Lancaster University

Catalytically generated N-acyliminium ions and their application in Diels-Alder reactions.

Niamh Jude Owen

36080976

Dr Mark McLaughlin

This thesis is submitted for the degree of [Master of Research in Chemistry]

Lancaster University

Department of Chemistry, Lancaster University, John Creed Ave, Bailrigg, Lancaster

LA1 4YB

Submitted: August 2022

Word count *(excluding references, captions & tables)* : 8,903

Abstract

Society is currently facing major challenges in providing resources such as healthcare in a more sustainable manner. The production of pharmaceuticals relies heavily on the use of precious transition metals such as palladium and rhodium to mediate single transformations on route to desired bioactive substances. Although these transformations are often high yielding, the need to mine great quantities of these metals remains a concern. Therefore, synthetic chemists must strive to develop more environmentally friendly and sustainable chemistry to access desirable and important scaffolds.

We report on the development of a novel route to tricyclic lactam products via a facile Aza-Diels-Alder reaction of catalytically generated N-acyliminium ions. Employing a $Ca(NTf_2)_2$ / nBu_4NPF_6 catalyst system in low loadings, to synthesise a diverse range of fused ring systems which differing electronic and steric properties in predominately good yields.

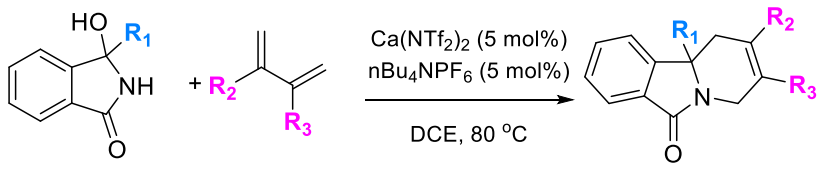

Contents

List of Tables:

List of Figures:

List of Schemes:

Acknowledgements

Firstly, I would like to thank my supervisor, Dr Mark McLaughlin, for his time and dedication to the project throughout the year. I would also like to thank him for the moral support during the periods of self-doubt and low motivation.

Another big thanks to Dr Nathan Halcovitch, for his expertise in crystallography and providing crucial data for the structural elucidation of novel compounds.

I would also like to thank the rest of the McLaughlin group for the support and most importantly the entertainment throughout the days in the lab.

Special thanks to my partner Ash, without him I wouldn't be where I am today. He's supported me inside the lab from day 1 showing me how to do a Grignard as well as outside the lab. He's been my shoulder to cry on as well as my person to celebrate the highs with over a glass of wine *(or two)*.

Last but definitely not least I'd like to thank my parents and family who've listened to countless Facetime updates on the highs and lows of research, this wouldn't have been possible without them.

Author's Declaration

"I declare that none of the work detailed herein has been submitted for any other award at Lancaster University or any other Institution."

"I declare that, except where specifically indicated, all the work presented in this report is my own and I am the sole author of all parts. I understand that any evidence of plagiarism and/or the use of unacknowledged third part data will be dealt with as a very serious matter"

Abbreviations

LUMO	Lowest unoccupied molecular orbital
HOMO	Highest occupied molecular orbital
FMO	Frontier molecular orbital
DMF	Dimethylformamide
THF	Tetrahydrofuran
DMSO	Dimethyl sulfoxide
DCM	Dichloromethane
DCE	Dichloroethane
EtOAc	Ethyl acetate
WERC	Water exchange rate constant
HFIP	Hexafluoro-2-propanol
PPTS	Pyridinium *p*-toluene sulfonate
TMSOH	Trimethylsilanol
m-CPBA	Meta-chloroperoxybenzoic acid
m-CBA	Meta-chlorobenzoic acid
NMO	*N*-methyl morpholine oxide
TMDS	Tetramethyldisiloxane
TMSCN	Trimethylsilyl cyanide
DA	Diels-Alder

1. Introduction

1.1. Lewis Acid Catalysis

1.1.1. Lewis Acid Concepts

A Lewis acid is a species that contains a vacant orbital which accepts an electron pair from a Lewis base, a process that is referred to as a σ-donation *(Figure 1)*. The strength of a σ-donation can be defined by the following: *(i)* charge of the metal, the larger the charge the stronger the Lewis acid *(ii)* ionic radius, the larger the radius the weaker the interaction and weaker the Lewis acid.

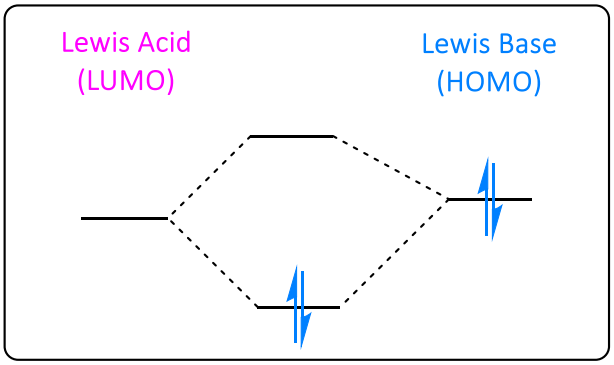

Figure 1. σ donation of Lewis bases.

Lewis acids and bases can be classified using hard/soft acid base theory, which explains the differing reactivity of Lewis acids. Hard acids typically have a small ionic radii and are highly charged and form electrostatic interactions with hard bases, whereas soft acids are larger in size with a more diffuse ionic charge and form strong covalent bonds with soft bases. Hard/soft acid base theory is helpful for choosing preparative conditions and predicting direction of reactivity *(Figure 2)*.[1]

	Hard	Borderline	Soft
Acids			
	H^+, Li^+, Na^+, K^+ Be^{2+}, Mg^{2+}, Ca^{2+} Cr^{3+}, Al^{3+} SO_3, BF_3	Fe^{2+}, Co^{2+}, Ni^{2+} Cu^{2+}, Zn^{2+}, Pb^{2+} SO_2, BBr_3	Cu^+, Au^+, Ag^+, Ti^+ Hg_2^{2+}, Pd^{2+}, Cd^{2+} Pt^{2+}, Hg^{2+} BH_3
Bases			
	F^-, OH^-, H_2O, NH_3 CO_3^{2-}, NO_3^-, O^{2-} SO_4^{2-}, PO_4^{3-}, ClO_4^-	NO_2^-, SO_3^{2-}, Br^- N_3^-, N_2 C_6H_5N, SCN^-	H^-, R^-, CN^-, CO, I^- SCN^-, R_3P, C_6H_6 R_2S

Figure 2. Classification of Lewis acids & bases.

1.1.2. Calcium as a Lewis acid.

There are many recognised types of Lewis acids, which are classified by frontier molecular orbital theory *(FMO)(Figure 3)*. FMO theory describes interactions between the HOMO and the LUMO.

This research focuses on calcium's application as a Lewis acid. Calcium is found in the s-block of the periodic table and like all s-block metals it is characterised by its stable oxidation state. The inner shells of metal(II) cations are inaccessible, this prevents back donation from the metal centre to its ligands and stops the metal cations acting as Lewis bases.

	Proton	s-LUMO	p-LUMO	Transition metal
			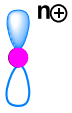	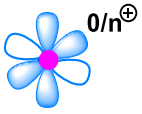
Examples	H^+	Li^+, Mg^{2+} Al^{3+}, Ca^{2+}	B^{3+}	Ag^+,Fe^{3+} Cu^{2+}

Figure 3. Types of Lewis acids.

1.1.3. Introduction to Calcium Catalysis

Many homogenous catalysts have been developed around transition metals, transition metals often have inherent disadvantages like cost, toxicity and shrinking availability, the

need for more sustainable catalysis has been reviewed in the literature.[2] One avenue which has been identified and becoming a key research topic is the Alkaline earth metals.

Alkaline earth metals are notable for their abundance in the earth's core, in particular calcium. Calcium is the 12th most abundant element in the earth's crust resulting in its low cost *($Ca(NTf_2)_2$ = £19.84 per mmol compared to $Sc(OTf)_3$ = £22.60 per mmol).* Calcium is air stable and environmentally benign and therefore does not require inert or anhydrous conditions. Its low redox potential *(Ca^{2+} = -2.869V)* minimises side redox reactions from occurring, making it highly selective as a Lewis acid.[3] This feature gives calcium the potential to be a synergistic catalyst. Synergistic catalysis is a specialised approach where at least two different catalysts act on different substrates simultaneously to enable the substrates to then react together. Finally, some calcium(II) complexes are ambiphilic and so display both nucleophilic and electrophilic behaviour, which is discussed in section 1.1.4 in further detail.

1.1.4. Weakly Coordinating Anions

Calcium(II) complexes display ambiphilic behaviour, which can be tuned through the manipulation of electronics, allowing for the tuning of catalytic properties *(Figure 4).*[4] The electropositive character of calcium(II) along with the polarisation of the metal/base bonding system provides a high degree of charge separation. This results in calcium(II) being a highly nucleophilic species and its Lewis acidic properties not prevailing.

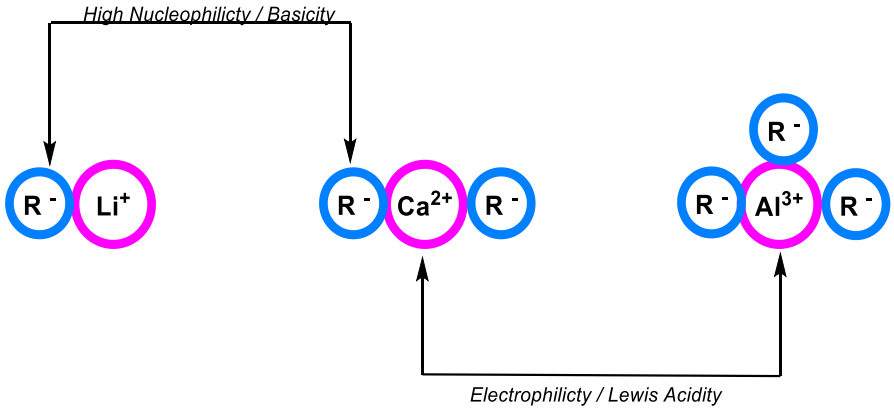

Figure 4. Amphiphilic properties of calcium(II).

Lewis acidity in s-block metals such as calcium directly correlates to the strength of the σ-donation between the cation and anion. For example, $CaCl_2$ is not Lewis acidic as the bonding in this compound is ionic.

The use of weakly/ non-coordinating anions *(^{-}OTf, $^{-}NTf_2$ & $^{-}PF_6$)* increases Lewis acidity of the species because the charge on the anion becomes delocalised across the complex, resulting in no singular point charge allowing the Lewis acidic properties to prevail. [5] This effect can be further enhanced by steric spatial hindrance and allows for ease of catalytic tuning *(Figure 5)*.

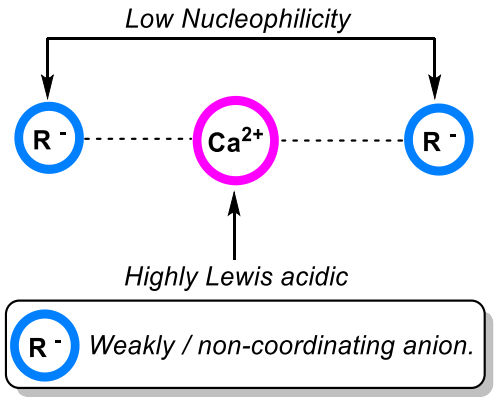

Figure 5. Catalytic tuning of calcium(II) complexes.

When designing a Lewis acid catalysed transformation it is important to consider factors that can impact catalytic activity such as solvent, presence of water and selection of ligands.

1.1.5. Effect of Solvent

Interactions between solvent and Lewis acids can often be observed and impact the reactivity. Many commonly used solvents such as DMF, THF and DMSO contain Lewis basic atoms which coordinate to the metal centre. Coordinating solvents can result in catalytic poisoning and should be avoided when using Lewis acids; if every coordination site is occupied the Lewis acidity of the metal centre decreases. Instead, the use of non-coordinating solvents such as DCM, DCE, EtOAc and toluene should be selected. When using calcium(II) complexes choice of solvent is highly important to maintain catalytic activity.

1.1.6. Water tolerance

Traditional Lewis acid catalysts such as $TiCl_4$ and $AlCl_3$ readily react with water to form hydroxides and so require inert atmospheres and anhydrous conditions to avoid poisoning of the catalyst and reactions plateauing.

Many group two metals will also react with water to form hydroxides but don't require inert and anhydrous atmospheres this can be explained by the water exchange rate constant (WERC) and the pK_h *(Scheme 1).*

$$x\ M^{n+} + yH_2O \rightleftharpoons M_x(OH)_y^{(xn-y)+} + yH^+$$

Scheme 1. Water and metal cation coordination.

Calcium(II) is tolerant to water so reaction conditions do not need to proceed under an anhydrous conditions. This stability can be explained by the hydrolysis constant pK_h. pK_h is a measure of a metal cation's stability towards hydrolysis and is seen in relation to the pK_w = 14 for pure water. A high pK_h value indicates a species' tolerance towards water. pK_w is defined as the negative log of K_w which is defined as the dissociation constant of water. [6]

Table 1. pk_h & WERC constants for metal cations.

	$M(H_2O)_x^{y+} + H_2O \overset{k = WERC}{\rightleftharpoons} M(H_2O)_{x-1}H_2O^{y+} + H_2O$						
	Li^+	Na^+	Mg^{2+}	Ca^{2+}	Ni^{2+}	Sc^{3+}	Al^{3+}
pK_h	13.64	14.18	11.44	12.85	9.89	4.30	1.14
WERC ($M^{-1}\ S^{-1}$)	$4.7x10^7$	$1.9x10^8$	$5.3x10^5$	$5.0x10^7$	$2.7x10^4$	$4.80x10^7$	$1.6x10^0$

Water is strongly coordinating which can impact catalytic activity. The effect of water on catalytic activity can be overcome when the exchange of the inner sphere ligands is fast this is defined as the WERC. The larger the WERC value the faster this exchange occurs, resulting in the maintenance of catalytic activity. Illustrated in Table 1 are the pK_h and WERC values for metal cations. focussing on calcium(II) we can explain its water stability. A pK_h value close to 14.0 indicates the metal cation will be less susceptible to hydrolysis, calcium(II) has a pK_h of 12.85 meaning it's unlikely to hydrolyse in the presence of water. The larger the WERC value the quicker the inner sphere exchange occurs; calcium(II)

exchange occurs at $5.0x10^7$ M^{-1} S^{-1}. From these 2 constants it's known that calcium(II) complexes are stable in water and don't require anhydrous atmospheres.

1.1.7. Calcium Catalysed Transformations

Many reactions employ Lewis acids catalysts. Lewis acids such as BF_3·OEt2 are used in stochiometric amounts because the oxygen boron bond formed during reaction activation is irreversible and poisons the catalyst. Reactions that utilise Lewis acids such as BF_3·OEt_2 often have harsh reactions conditions making the functional group tolerance low. Work from Perlmutter employed BF_3·OEt_2 as catalysts in Diels-Alder reactions of 1,2-Napthoquinones, the scope of functional groups which were tolerated was limited to electron donating group methoxy's only.[7] This lack of functional group tolerance has pushed research into the development of milder catalyst systems, one of these being calcium bistriflimide, which has been utilised in a range of transformations.

The triflimidate ion is a highly delocalised counterion, which causes the metal centre to bear a high positive charge. Calcium bistriflimide **1** is often treated with a source of weakly coordinating anions such as tetrabutylammonium hexafluorophosphate **2**. The treatment of Lewis acids with a source of weakly coordinating anions results in the increased acidity of the metal centre and often the generation of the active catalyst **4.** The treatment of Lewis acids with weakly coordinating anions is defined as anion dissociation, which is driven by the formation of the insoluble tetrabutylammonium triflimidate **3** *(Scheme 2).*[8]

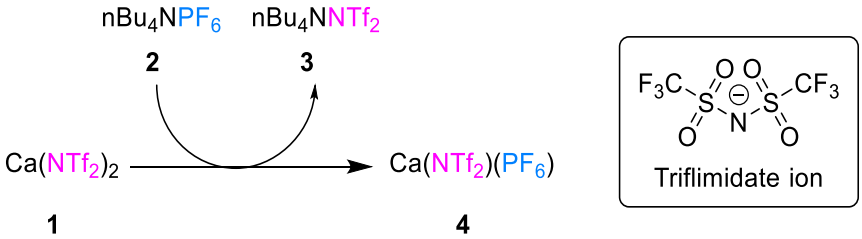

Scheme 2. Anion dissociation.

The seminal work surrounding the generation of reactive intermediates with calcium catalysis was reported by Niggemann in 2010. They employed catalytic calcium bistriflimide to generate carbocations via alcohol dehydration, and carbocations **8** were then trapped out with carbon nucleophiles **6** *(Scheme 3A).* [9] This work was further developed by the Niggemann group, who introduced heteroatomic nucleophiles **10**

(Scheme 3B). [8] In 2014 the Leboeuf group took these principles and applied this theory to a range of substituted furans **12** which were used as oxygen/carbon reactive intermediates - oxocarbenium ions **15**. *(Scheme 3C).* [10]

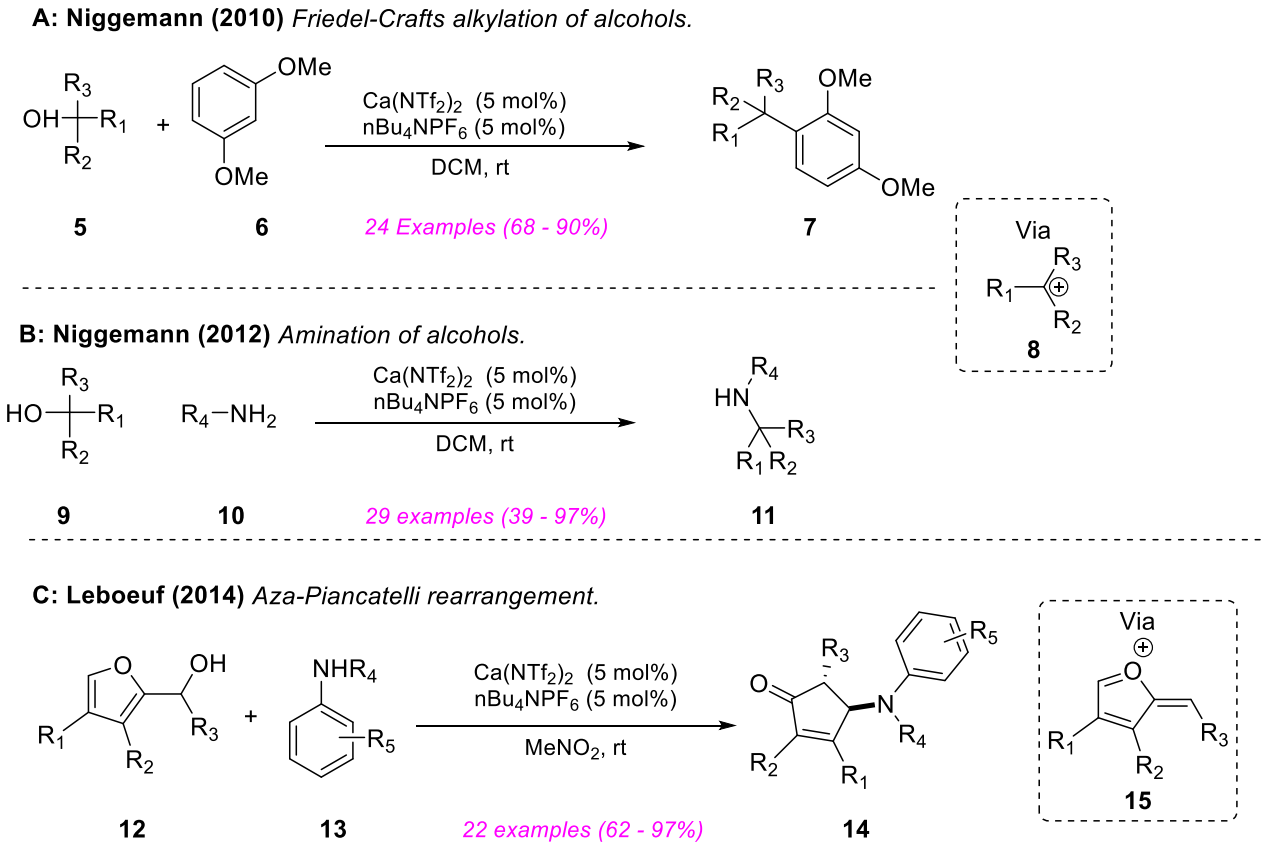

Scheme 3. Seminal calcium-catalysed transformations.

The McLaughlin group then focused their research on the generation of nitrogen containing reactive intermediates, specifically N-acyliminium ions. They identified 3-hydroxyisoindolinones **16** and N,O-acetals **22** as N-acyliminium ion **21&25** precursors and utilised them in a range of transformations. *(Scheme 4)* [11-13] The nucleophilic trapping of N-acyliminium ions is a robust and high yielding method, which affords a range of highly substituted products and requires low catalytic loading. They introduced heteroatomic nucleophiles including nitrogen and sulfur moieties such as; indoles, thiophenols, sulfonamides, benzyl carbamates and secondary amines. Functionalisation at 3 points with heteroatoms was previously absent in the literature *(Scheme 4B)*.

In 2021 McLaughlin and co-workers developed a new methodology utilising N-acyliminium ions for the synthesis of oxazoles and thiazoles *(Scheme 4C).* Employing isocyanides **23** as nucleophiles and the N-acyliminium ions as electrophiles resulted in

their cyclisation to form heterocycles **24**. This was presented as an alternative method to traditional oxazole and thiazole synthesis which typically required their synthesis to be conducted at high temperatures in concentrated HCl.[14]

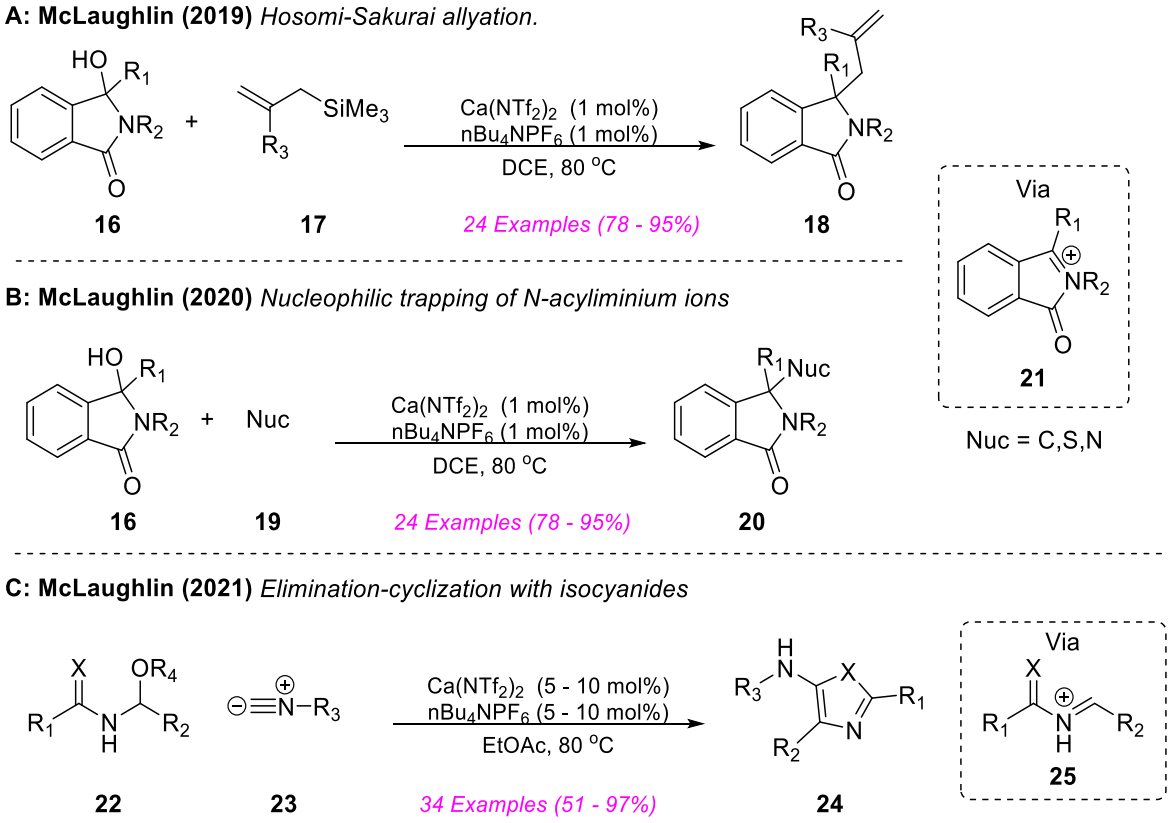

Scheme 4. Calcium-catalysed generation of N-acyliminium ions.

Kobayashi and co-workers also explored calcium catalysis, employing $Ca(O^iPr)_2$ for the asymmetric addition of α-amino acid derivatives **27** to α,β-unsaturated carbonyl **26** compounds.[15] They also employed $Ca(OAr)_2$ *(Ar = p-MeOC$_6$H$_4$)* for the enantioselective 1,4 addition of 1,3-dicarbonyls **30** to nitroalkenes **31** *(Scheme 5)*. [16]

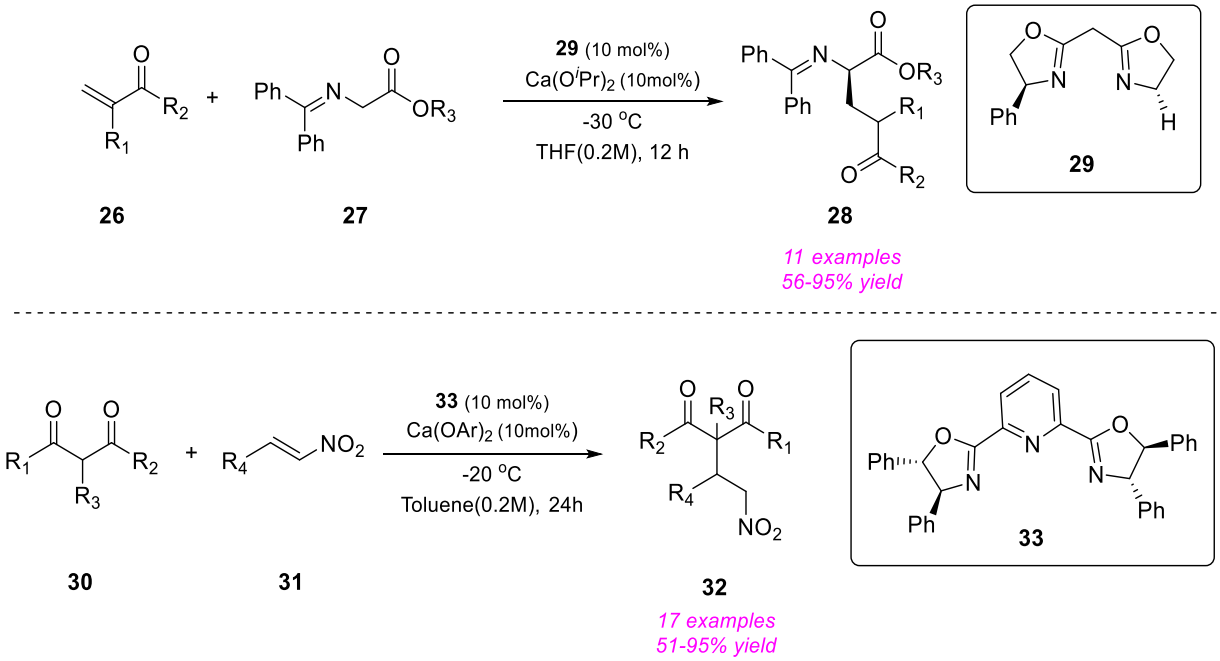

Scheme 5. Kobayashi's calcium-catalysed transformations.

1.2. Diels-Alder reaction

Pericyclic reactions by definition are reactions which proceed through a concerted mechanism involving a single cyclic transition state. Pericyclic reactions are classified into 3 categories; electrocyclic, sigmatropic rearrangement and cycloaddition reactions *(Table 2)*.

Table 2. Classes of pericyclic reactions.

Reaction	Bond changes	
	Sigma *(σ)*	Pi *(π)*
Electrocyclic	+1	-1
Sigmatropic rearrangement	0	0
Cycloaddition	+2	-2

The Diels-Alder reaction is a [4+2] cycloaddition between an electron-rich conjugated diene and electron deficient dienophile *(Scheme 6)*. The prefix [4+2] arises from the number of π-electrons which participate in the 2 reacting species. Dienes **34** contain 4 pi-electrons and dienophiles **35** contain 2 pi-electrons. Diels-Alder reactions are commonly used throughout organic chemistry as they provide easy access to cyclic structures **36**.

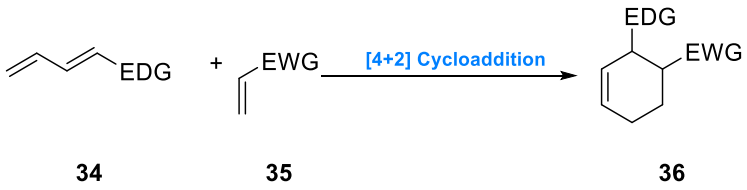

Scheme 6. Diels-Alder reaction.

1.2.1. Frontier molecular orbital theory

Diels-Alder reactions are believed to occur in a single transition state with no generated intermediates. Frontier molecular orbital theory explains how the HOMO *(ψ_2)* of the diene interacts with the LUMO *(π^*)* of the dienophile, resulting in the in-phase suprafacial/suprafacial orbital interaction *(Figure 6)*. This in-phase interaction is what forms the new sigma bonds. [4+2] cycloadditions are thermally allowed and so do not require activation with light.

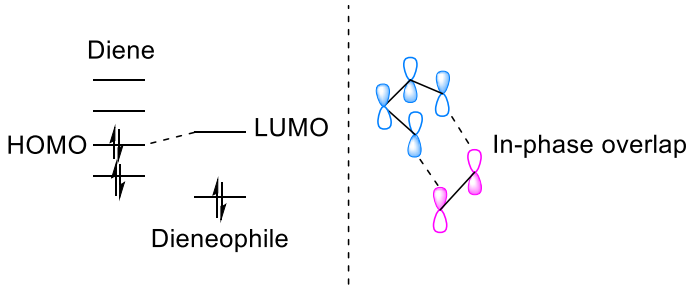

Figure 6. Frontier molecular orbital diagram of a Diels-Alder reaction.

1.2.2. Selectivity

Diels-Alder reactions are stereoselective, which can be explained using the *endo*/*exo* rule *(Figure 7)*.

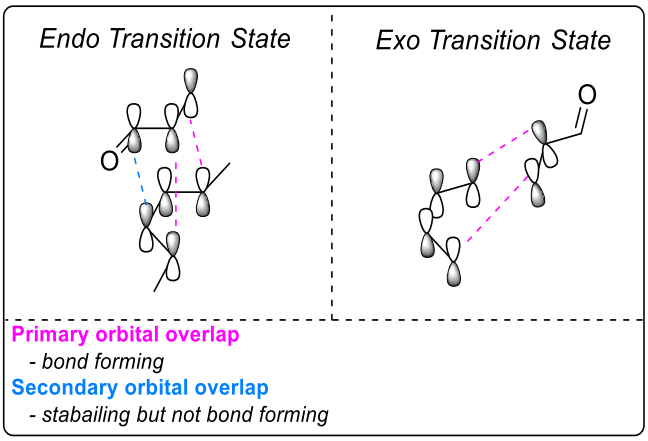

Figure 7. Endo/exo rule.

Typically, Diels-Alder reactions result in *endo* products as secondary orbital interactions stabilise the transition state, lowering its energy, making it more favourable than the *exo* transition state. Secondary orbital interactions aren't observed in the *exo* transition state as the orbitals lie too far apart to interact with one another. It should be noted that secondary orbital interactions are not bond forming, they are only stabilising.

1.2.3. Lewis Acid facilitated Diels-Alder reactions

The use of catalysts in Diels-Alder reactions has been found to lower the energy of the LUMO of the dienophile, which subsequently results in a smaller energy gap between the reacting orbitals, and so more stabilising orbital interactions *(Figure 8)*. [17]

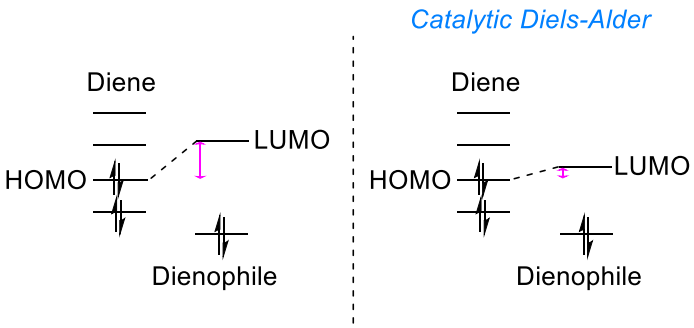

Figure 8. Frontier molecular orbital diagram of a catalytic Diels-Alder reaction.

Section 1.2.3 will primarily focus on Lewis acid facilitated Diels-Alder reactions. Recent computational studies found that Lewis acids do not enhance reactivity as described in Figure 8, but they have been found to accelerate the reaction by reducing the four-electron *(Pauli)* repulsion between the pi-systems of the dienophile and reacting diene *(Figure 9)*. [18]

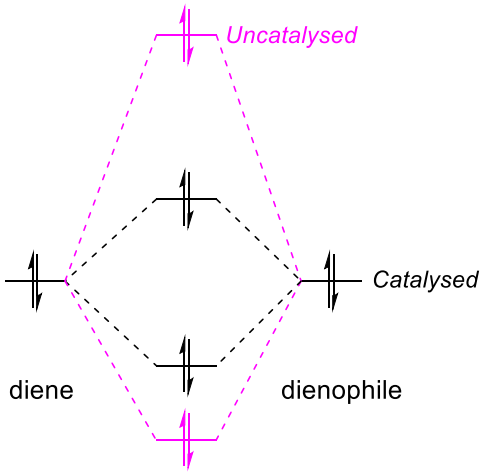

Figure 9. Pauli repulsion-lowering catalysis.

This reduced Pauli repulsion is induced by the co-ordination of Lewis acid with carbonylic oxygen of the dienophile, which causes polarization of the conjugated pi-system away from the sp^2 carbons and the lowering of the activation energy of the reaction. [17]

In 1995 metal triflimidates were first utilised as Lewis acid catalysts in a Diels-Alder cycloaddition of cyclopentadiene **37** with methyl vinyl ketone **38**.[19] Gas chromatography analysis of reaction mixtures found that Lewis acids; $Mg(NTf_2)_2$, $Zn(NTf_2)_2$ and $La(NTf_2)_3$ yielded product at more than 95% yield at highly accelerated rates of reaction when as little as 1 mol% was used. Reactions which were uncatalysed proceed 1440 times slower *(Scheme 7)*.

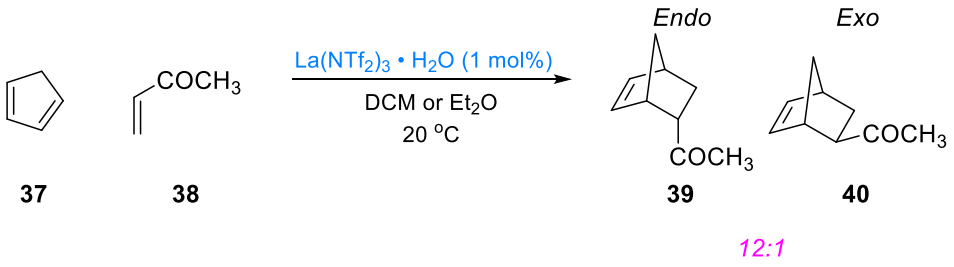

Scheme 7. First Lewis acid-catalysed reaction.

Shi and co-workers developed a Lewis acid catalysed Aza-Diels-Alder for the direct synthesis of piperidine scaffolds **42**. They tested the effects of multiple Lewis acids and found $Sc(OTf)_3$ at 10 mol% loading, yielded the best results, with reaction times ranging between 5-23 hours depending on the sterics and electronics of the diene **42** and dienophile **41**. Overall, they reported excellent yields and control experiments indicated

the catalyst system was essential for the formation of piperidine products **43** *(Scheme 8)*.[20]

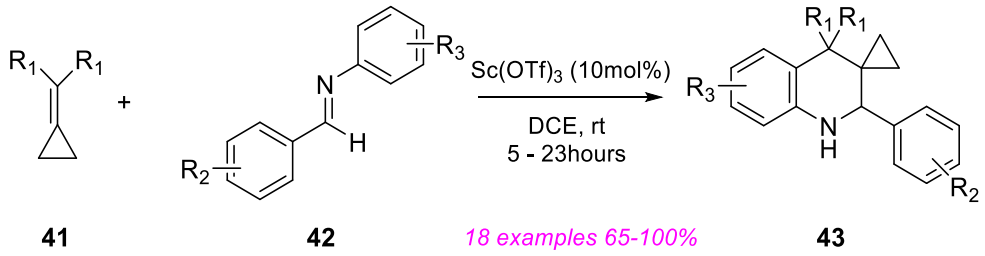

Scheme 8. Lewis acid-catalysed Aza-Diels-Alder.

Song and co-workers wanted to explore selectivity of Diels-Alder reactions, they reported that the use of a bis-silane **44** forces the reaction through the *exo* transition state *(95:5)* due to the sterics of the silane groups. They screened multiple Lewis acids and found that bulkier ligands resulted in increased yields and higher diastereoselectivity. 0.6 equivalents of the Lewis acid $AlClEt_2$ was responsible for the activation of the dienophile **45** through coordination of the oxygen lowering the LUMO *(Scheme 9)*.[21]

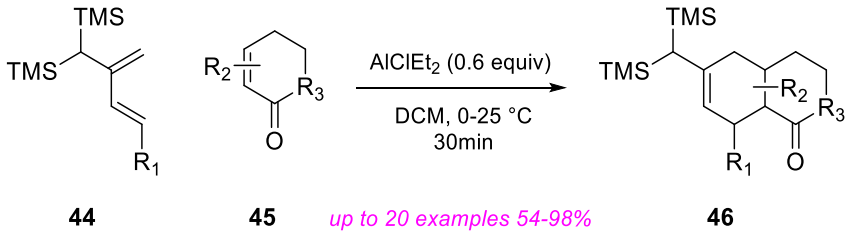

Scheme 9. Selectivity of Diels-Alder reactions.

1.3. N-acyliminium ions

We identified N-acyliminium ions to have potential as dienophiles in Diels-Alder reactions as they are highly electrophilic in nature. Their reactivity as dienophiles in Diels-Alder reactions is not heavily explored. The current focus in the literature explores their reactivity as electron deficient dienes in the inverse electron demand Diels-Alder which are detailed below.

N-acyliminium ions **51** are highly reactive electrophiles that are used in the formation of carbon-carbon and carbon-heteroatom bonds. They are more electrophilic than iminium ions **50** due to the electron withdrawing nature of the carbonyl group, which makes them a more reactive species *(Figure 10)*.

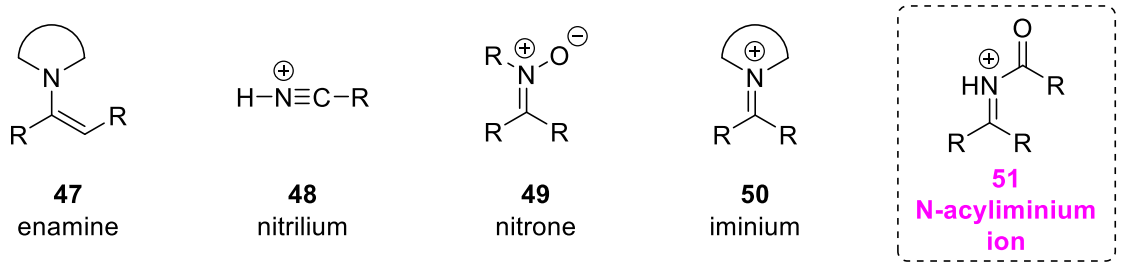

Figure 10. Summary of nitrogen containing reactive species.

Their use features in named reactions such as the Mannich and Pictet-Spengler reactions.[22, 23] The Pictet-Spengler reaction is a condensation reaction of an aldehyde or ketone with a β-arylethylamine **52**. The Mannich reaction is a three-component reaction which is used to synthesise β-amino-carbonyl compounds **58**. Which are also referred to as Mannich bases.[24] *(Scheme 10).* [25]

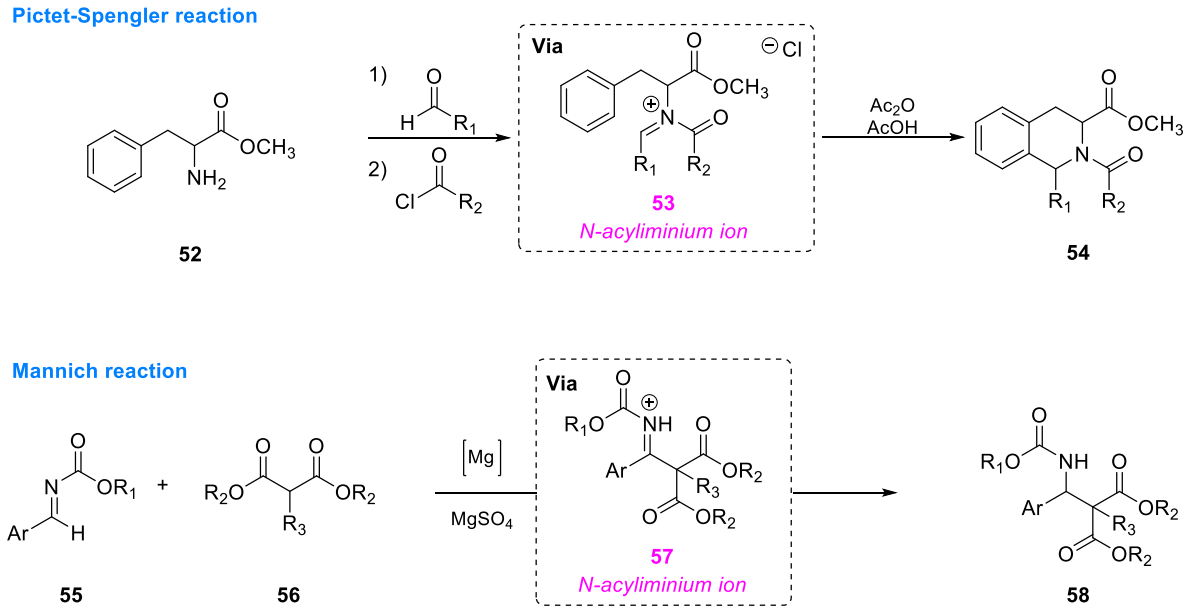

Scheme 10. Named reactions employing N-acyliminium ions.

1.3.1. Accessing N-acyliminium ions

There are multiple established routes to access N-acyliminium ions; they are generated in situ and cannot be isolated (Scheme 11). Traditional non-catalytic methods to generate N-acyliminium ions **66'** include the condensation of an amide **59** with an aldehyde **60** as well as the acylation of an imine **61** with an acyl chloride **62.** Catalytic methods used to generate N-acyliminium ions commonly include the liberation of a leaving group **63** activated by catalytic Lewis or Brønsted acids, this is often a controlled way of accessing these species, as catalytic amounts of the acid are used. Hydroxyls are the most widely

used leaving group, however halogen, alkoxy, acetoxy and arylsulfony leaving groups have also been utilised.[26] Protonation of enamides **64** is another mode of accessing N-acyliminium ions. Anodic oxidation **65** (commonly referred to as Shono oxidation) can also be used to access N-acyliminium ions **66'**, however isn't widely used since it requires bulk electrosynthesis and specialised reaction setups. [27]

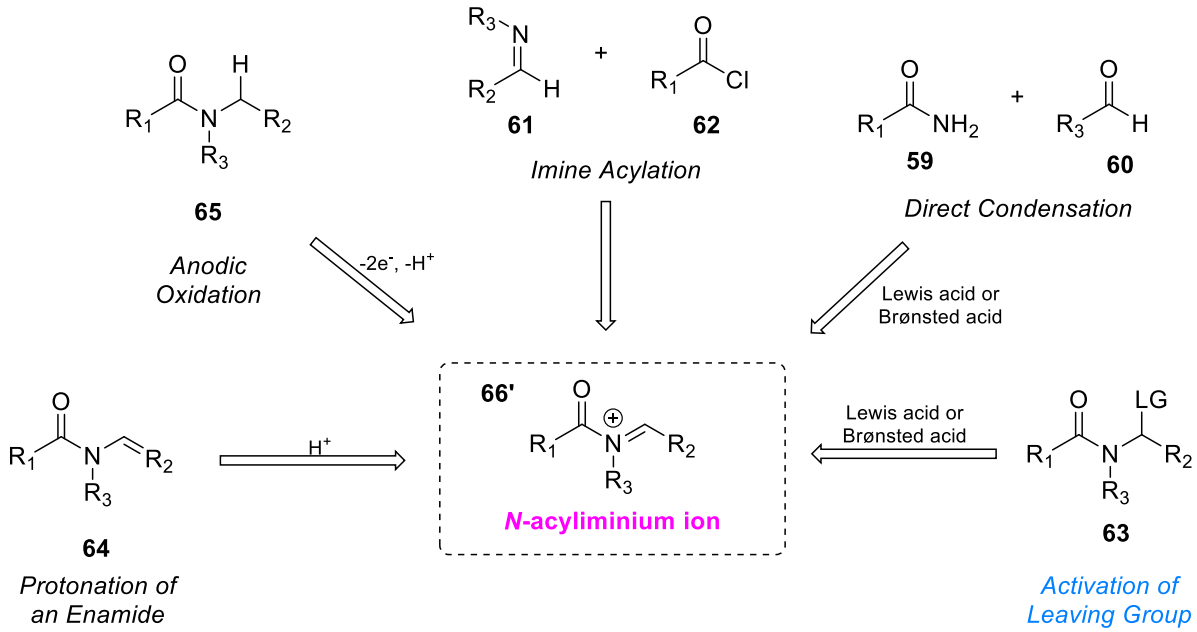

Scheme 11. Accessing N-acyliminium ions.

1.3.2. N-acyliminium Ions as Dienes/Dienophiles in Aza-Diels Alder reactions

N-acyliminium ions have been identified as suitable components in Aza-Diels-Alder reactions as they are capable of reacting as both dienophiles **68** and dienes **69**. This reactivity has been reviewed in the literature *(Figure 11)*. [28, 29]

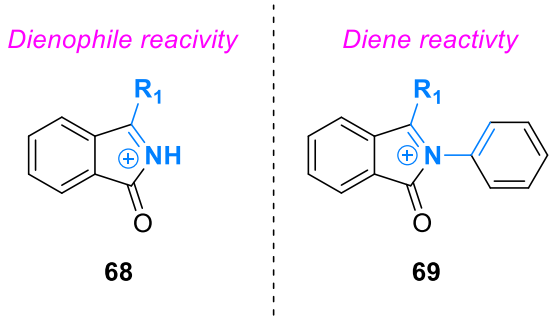

Figure 11. Reactivity of N-acyliminium ions.

N-acyliminium ion reactivity is determined by the substituent located on the nitrogen. Most literature studies focus on the reactivity of N-acyliminium ions as dienes **69** rather

than their application as dienophiles **68**. N-acyliminium ion reactivity as dienes has been considered from a mechanistic viewpoint. Schmidt suggested in his pioneering work that these reactions should be classified as *"polar cycloadditions"*. [30]

It is believed that polar cycloadditions occur via transition state **1** and not transition state **2**; this process is concerted and results in heterocycles **71** *(Scheme 12)*.

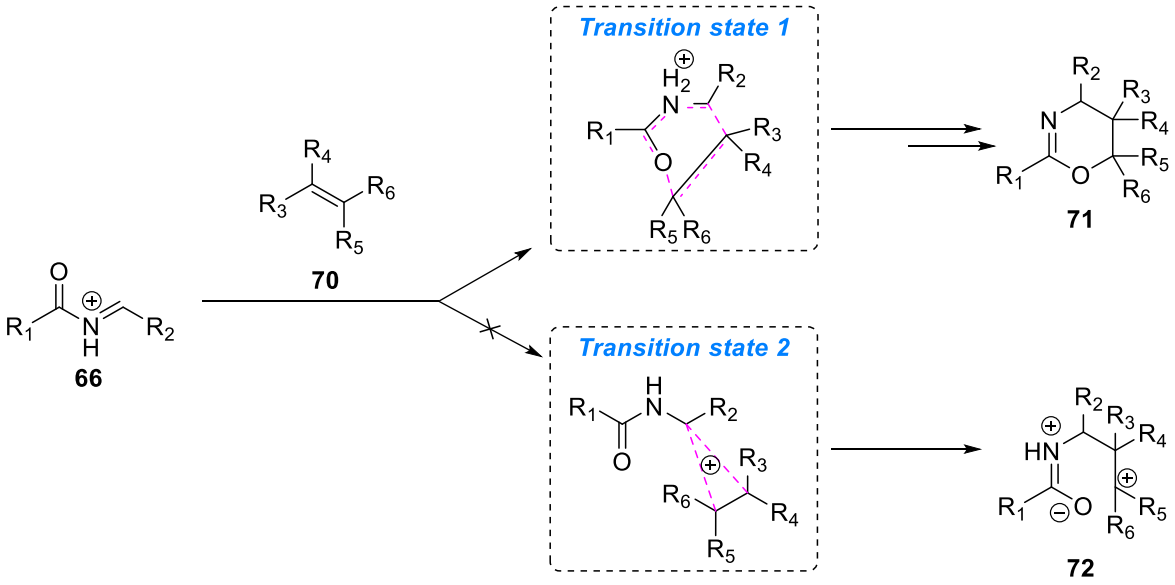

Scheme 12. Transition state of polar cycloadditions.

In 2014 Jha and co-workers reported how steric factors impact reaction pathways in an inverse electron demand Aza-Diels-Alder. Stoichiometric amounts of $BF_3{\cdot}Et_2O$ were employed to liberate hydroxide and generate the N-acyliminium ion **76**. N-phenyl phthalimide **73** was used as the N-acyliminium precursor, which went on to react as a diene. N-vinyl lactam **74** was used as an electron rich dienophile to synthesise a range of substrates in fair to good yield. The study found that *ortho* substituents on the N-acyliminium ions were detrimental to cyclisation and so should not be used. The use of electron donating groups typically led to higher yields when compared to electron withdrawing groups, as electron donating groups will give rise to a more nucleophilic diene *(Scheme 13)*. [31]

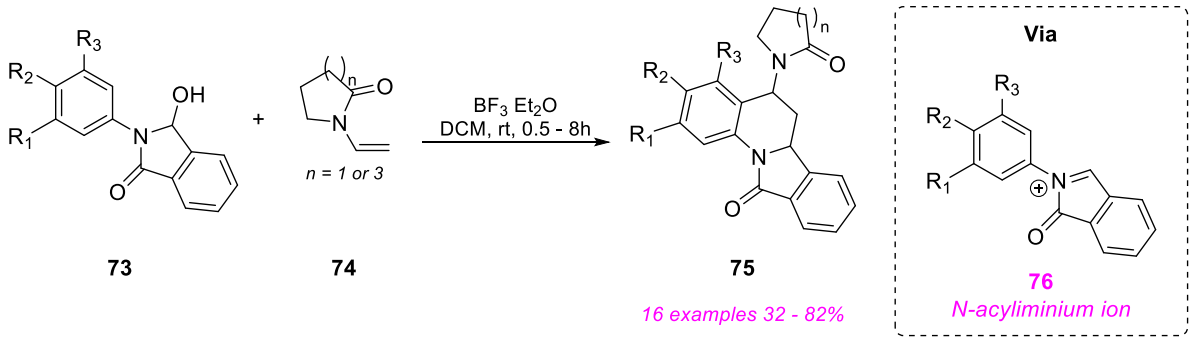

Scheme 13. Aza-Diels–Alder reaction between N-aryl-1-oxo-1H-isoindolium ions and tert-enamides.

Most examples which utilise N-acyliminium ions found in the literature generate the N-acyliminium ion through the liberation of a leaving group. Suga and co-workers used anodic oxidation to generate N-acyliminium ions **79** using low temperature electrolysis and carbamate **77**. These N-acyliminium ions then reacted as dienes to result in the 6-membered heterocycles **78**. The substrate scope was limited to simple alkyl substituents, suggesting this method is sensitive to functional groups either sterically or electronically *(Scheme 14)*. [32]

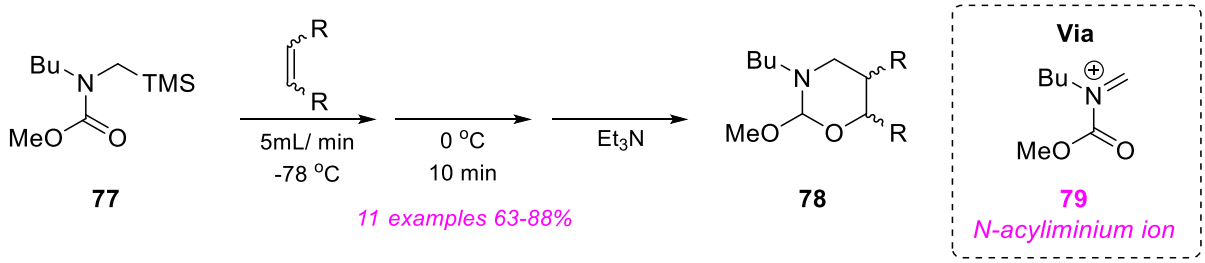

Scheme 14. Cycloaddition of "N-acyliminium pools"

In the 1970's Ishai and co-workers developed a route to synthesise 1,3-oxazines. N-acyliminium ions **66** were key intermediates and were generated using stoichiometric $BF_3{\cdot}Et_2O$. N-acyliminium ions reacted as dienes when olefin **80'** was added to the reaction mixture to synthesise 1,3-oxazines **81** *(Scheme 15)*.[33]

Nelson and co-workers also worked on similar chemistry many years later in 2015, where they also took N,O-acetals **82** as N-acyliminium precursors and generated N-acyliminium ion intermediate **66** using sulfuric acid. The use of sulfuric acid will impact the functional group tolerance of the reaction as the acidic conditions will lead to functional groups becoming protonated and potentially collapsing and breaking apart *(Scheme 15)*.[34]

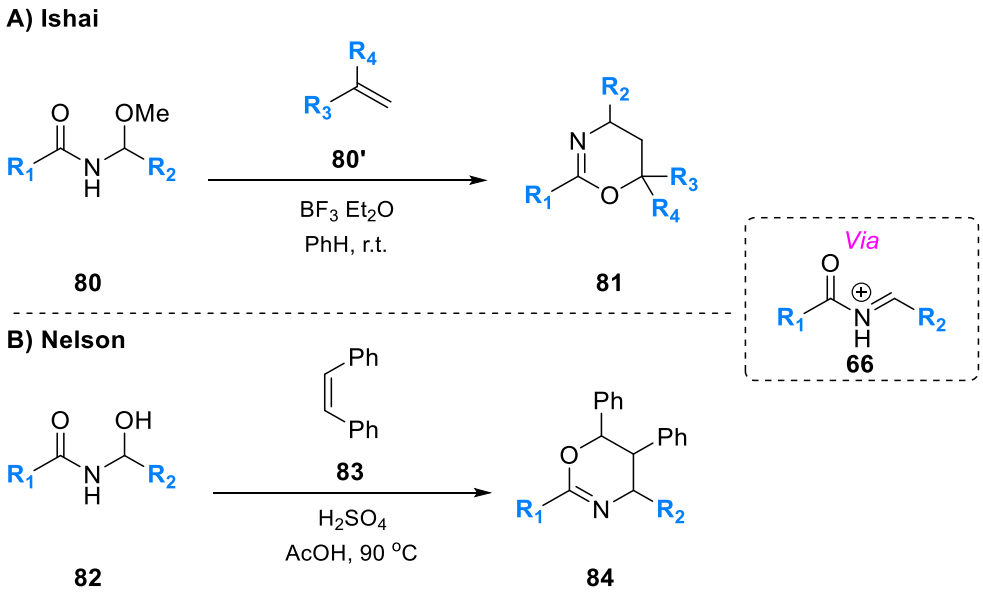

Scheme 15. N,O-acetal cyclisation to form 1,3-oxazines.

There are very few examples in the literature of N-acyliminium ions reacting as dienophiles in Diels-Alder reactions, however Ueda explored this reactivity. Early work by Ueda and co-workers looked at using N-acyliminium ions as dienophiles in Aza-Diels-Alder reactions. They used 4-membered lactams **85** as N-acyliminium ion precursors, which they accessed using $ZnCl_2$. The liberation of acetic acid allowed access to the N-acyliminium ions **88,** which then readily underwent the Aza-Diels-Alder reactions with diene **86** to generate fused 4,6-bicycles **87** *(Scheme 16)*.[35]

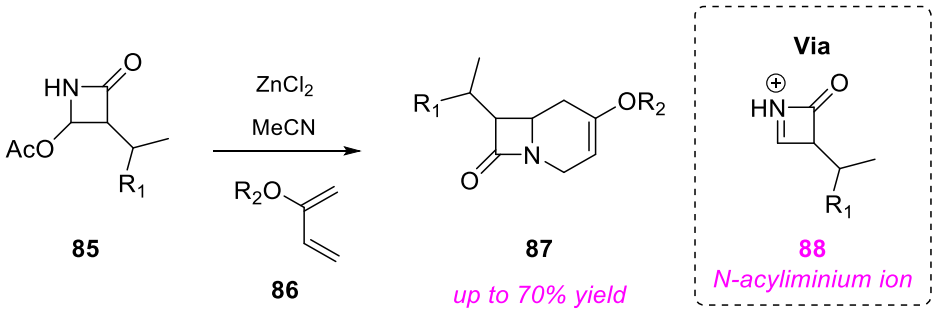

Scheme 16. Asymmetric Aza-Diels-Alder of N-acyliminium ion.

1.4. Isoindolinones

The isoindolinone structure **91** is a common pharmacophore and is found in many bioactive compounds making it a desirable structure for functionalisation. Figure 12 illustrates the isoindolinone family and its derivatives. This research makes use of phthalimides **92** to access 3-hydroxisoindolinones **93**, which we identified as N-

acyliminium precursors. The ability to functionalise these cores is advantageous, due to their medical relevance *(Figure 12)*.

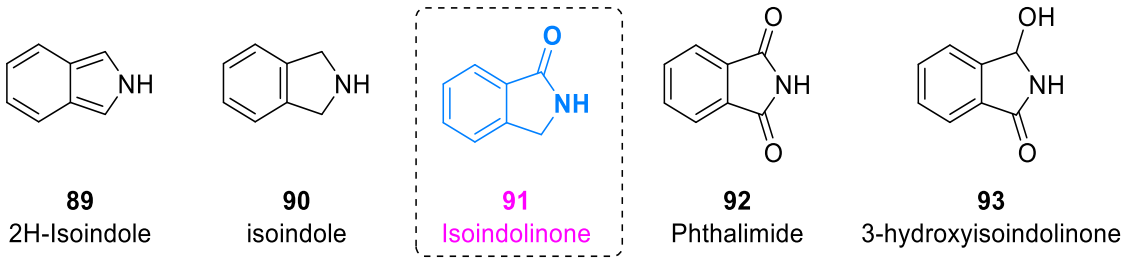

89 2H-Isoindole | **90** isoindole | **91** Isoindolinone | **92** Phthalimide | **93** 3-hydroxyisoindolinone

Figure 12. Structural features of isoindolinones.

1.4.1. Medicinal Relevance of Isoindolinones

In the 1950's thalidomide **94** was prescribed to many pregnant women as morning sickness relief medication. It soon became the most infamous drug in human history and caused thousands of fatalities and severe birth defects, it's now used to treat multiple myeloma. This discovery led to the modification of thalidomide to give new drugs such as Pomalidomide **95** and highly selective Lenalidomide being developed. Many bioactive compounds contain the isoindolinone core giving them desirable properties such as sedatives **96**, dopamine antagonists **97**, anti-inflammatories **98** and organic dyes **99** etc *(Figure 13)*.[36]

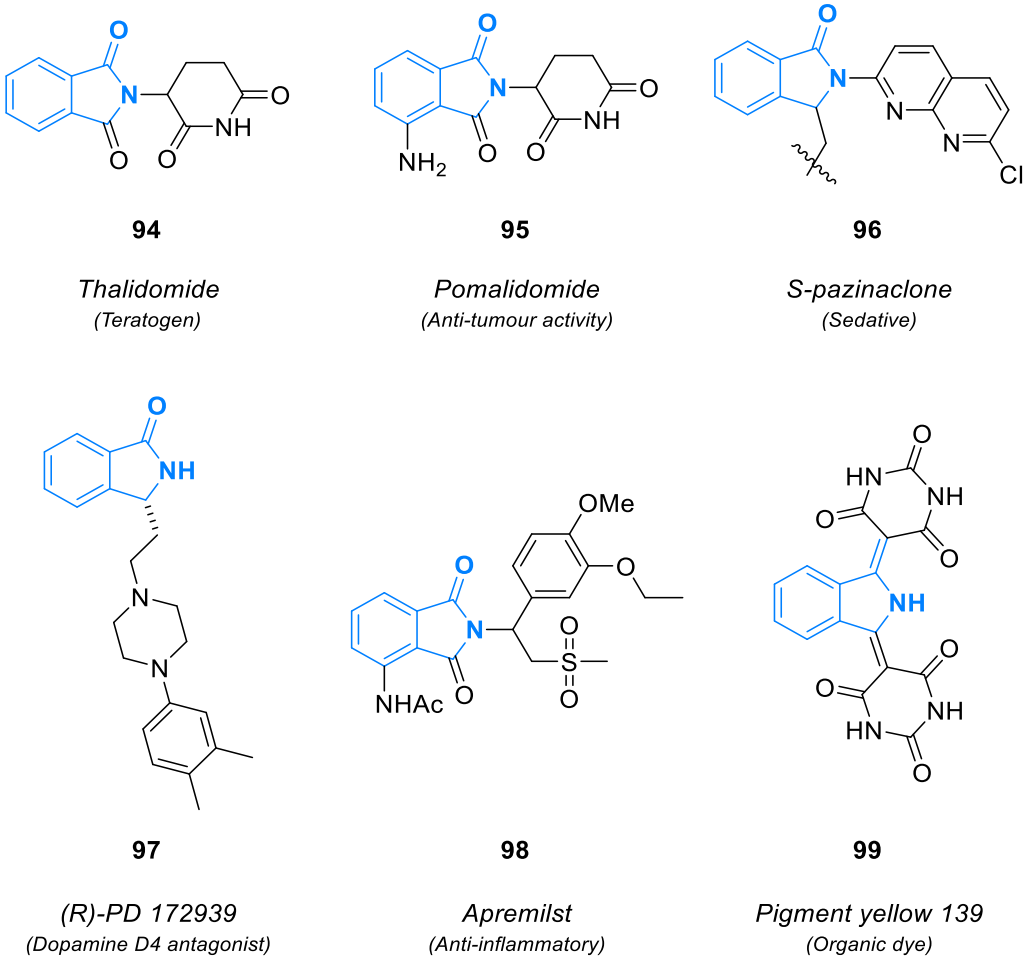

Figure 13. Biologically active species with an isoindolinone core.

1.4.2. Functionalisation of Isoindolinones

Research into the functionalisation of isoindolinones is still prevalent in synthetic organic chemistry. Many of the examples displayed in Figure 13 contain functionalisation at the 3 position, but there are currently very few examples of how to easily install functionalisation at this position in a modular single-step route. The ability to easily install functional groups and develop large screening libraries is highly desirable to medicinal chemists. Most studies explore functionalisation of isoindolinones installing single points of substitution at the 3-position to form single carbon-carbon or carbon-heteroatom bonds. Scheme 17 displays some selected recent studies, which look at single carbon-carbon or carbon-heteroatom bond formation to functionalise isoindolinones. Dunach and co-workers developed a methodology for the direct installation of a substituent at the activated 3-position **100** using $Sn(Tf)_2$. They explored a range of cyclic and alkyl enol nucleophiles, which provided handles for further functionalisation *(Scheme 17A)*. [37] Li and

co-workers also developed a methodology for the single substitution at the 3-position of isoindolinones using a range of benzyl amines **103** as chelating groups to access benzolactams **104**. Reactions required the use of 1 atm CO and required a functionalised amine **103** starting material *(Scheme 17B).*[38] Both reactions described demonstrate effective ways to functionalise the isoindolinone core, however the drawback is they only allow for the installation of 1 functionality using carbon nucleophiles. In 2020 McLaughlin and co-workers developed a methodology which allowed for 3 points of substitution, disubstitution at the 3-position and also the amine functional handle, **106** and introduced the working idea of functionalisation with nucleophiles such as, indoles, thiophenols, sulfonamides, benzyl carbamates and secondary amines *(Scheme 17C).*[12]

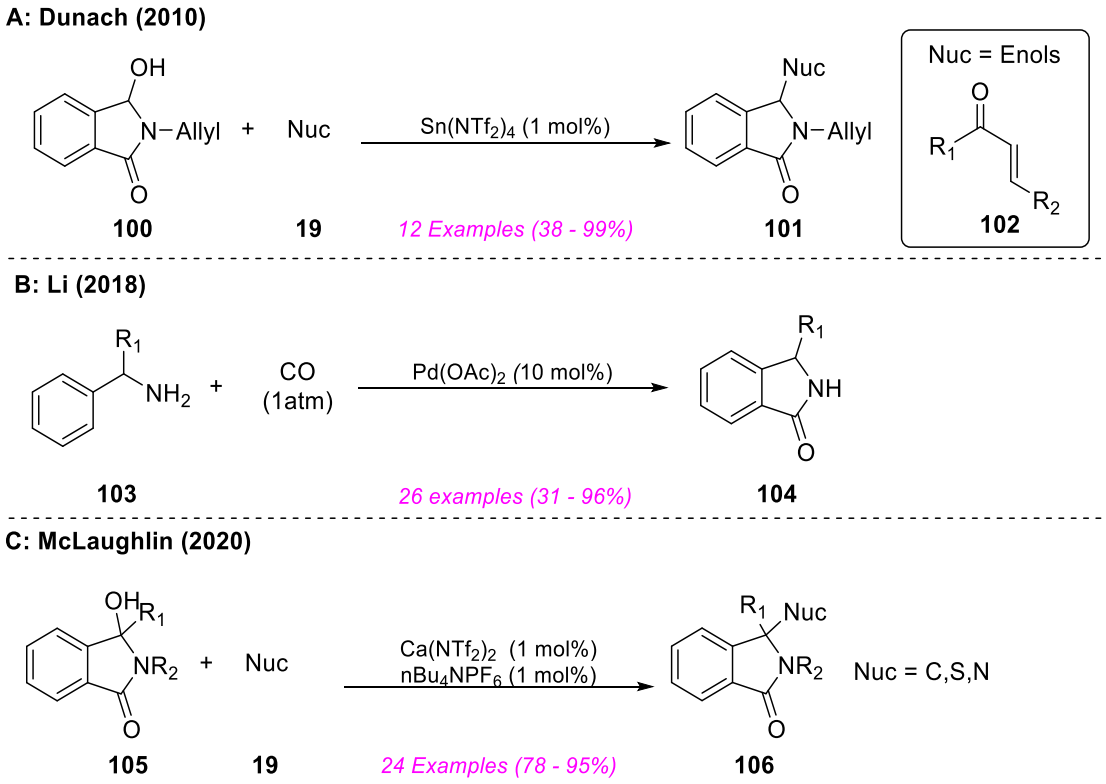

Scheme 17. Functionalisation of Isoindolinones.

They are many examples which develop methodology for the installation of functionality at the 3-position. The introduction of fused ring system onto the isoindolinone core is synthetically more challenging method to develop. In 2022, McLaughlin and co-workers developed a unified approach to the synthesis of 6,5,5,6 fused cyclic scaffolds **108**, which contain the isoindolinone core, utilising catalytic calcium bistriflimide. They reported

successes using tethered indoles as well as employing amides which introduced a lactam ring into the products *(Scheme 18)*.[39]

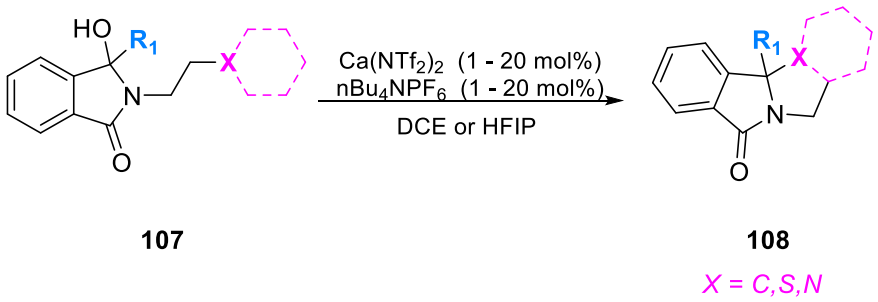

107 **108**

X = C,S,N

Scheme 18. Synthesis of fused fragments.

In 2022, Schneider and co-workers reported on the enantioselective annulation of α,β-unsaturated 3-hydroxyisoindolinones **109** with β-keto ester enolates **110** to install fused bicycles onto the isoindolinone core **111**. Substrate scopes included heterocycles, R_1 was limited to phenyl or *p*-substituted phenyl and when ^{t}Bu group was changed to alternate alkyl chains yields dropped *(Scheme 19)*.[40]

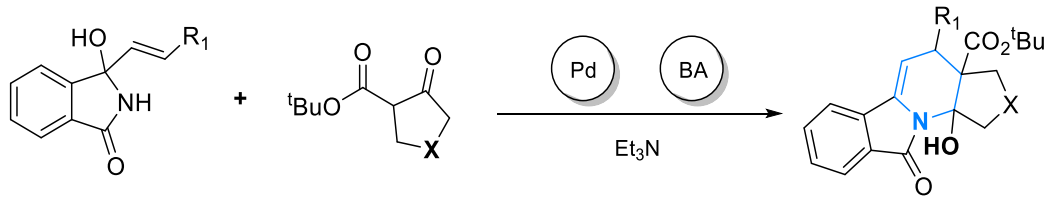

109 **110** *23 examples up to 87% yield* **111**

Scheme 19. Installation of a 6-membered nitrogen containing ring onto isoindolinone core

The literature demonstrates how calcium bistriflimide can be utilised to generate N-acyliminium ions. Calcium bistriflimide is derisible option for catalysis as its easily tuned, its low in cost and reaction by-products are innocuous. I want to generate N-acyliminium ions as they are highly electrophilic in nature and so have the potential to react as dienophiles in Diels-Alder reactions, currently this type of reactivity isn't heavily represented in the literature and so leaves a gap for this exploration. We know from the literature that isoindolinones are great N-acyliminium ion precursors so we can utilise isoindolinones as starting materials, not only this but isoindolinones are high interest in medicinal chemistry due to the reoccurrence of its structure in many bioactive compounds. The ability to develop a new methodology to functionalise its core is highly desirable to medicinal chemists.

2. Aims

This research aims to catalytically generate N-acyliminium ions, utilising the sustainable calcium bis triflimidate catalyst system previously developed by the McLaughlin group.[11] 3-Hydroxisoindolinones are isoindolinone derivatives that possess medicinal relevance and have been identified as excellent N-acyliminium precursors.[11, 12] We aim to use the electrophilic N-acyliminium ions as dienophiles in formal Aza-Diels-Alder reactions to install a 6-membered ring directly onto the isoindolinone core, with handles for further functionalisation *(Figure 14)*.

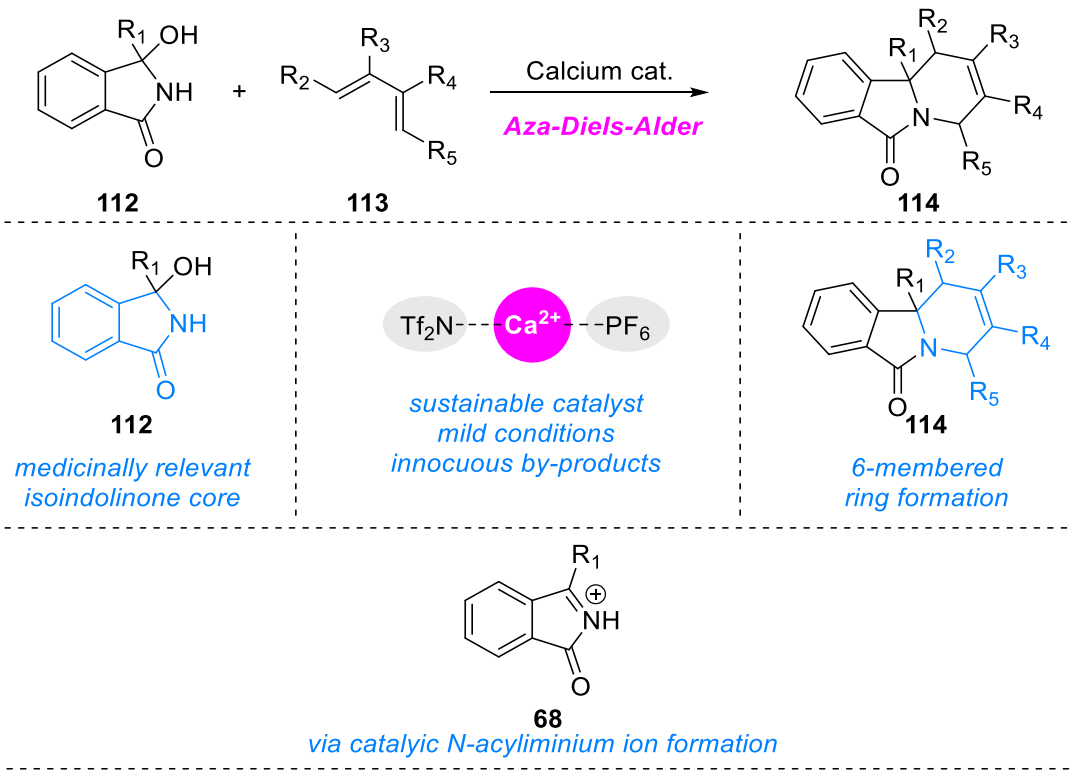

Figure 14. Project aims.

3. Results & Discussion

3.1. Preparation of starting material

3-Hydroxyisoindolinones **112**, N,O-acetals **115** and N-phenyl phthalimide **118** were prepared according to known literature procedures *(Scheme 20)*. [41-43] Synthesis of 3-hydroxyisoindolinones **112** was carried out using Grignard addition and/or halogen lithium exchange **92** to furnish a range of 3-substiuted 3-hydroxyisoindolinones **112** *(Scheme 20A & B)*. N,O-Acetals **115** were synthesised through the Grignard-mediated addition of an amide **60** to an aldehyde **59** followed by acid catalysed transacetalisation to synthesise hemiaminals **115** *(Scheme 20C)*. N-Phenyl phthalimides **118** was synthesised by the direct condensation of phthalic anhydride **116** and aniline **117** *(Scheme 20D)*.

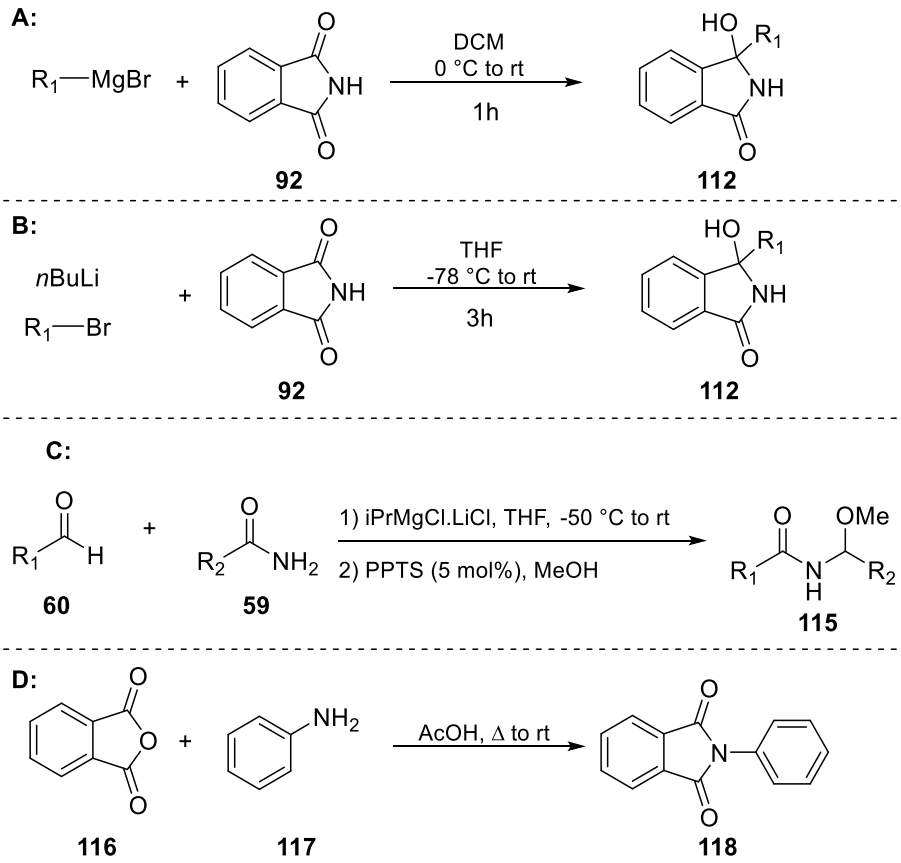

Scheme 20. Preparation of starting materials.

3-Hydroxyisoindolines **112** were synthesised as N-acyliminium precursors using halogen lithium exchange to produce a range of substrates in a moderate to good yield. These precursors were carefully chosen to assess the full range of electronics, sterics and Lewis basic properties of Diels-Alder reactions *(*

Table 3*)*. The substrate scope included the use of electron withdrawing groups **112a** as well as *ortho*, *meta* and *para* substitution patterns **112b** – **112d.** Lewis basic oxygen and nitrogen-containing heterocycles **112e – 112h** were synthesised in good yield. N-acyliminium precursors **112i** – **112n** when synthesised led to complex inseparable mixtures.

Table 3. 3-hydroxyisoindolinone substrate scope.

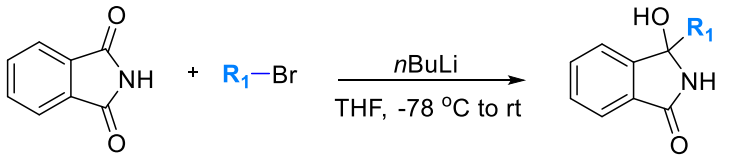

92 **112**

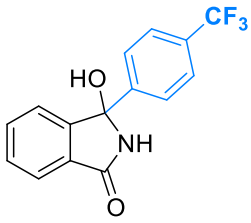

112a, 76%

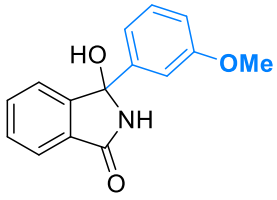

112b, 79%

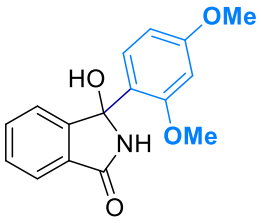

112c, 22%

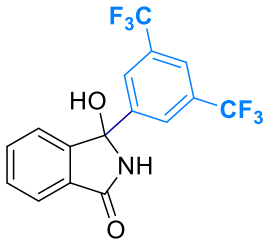

112d, 51%

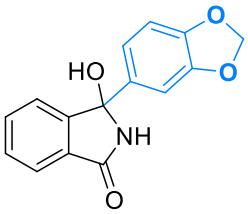

112e, 79%

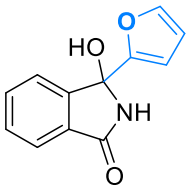

112f, 63%

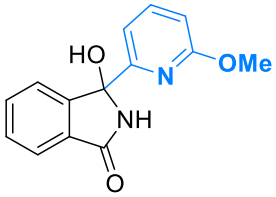

112g, 77%

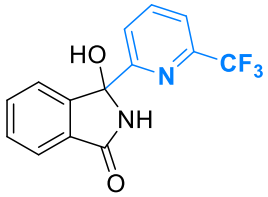

112h, 68%

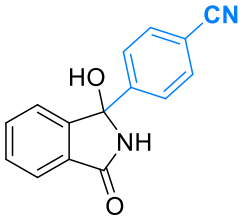

112i, 0%

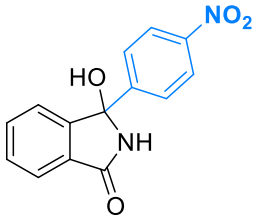

112j, 0%

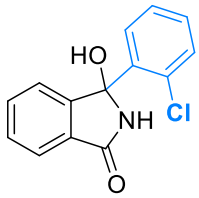

112k, 0%

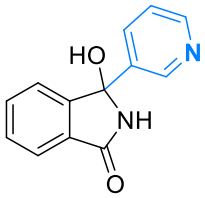

112l, 0%

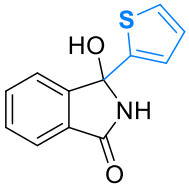

112m, 0%

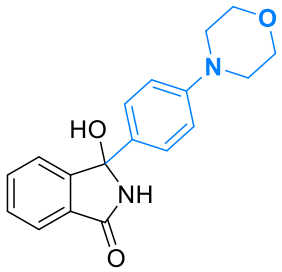

112n, 0%

3-Hydroxyisoindolines **112** were synthesised as N-acyliminium precursors using Grignard addition to produce a range of substrates in a moderate to good yield. The substrate scope included the electron donating group **112p**. Synthesis of **112q** led to a complex inseparable mixture *(Table 4)*.

Table 4. 3-hydroxyisoindolione substrate scope.

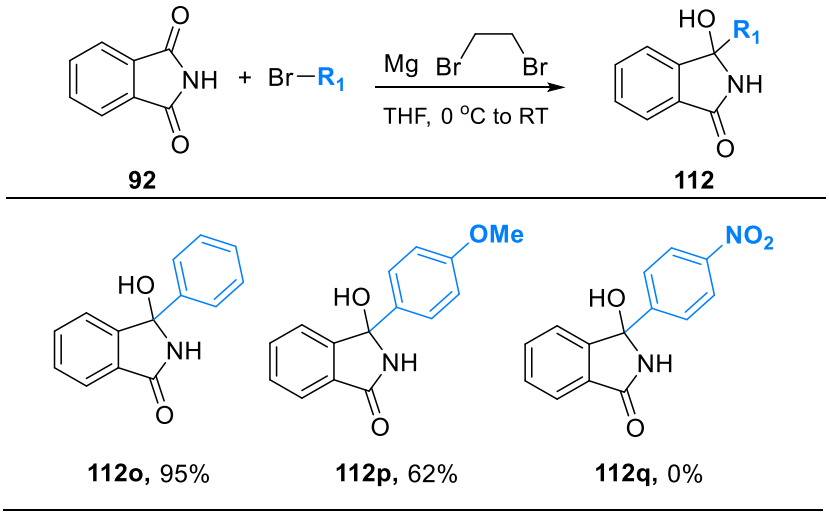

Preparation of N,O-Acetal **121** was synthesised by the grignard mediated addition of aldehyde **119** to amide **120** followed by the acid catalysed transacetalisation to form hemiacetal **121** in a good yield *(Scheme 21)*.

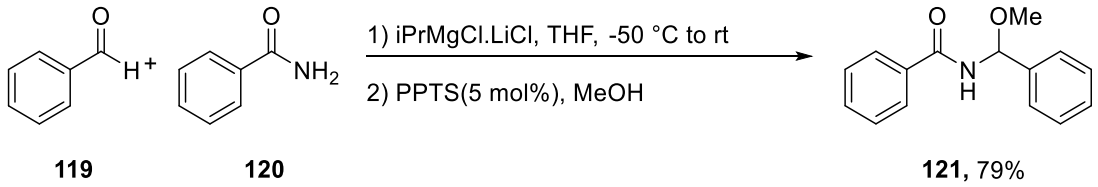

Scheme 21. Synthesis of N,O-acetal

The direct condensation of phthalic anhydride **116** and aniline **117** led to synthesis of N-phenyl phthalimide **118**in high yield *(Scheme 22)*.

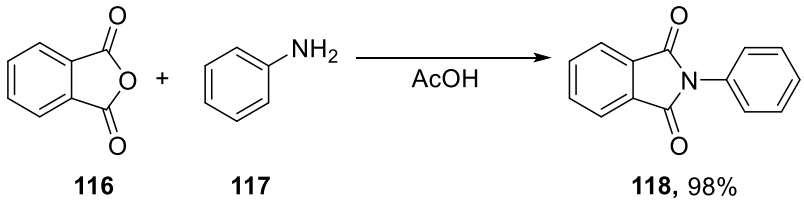

Scheme 22. Synthesis of N-phenyl phthalimide.

3.2. Isoindolinones

We first focussed our attention on isoindolinones as N-acyliminium ion precursors, for their use in Diels-Alder reactions as dienophiles.

3.2.1. Danishefsky's Diene

Previous work carried out in the McLaughlin group showed that when 3-hydroxyisoindolinones **112** are reacted with calcium bistriflimide they undergo dehydration to generate N-acyliminium ions **68**. [11, 12] We first identified Danishefsky's diene **122** as a suitable counterpart in the Diels-Alder reaction. Danishefsky prepared diene **122** in the 1980's to be a highly reactive nucleophile. He then tested diene **122's** nucleophilicity in Diels-Alder reaction with maleic anhydride and found the two compounds readily underwent [4+2] cycloadditions.[44]

Scheme 23 illustrates a plausible catalytic cycle for the reaction of diene **122** with 3-hydroxyisoindolinones **112** in the presence of catalytic calcium bistriflimide and tetra butyl-ammonium hexafluorophosphate. The loss of weakly coordinating anion $^{-}PF_6$ generates the active catalyst also generating N-acyliminium ion **68** through the loss of a hydroxyl group. Entrance of diene **122** to the catalytic cycle generates intermediate **123** which then cyclises to generate a hemiacetal intermediate **124** which can then re-enter the catalytic cycle to liberate the desired product **125** and by-products; methanol and trimethyl silanol.

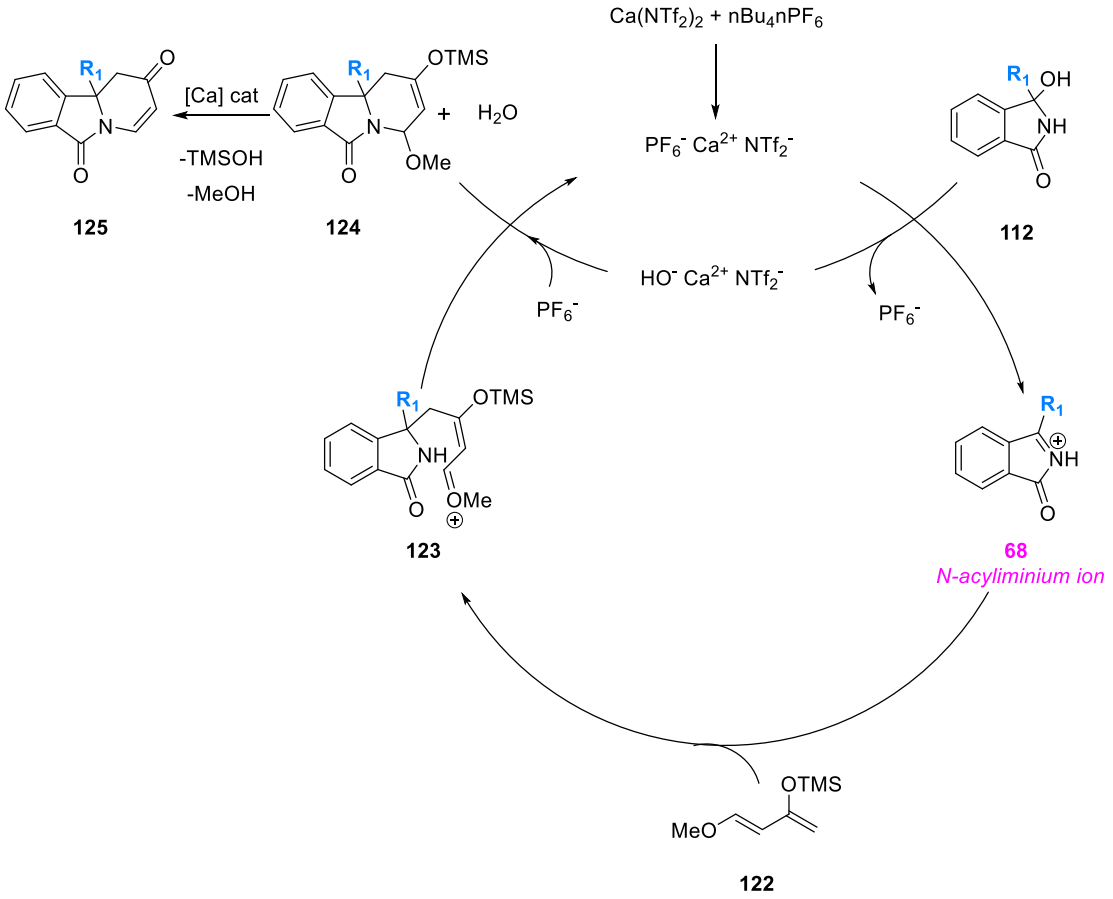

Scheme 23. Plausible reaction mechanism for the reaction of 3-hydroxyisindolinones and Danishefsky's diene.

Initial optimisation was conducted on 3-hydroxyisoindolinone **126** and Danishefsky's diene **122**. The reaction was first set up using 10 mol% of calcium bistriflimide in DCM at 40 °C with 1.20 equivalents of diene **122**. When the reaction was left to stir for 1 hour no consumption of starting material was observed *(Scheme 24)*.

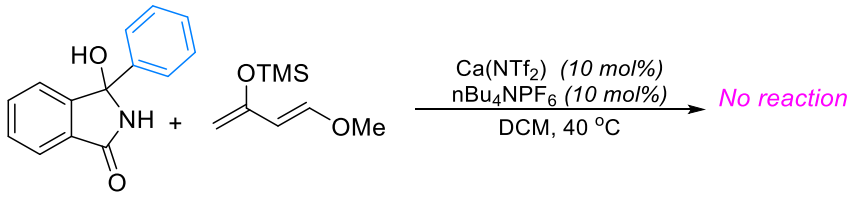

Scheme 24. Reaction of 3-hydroxyisoindolinone and Danishefsky's diene.

An optimisation study varying catalytic loading, solvent choice and temperature was carried out *(Table 5)*.

Attempted optimisation of the reaction was carried out beginning with a solvent screen of DCM, EtOAc, toluene, HFIP and DCE *(entries 1-5)* however all reactions led to rapid decomposition of starting material **126**. These results led to the conclusion that **126** was degrading quicker than the productive rate of reaction. To counteract this a temperature increase to 80 °C was implemented *(entry 6)* however degradation was still observed. A decrease in catalyst loading to 5 mol% and 1 mol% *(entries 8&9)* was carried out to test if catalyst loading was impacting the rate of degradation, however there was no change to previously observed results. The degradation of the 3-hydroxyisoindolinone **126** wasn't expected to be observed, as the literature reports on their high stability under similar conditions to those used throughout optimisation study 1.[11, 12]

Table 5. Optimisation study 1.

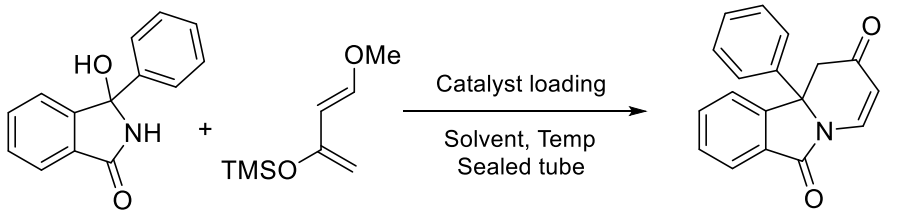

126 **122** **127**

Entry	Catalyst	Additive	Loading	Temp	Solvent	Time	Yield
1	$Ca(NTf_2)_2$	nBu_4NPF_6	10 mol%	40 ºC	DCM	1h	n.r
2	$Ca(NTf_2)_2$	nBu_4NPF_6	10 mol%	40 ºC	EtOAc	1h	Degradation
3	$Ca(NTf_2)_2$	nBu_4NPF_6	10 mol%	40 ºC	Toluene	1h	Degradation
4	$Ca(NTf_2)_2$	nBu_4NPF_6	10 mol%	40 ºC	HFIP	1h	Degradation
5	$Ca(NTf_2)_2$	nBu_4NPF_6	10 mol%	40 ºC	DCE	1h	Degradation
6	$Ca(NTf_2)_2$	nBu_4NPF_6	10 mol%	80 ºC	DCE	1h	Degradation
7	$Ca(NTf_2)_2$	nBu_4NPF_6	10 mol%	60 ºC	DCE	1h	Degradation
8	$Ca(NTf_2)_2$	nBu_4NPF_6	5 mol%	60 ºC	DCE	1h	Degradation
9	$Ca(NTf_2)_2$	nBu_4NPF_6	1 mol%	60 ºC	DCE	1h	Degradation

A control experiment *(Scheme 25)* was carried out reacting diene **122** and the catalyst system to see if any side reactions were taking place. Results from this control indicated the degradation observed in optimisation study 1 was caused by the reaction of diene **122** and calcium bis triflimide/tetrabutylammonium hexafluorophosphate.

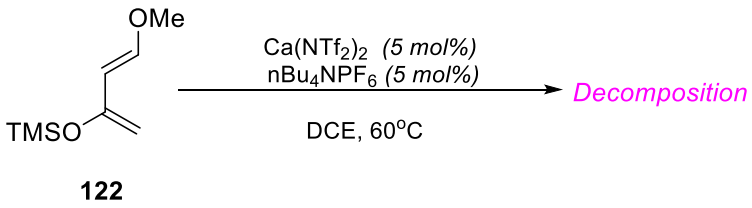

122

Scheme 25. Control experiments on Danishefsky's diene.

NMR confirmed the degradation of diene **115** caused by the catalyst system *(Figure 15)*. Further control experiments were run to attempt to minimise the levels of degradation observed *(Scheme 26)*.

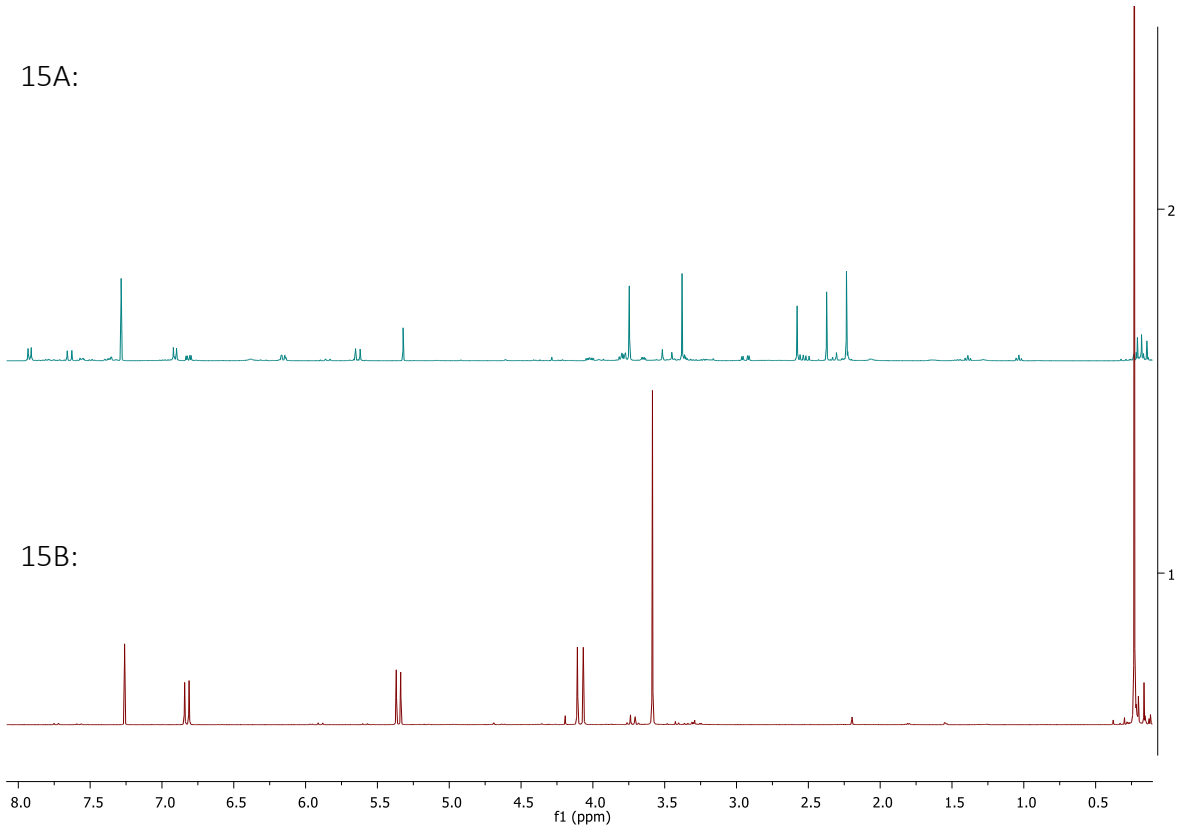

Figure 15. ^{1}H NMR collected in $CDCl_3$, (A) Danishefsky's diene reacted with $Ca(NTf_2)_2$ and nBu_4NPF_6 (B) Pure Danishefsky's diene.

Control experiment A was set up using $Ca(NTf_2)_2$ in the absence of nBu_4NPF_6, as we postulated that reactivity between diene **122** and the catalyst would be more controlled if the Lewis acidity was decreased, however decomposition was still observed. Control experiment B employed triethylamine to try and reduce the acidity, however degradation was still observed. Lastly, control experiment C added the catalyst to the reaction mixture

in a 0.1M solution in THF to dilute the reaction mixture, which also proved unsuccessful *(Scheme 26)*.

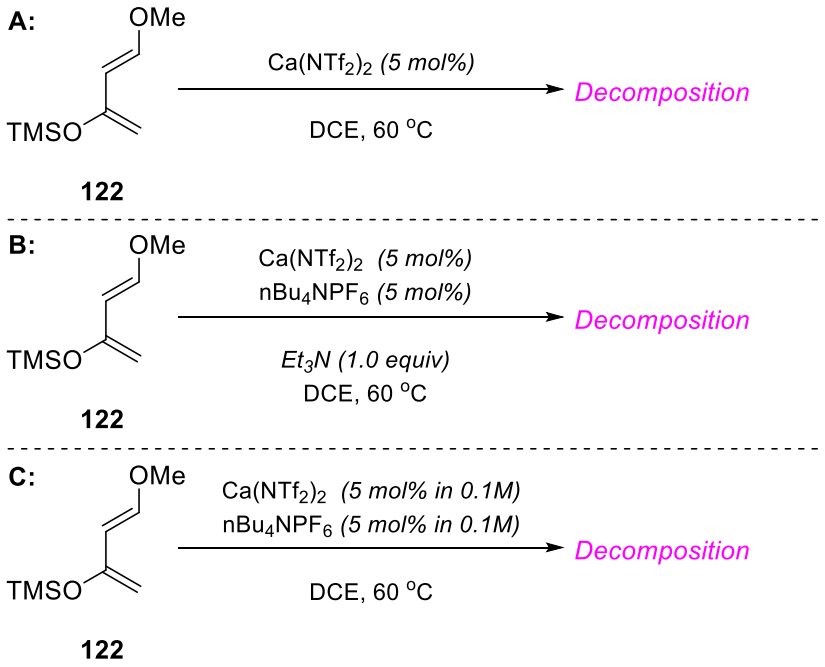

Scheme 26. Control experiments with Danishefsky's diene.

We concluded that oxygen-containing dienes wouldn't be suitable for the proposed reaction conditions, so moved our focus to the more traditional dimethyl-butadiene.

3.2.2. Optimisation of reaction conditions

After finding incompatibilities with oxygen containing dienes, we identified diene **129** to utilise in reaction optimisation. Dimethyl butadiene **129** readily undergoes Diels-Alder reactions, its effectiveness in cycloadditions is partly down to the *s-cis*-conformation which stabilises the reactivity *(Figure 16)*.[45] The stability of the *s-cis*-conformation is a result of steric impact of the methyl groups, which slows reactivity making it more controlled when in comparison to the *trans*-conformation.

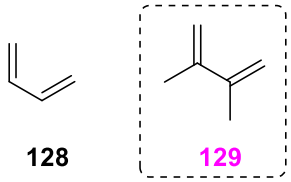

Figure 16. Structure of butadiene and dimethyl-butadiene.

Optimisation study 2 was carried out using diene **129** and 3-hydroxy-3-phenyl-isoindolin-1-one **126** *(Table 6)*. Our investigation began with a solvent screen *(entries 1-5)* which found DCE and EtOAc to furnish the highest yields of 82% and 81% respectively in 30 minutes. Decreasing the temperature from 65 °C to 40 °C led to no consumption of **126**, indicating the temperature needed to be at least 65 °C. Increasing the temperature to 80 °C *(entries 8-10)* had very little impact on yield. Decreasing catalyst loading to 5 mol% *(entry 11)* gave no impact on the yield. Increased equivalents of diene **129** from 1.20 to 1.50 *(entry 12)* saw the highest yield of 88%. 1 mol% of catalyst resulted in a large decrease in yield *(entry 13)* indicating that optimal catalyst loading is 5 mol%. Controls were run *(entries 15-17)* showing that the catalyst system required both $Ca(NTf_2)_2$ and nBu_4NPF_6 for reactivity. Optimised conditions for their reactivity were entry 12: DCE at 80 °C with 5 mol% catalyst and 1.5 equivalents of diene **129.** These conditions led to the full consumption of **126** and an isolated yield of 88% of the desired product **130**.

Table 6. Optimisation study 2.

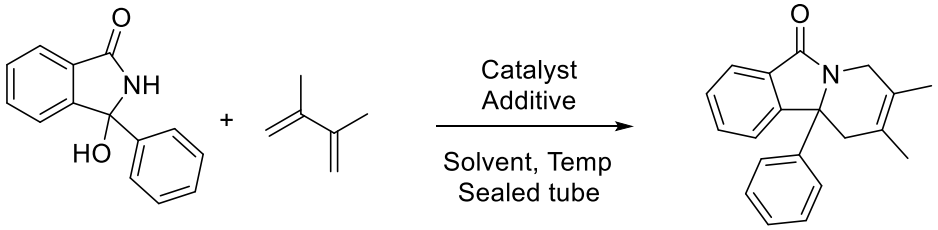

126 **129** **130**

Entry	Catalyst	Additive	Loading	Temp	Solvent	Time	Yield
1	$Ca(NTf_2)_2$	nBu_4NPF_6	10 mol%	65°C	DCM	30m	73 %
2	$Ca(NTf_2)_2$	nBu_4NPF_6	10 mol%	65°C	EtOAc	30m	81 %
3	$Ca(NTf_2)_2$	nBu_4NPF_6	10 mol%	65°C	DCE	30m	82 %
4	$Ca(NTf_2)_2$	nBu_4NPF_6	10 mol%	65°C	HFIP	30m	57 %
5	$Ca(NTf_2)_2$	nBu_4NPF_6	10 mol%	65°C	Toluene	30m	71 %
6	$Ca(NTf_2)_2$	nBu_4NPF_6	10 mol%	40ºC	DCM	30m	n.r
7	$Ca(NTf_2)_2$	nBu_4NPF_6	10 mol%	50°C	HFIP	60m	57 %
8	$Ca(NTf_2)_2$	nBu_4NPF_6	10 mol%	80°C	EtOAc	90m	70 %
9	$Ca(NTf_2)_2$	nBu_4NPF_6	10 mol%	80°C	DCE	90m	82 %
10	$Ca(NTf_2)_2$	nBu_4NPF_6	10 mol%	80°C	Toluene	90m	76 %
11	$Ca(NTf_2)_2$	nBu_4NPF_6	5 mol%	80°C	DCE	60m	82 %
12	**$Ca(NTf_2)_2$**	**nBu_4NPF_6**	**5 mol%**	**80°C**	**DCE**	**30m**	**88 %[a]**
13	$Ca(NTf_2)_2$	nBu_4NPF_6	1 mol%	80°C	DCE	90m	32 %
14	$Ca(NTf_2)_2$	nBu_4NPF_6	1 mol%	80°C	DCE	120m	74%[a]
15	$Ca(NTf_2)_2$	-	5 mol%	80°C	DCE	30m	n.r
16	-	nBu_4NPF_6	5 mol%	80°C	DCE	30m	n.r
17	-	-	-	80°C	DCE	30m	n.r

a - 1.5 eqivalents of diene

other entries use 1,2 equivalents of diene

Illustrated in Scheme 27 is a plausible mechanism for the formation of the Diels-Alder product **132** synthesised from the catalytically generated N-acyliminium ion. 3-Hydroxyisoindolinone **112** undergoes catalytic dehydration to generate N-acyliminium ion **68**, which then undergoes the formal Diels-Alder rection with diene **129** to generate intermediate **131.** Intermediate **131** is then deprotonated by the previously liberated hydroxyl anion to form a water by-product and desired product **123**.

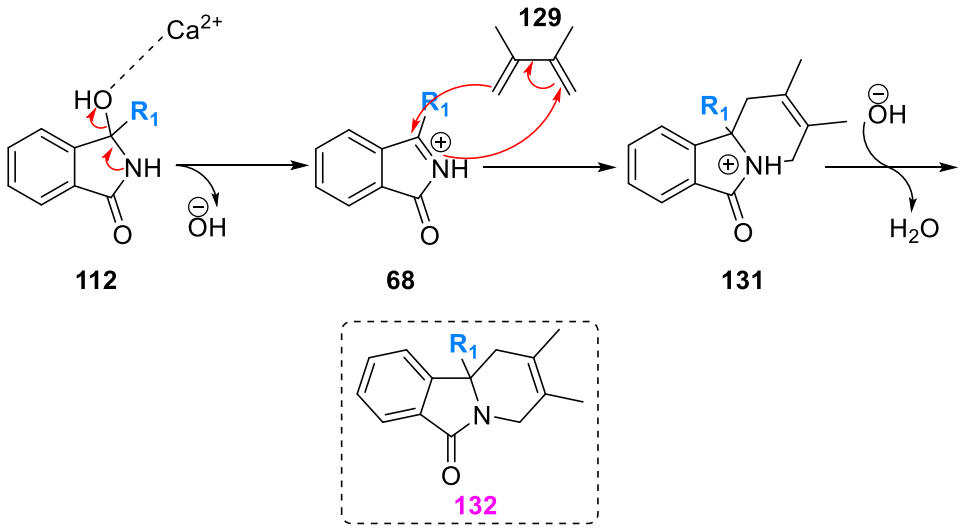

Scheme 27. Plausible mechanism of formal Diels-Alder reaction.

3.2.3. Substrate scope

The optimised conditions were used on a range of 3-hydroxyisoindolinones **112** to produce a substrate scope with varying electronic and steric properties. The substrate scope of the formal [4+2] cycloaddition was probed over 13 substrates *(Table 7)*. Electron donating groups **132b** and electron withdrawing groups **132c** worked well, providing the desired products in good to excellent yields. *Meta* **132d** and *ortho* **132e** substituents were also well tolerated in moderate to good yields. Heterocycles with Lewis basic atoms including oxygen **132f**, nitrogen **132g**-**132h** and sulfur **132i** furnished product in low to good yield. Lewis basic nitrogen yielded the biggest discrepancy of 60% and 35% from substrates **132g** and **132h** respectively. We postulated the difference in isolated yields could be explained by the fact that **132h** is more Lewis basic than **132g** due to the electron donating nature of the *ortho* methoxy substituent. Substrates **132j** – **132l** resulted in complex inseparable mixtures, even when the optimised conditions were altered slightly. We suspect that when there is alkyl substitution **132l** at the 3 position we can observe an

elimination reaction which quenches the N-acyliminium ion, this is described further in Scheme 28. **132m** was synthesised in trace amounts, however rapid decomposition of the product occurred.

Table 7. Substrate scope of [4+2] cycloaddition of 3-hydroxyisoindolinones and 2,4-dimethyl-2,3-butadiene.

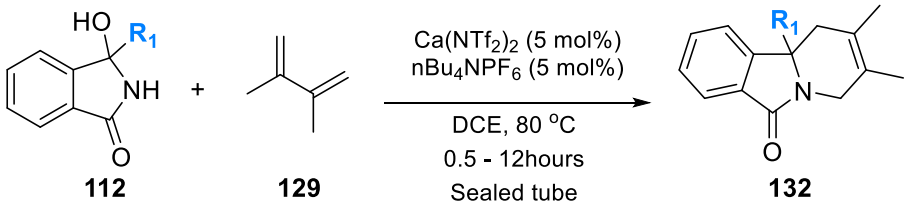

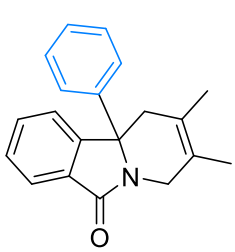

132a, 88%

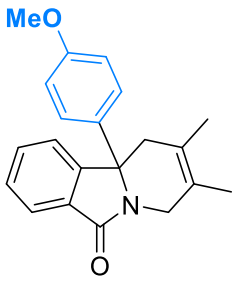

132b, 79%

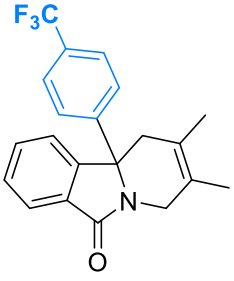

132c, 66%[a]

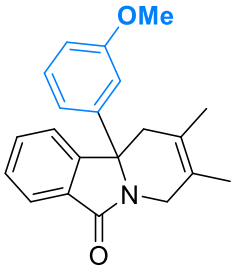

132d, 75%

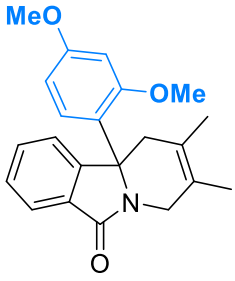

132e, 60%

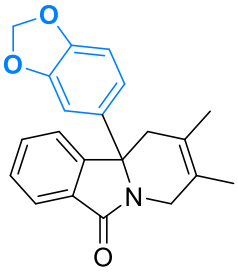

132f, 67%

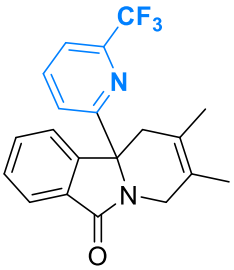

132g, 60%

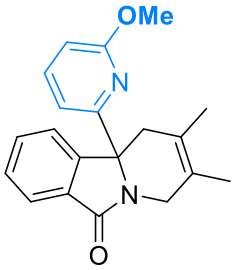

132h, 35%[b]

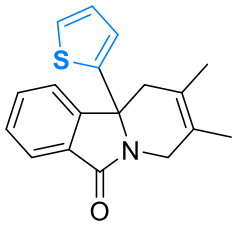

132i, 56%

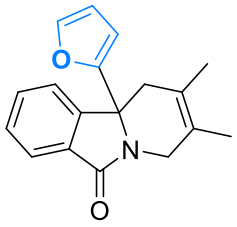

132j, 0%

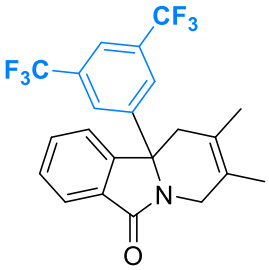

132k, 0%

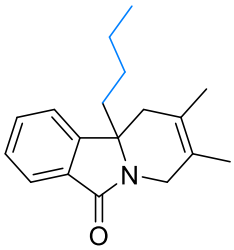

132l, 0%

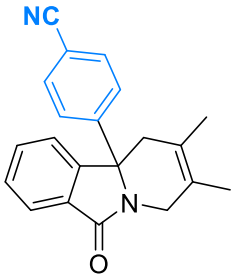

132m, 0%

a = 100°C
b = 10mol%

When 3-hydroxyisoindolinoes with alkyl substitution **133** at the 3 position are stirred with calcium bistriflimide the generated N-acyliminium ion **135** undergoes an elimination

reaction to quench the nitrogen positive charge and liberate product **134**. This elimination occurs because it is more facile than the reaction of the N-acyliminium ion *(Scheme 28)*.

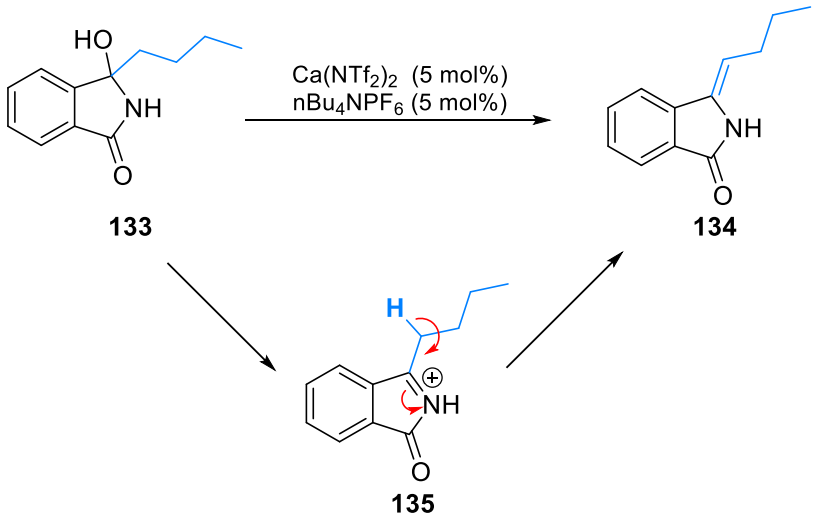

Scheme 28. Elimination of alkyl chain with $Ca(NTf_2)_2$.

3.3. Scope of dienes

After successes with dimethyl-butadiene **129**, we wanted to probe the scope of dienes further to see how the 4π component affected the reactivity of Aza-Diels-Alder reactions with N-acyliminium ion dienophiles.

We identified 3 structural isomers of 1,3-dienes which we wanted to subject to our optimised reaction conditions; linear dienes **136**, 2,4-substituted dienes **137** and asymmetric dienes **138** *(Figure 17)*.

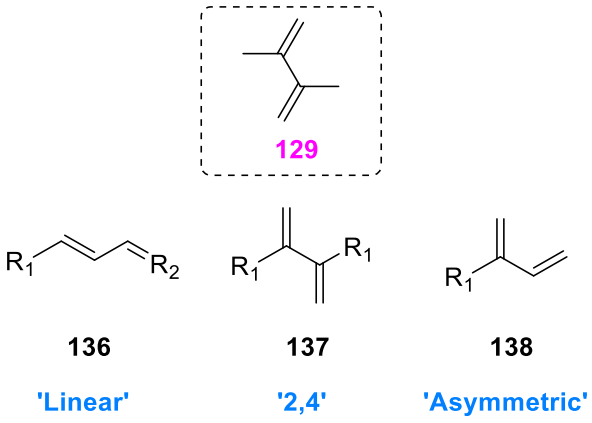

Figure 17. Structures of 1,3 dienes.

3.3.1. Linear dienes

We first prepared a range of linear dienes to employ according to procedures from the literature which utilise the Wittig reaction *(Scheme 29)*.[37]

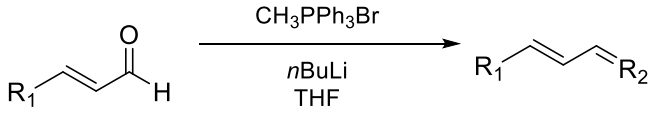

139 **136**

Scheme 29. Synthesis of 'linear' 1,3-dienes.

Dienes **136a** – **136d** were synthesised in low yields using a Wittig reaction on α, β-unsaturated aldehydes **139** to install a terminal olefin bond. The scope included electron donating group **136b**, electron withdrawing group **136c** and tertiary amine **136d** *(Table 8)*.

Table 8. Substrate scope of 4-substituted 1,3-dienes.

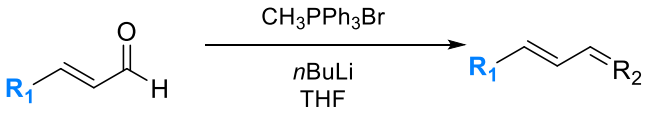

139 **136**

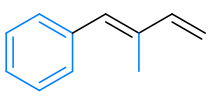

136a, 20%

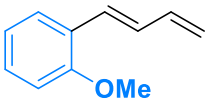

136b, 36%

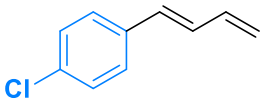

136c, trace

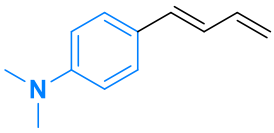

136d, trace

We then carried out a substrate scope of the dienes which we synthesised in Table 8, using our optimised conditions. The substrates included varying electronic and sterics *(Table 9)*

All substrates led to complex inseparable mixtures. Halide **141b**, *ortho* substitution **141c**, tertiary amine **141d** and sterically hindered diene **141e** all had the same effect and were not tolerated. We concluded the use of linear dienes **136** was unsuccessful due to the positioning of the olefin bonds not being terminal.

Table 9. substrate scope of linear 1,3-dienes.

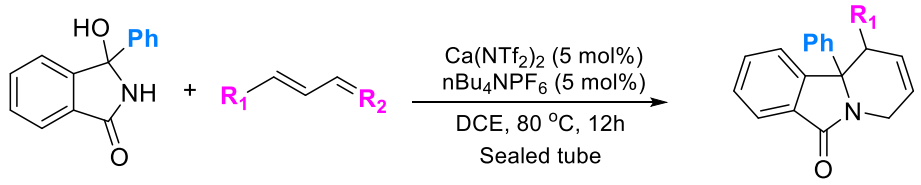

140 **136** **141**

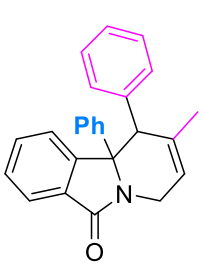

141a, 0%

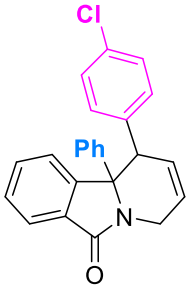

141b, 0%

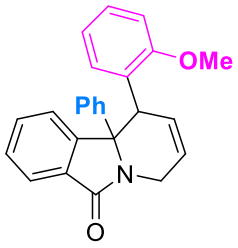

141c, 0%

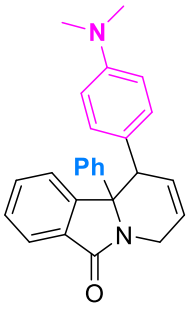

141d, 0%

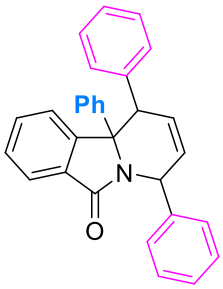

141e, 0%

3.3.2. 2,4-substituted dienes

After no success with 'linear' 1,3-dienes we moved our attention to synthesising a range of 2,4-substituted 1,3-dienes *(Figure 18)*. We predicted that reactivity of dimethyl diene **129** and diphenyl diene **142** would be the same as structurally they are very similar.

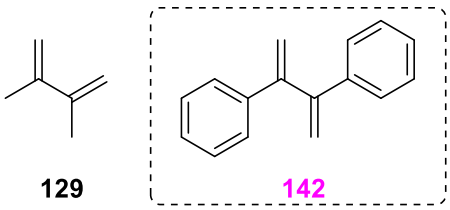

Figure 18. Dimethyl diene and diphenyl diene.

We prepared a range of 2,4-substituted dienes from a known procedure in the literature, employing a double Wittig reaction on di-ketones **143** to synthesise the 2,4-substituted dienes **137** *(Scheme 30)*.[37]

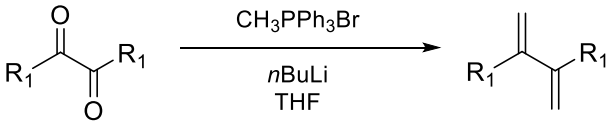

143 **137**

Scheme 30. Synthesis of 2,4-substituted 1,3-dienes.

Dienes **137a** – **137c** were synthesised in low yields from benzil and benzil derivatives using a double Wittig reaction. The substrate scope included electron donating groups **137b** and electron withdrawing groups **137c**, as we wanted to explore the effects of electron-deficient and electron rich-dienes on reactivity *(Table 10)*.

Table 10. Substrate scope of 2,4-substituted 1,3-dienes.

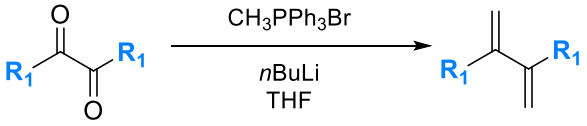

143 **137**

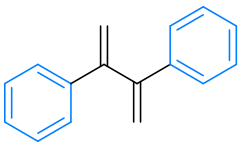	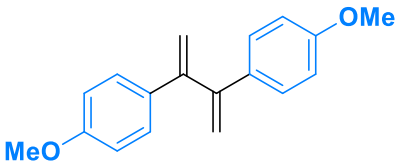	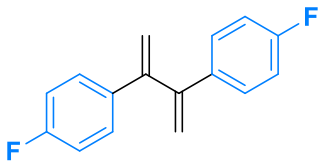
137a, 31%	**137b**, 24%	**137c**, 28%

We postulated that diphenyl diene **142** and 3-hydroxyisoindolinone **140** would undergo a formal [4+2] cycloaddition to form product **144** *(Scheme 31)* through the same mechanism shown in Scheme 27 when the optimised conditions were used.

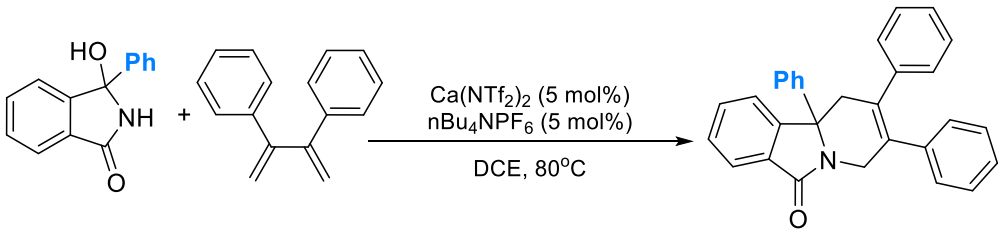

140 **142** **144**

Scheme 31. Proposed reactivity of diphenyl diene with 3,3-hydroxy-phenyl isoindolinone.

TLC analysis showed full consumption of the starting material and the formation of 2 products, in under 1 hour. NMR characterisation led to the assignment of structure **144** and **145** *(Scheme 32).*

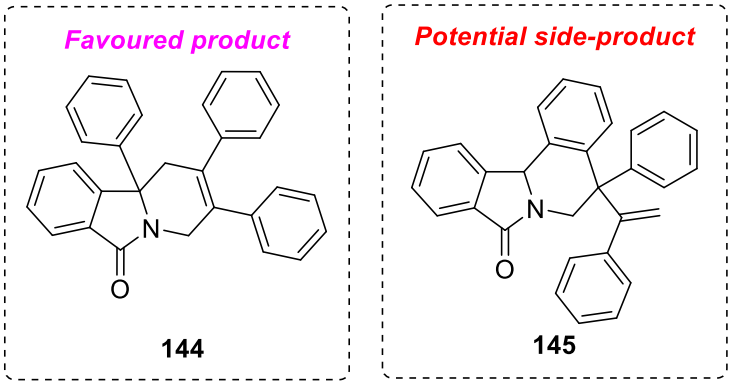

Scheme 32. Products of formal Diels-Alder with diphenyl diene.

We hypothesised that side-product **145** was the product of the inverse electron demand [4+2] reaction occurring simultaneously alongside the traditional [4+2] cycloaddition. We know N-acyliminium ions have the capability of reacting as both dienophiles and dienes. We knew that the formation of **144** would occur through the formal [4+2] previously observed. However, product **145** we postulated that N-acyliminium ion **146** reacted as a diene through the phenyl substituent at the 3 position and then underwent an inverse electron demand Diels-Alder with diphenyl diene **142** to generate intermediate **147** *(Scheme 33)*. Intermediate **147** will then be susceptible to deprotonation likely by the previously liberated hydroxyl anion to liberate a water by-product and intermediate **148**. Re-aromatisation of intermediate **148** will furnish the inverse electron demand product **145**.

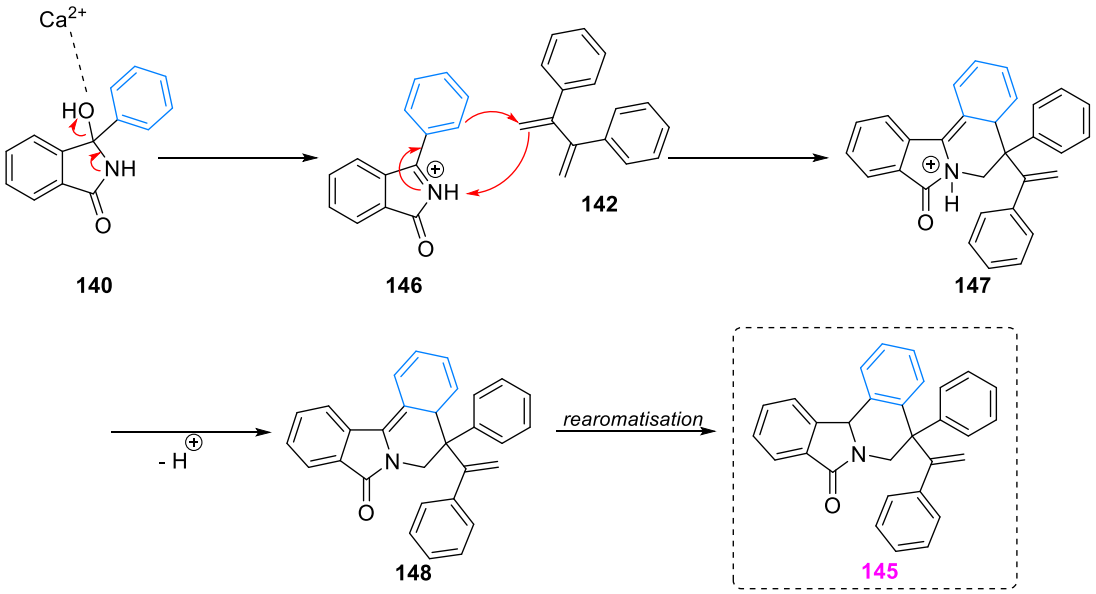

Scheme 33. Plausible mechanism for the inverse electron demand Diels-Alder of diphenyl diene and 3-hydroxyisoindolinone

The occurrence of the inverse [4+2] indicated that diphenyl diene **142** wasn't reactive enough as a diene to out compete its reactivity as a dienophile. To selectively have control over which reaction occurred we altered the electronics of the 3-hydroisoindolinones **149** *(Scheme 34)*.

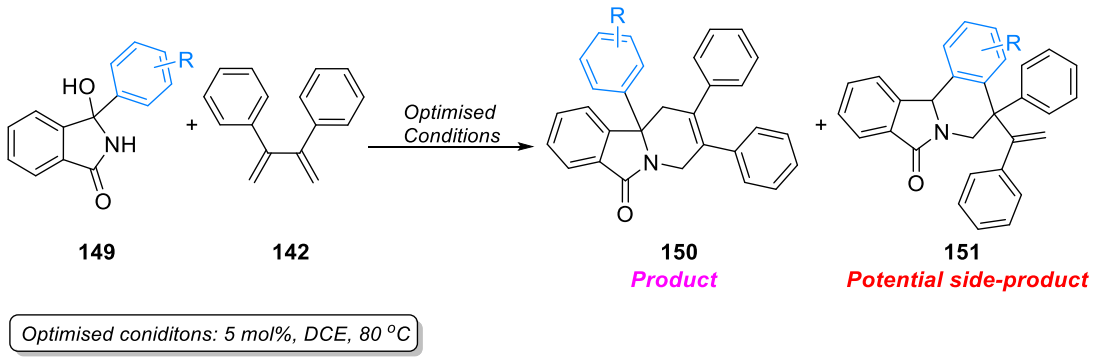

Scheme 34. Simultaneous Diel-Alder and inverse electron demand Diels-Alder.

By altering the electronics of 3-hydroxyisoindolinone **140** *(Figure 19)* to contain an electron donating/ withdrawing group we hoped to manipulate the reaction pathway. We predicted that electron-withdrawing isoindolinone **153** would result in a more electron deficient N-acyliminium bond, forcing diphenyl diene **142** to react as a diene, favouring the Diels-Alder pathway and its respective product. Electron donating isoindolinones **152** would have the opposite effect and favour the inverse electron demand Diels-Alder pathway.

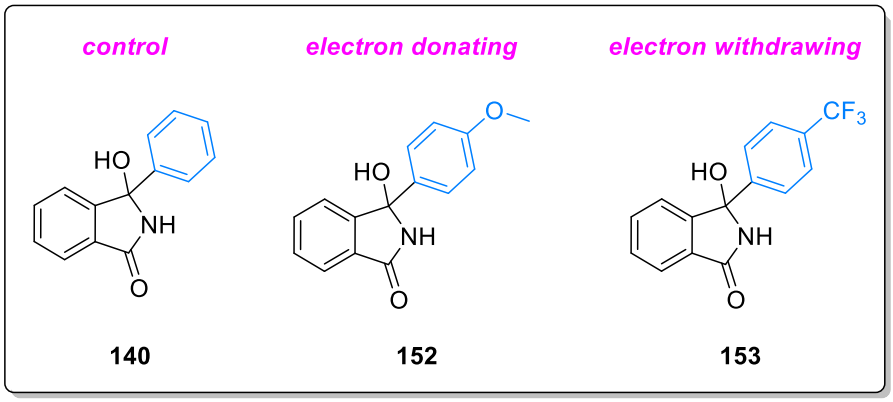

Figure 19. 3-substituted, 3-hydroxyisoindolinones for electronic probing.

The experimental studies found that the electronics of the 3-hydroxyisoindolinones had no major effect on the ratio of products *(Table 11)*. We concluded that the reaction pathway must therefore be entirely controlled by the electronics of the diene.

Table 11. Electronics study on 3-hydroxyisoindolinones.

R Group	Yield		Ratio (P:BP)
	Product	By-product	
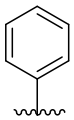	*32%*	*57%*	*0.56 : 1*
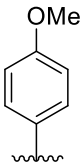 OMe	*20%*	*15%*	*1 : 0.73*
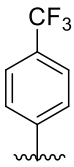 CF_3	23%	38%	*0.61 : 1*

After these results, we focused our attention on altering the electronics of diphenyl diene **142**, employing electron donating diene **154** and electron withdrawing diene **155** to probe the reactivity. We predicted that diene **154** would favour the Diels-Alder pathway and diene **155** would favour the inverse electron demand pathway. As we knew the electronics of the 3-hydroxyisoindolinones made no difference to reaction outcome, we used 3-phenyl 3-hydroxyisoindolinone **140** as the starting material *(Figure 20)*.

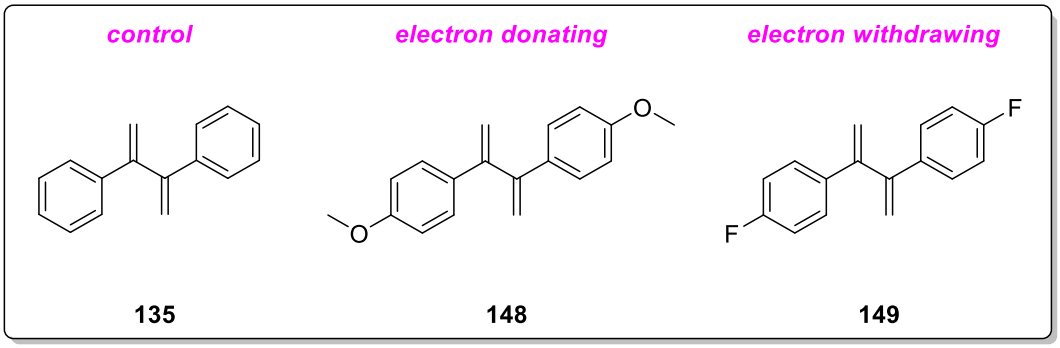

Figure 20. 4,4-substituted diphenyl dienes for electronic probing.

Results shown in Table 12 were not as predicted. We expected the electron withdrawing diene **155** to favour the inverse electron demand Diels-Alder, the results obtained did not support this *(2:1 ratio favouring the DA)*. We then queried the original structural assignment of side-product **145** and to obtain confirmation we used X-ray crystallography.

Table 12. Electronic study on diphenyl dienes.

Diene	Yield		Ratio *(P:BP)*
	Product	By-product	
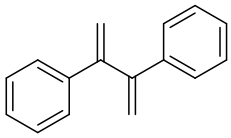 **142**	*32%*	*57%*	*0.57 : 1*
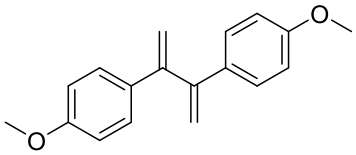 **154**	*88%*	*8.7%*	*10 : 1*
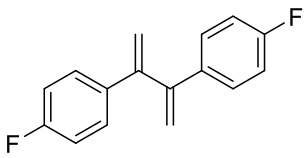 **155**	50%[a]	24%[a]	*2 : 1*

[a] - NMR yield.

Results from the X-ray crystallography disproved the original assignment *(Figure 22)*.

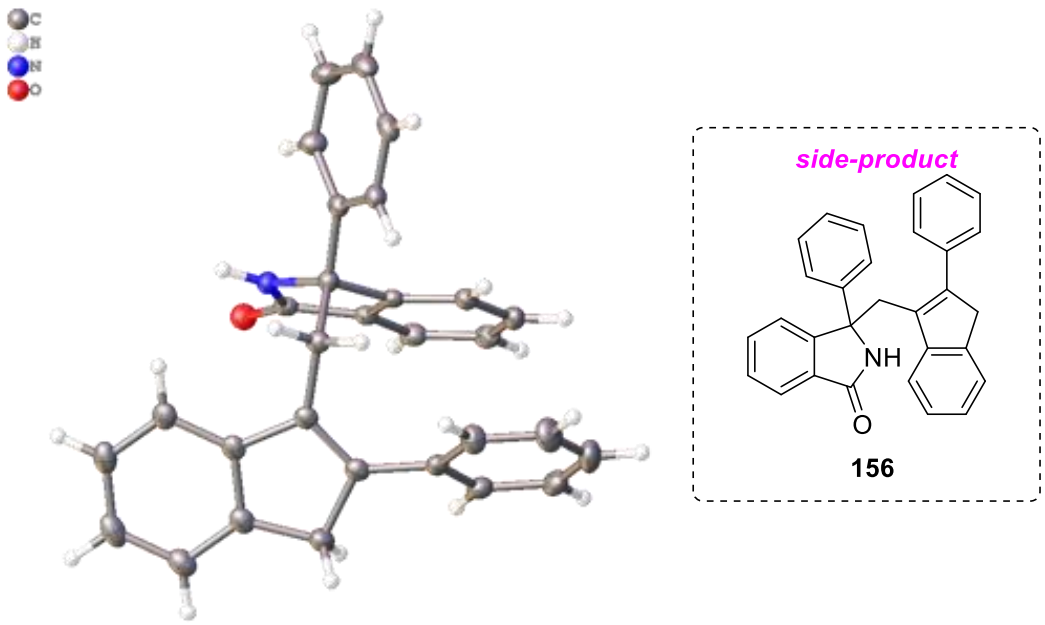

Figure 21. Crystal structure of side-product, 156.

After disproving structure **145**, we gathered data from the electronic studies and drew some conclusions on the formation of the indene by-product **156**. Electronics appeared to have an effect on the formation of by-product **156**, as electron donating groups majorly reduced the formation of the side-product **156** *(Figure 22)*.

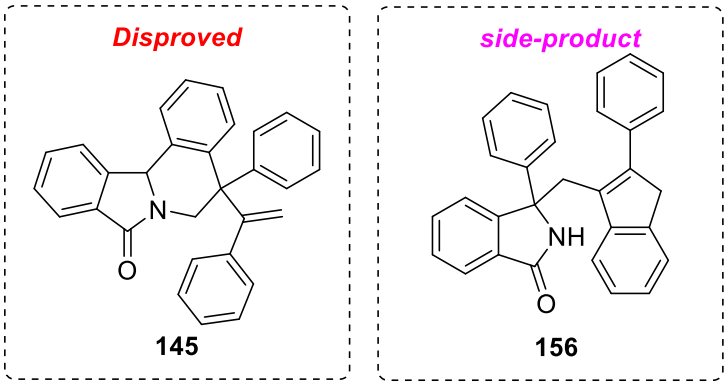

Figure 22. Structure of indene by-product, 156.

Illustrated below in Scheme 35 describes a plausible mechanism for the formation of the indene side-product **156**. 3-Hydroxyisoindoline **140** undergoes catalytic dehydration to form N-acyliminium ion **146**, which then accepts electrons from diene **157** to quench the nitrogen positive charge. This generates tertiary carbocation intermediate **158**, which cyclises to install the 5-membered ring shown in intermediate **159** and a new tertiary carbocation, which undergoes re-aromatisation to generate the indene by-product, **160**.

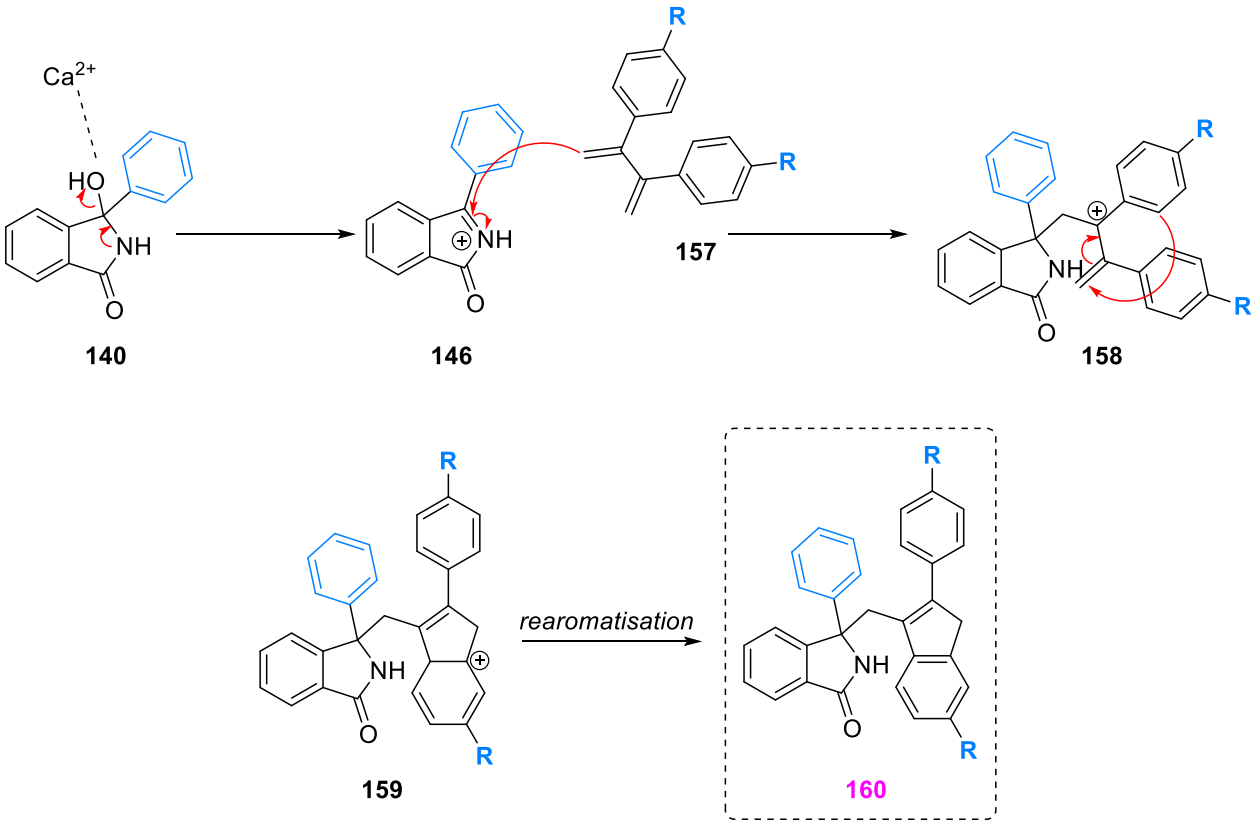

Scheme 35. Plausible mechanism for the formation of indene by-product, 160.

Diels-Alder products **161.1** were synthesised from a range of 3-hydroxyisoindoliones **112** and dienes **157** in low to good yield *(Table 13)*. The substrate scope included electron donating **161.1b** and electron withdrawing **161.1c** resulting in low yields. The use of electron rich dienes **161.1d** – **161.1h** and electron withdrawing diene **161.1i** resulted in the preferential formation of the Diels-Alder product in increased yields. The reaction was tolerated by oxygen **161.1g** and nitrogen **161.1h** heterocycles too.

When reacting 3-hydroxyisoindolinones **112** with diphenyl diene **157** we also observed the formation of an indene side-product **161.2** in moderate to low yields *(Table 13)*. Substrate scope included electron donating **161.2b** and electron withdrawing **161.2c** groups, furnishing a low to moderate amount of product. The use of an electron-rich **161.2d** and electron-deficient diene **161.2i** resulted in a decreased yield. Products **161.2f** - **161.2g** were synthesised in trace amounts, however rapid decomposition of the product occurred. The side-product formation can be minimised through the electronic properties of the diene. When dienes that are electronically 'neutral' are used, a mixture of products results; to minimise this ratio electron donating groups on the diene should be present.

Table 13. Substrate scope of Diels-Alder products.

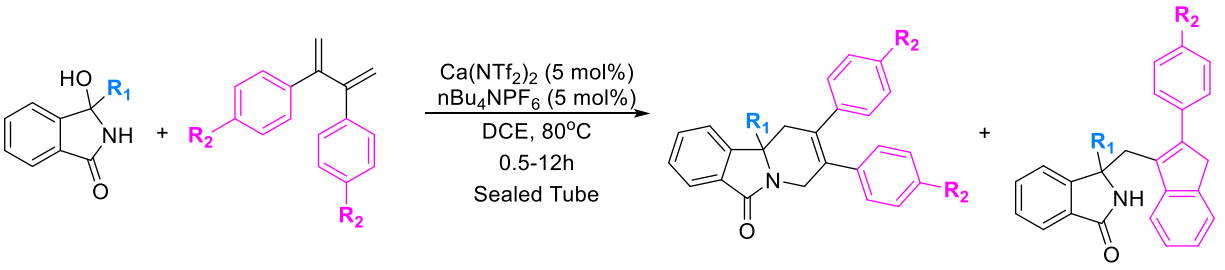

112	157		161.1	161.2

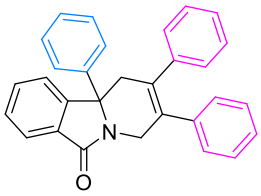	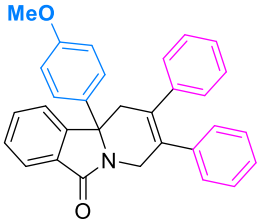	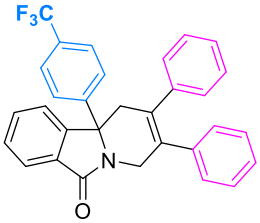
161.1a 32% **161.2a** 57%	**161.1b** 20% **161.2b** 15%	**161.1c** 23% **161.2c** 38%
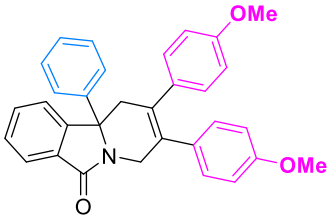	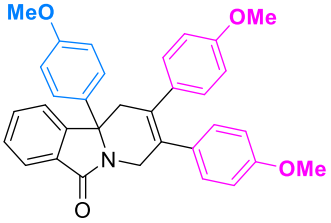	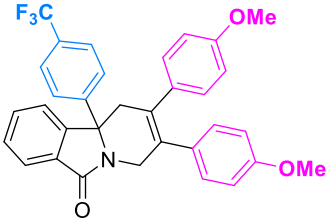
161.1d 88% **161.2d** 8.7%	**161.1e** 88% **161.2e** 0%	**161.1f** 22% **161.2f** 0%
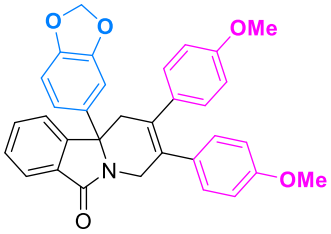	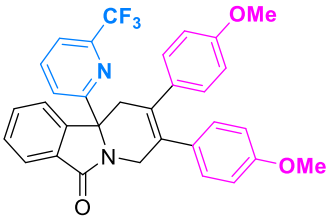	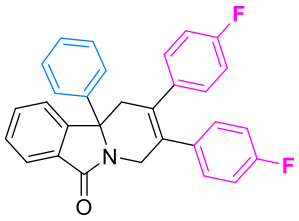
161.1g 74% **161.2g** 0%	**161.1h** 65% **161.2h** 0%	**161.1i** *50%*[a] **161.2i** *24%*[a]

[a] - NMR yield.

We were unable to separate **161.1i** and its structural isomer **161.2i** so we utilised NMR to calculate yields for each, this can be seen in Figure 23 and Table 14.

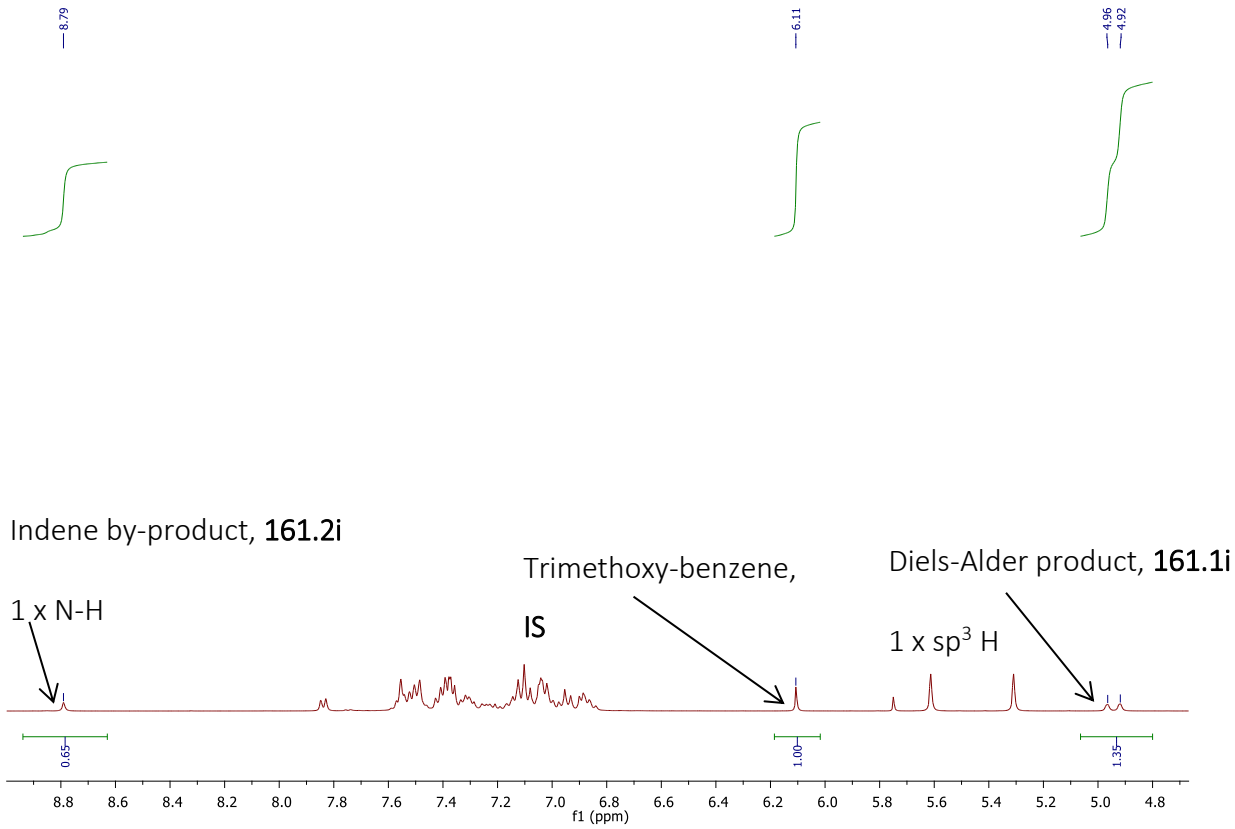

Figure 23. ^{1}H NMR in DMSO for yields of substrates 161.1i and 161.2i

We used trimethoxy-benzene as the internal standard for the NMR yield calculations, we were able to pick out the peaks which we knew corresponded to each product, so a free NH in the indene, **161.2i** and a sp^3 proton in the Diels-Alder **161.1i**.

Table 14. NMR yield calculations.

Diels-Alder product, **161.1i**	Indene by-product, **161.2i**
$n_A = n_{IS} \times r_{A/IS}$ n_{IS} =0.02735*mmol* $r_{A/IS}$ = (1.35/1) / (1/3) = 4.05 n_A = 4.05 X 0.02735 = 0.1108*mmol* 0.222*mmol* in 0.9mL of DMSO **NMR Yield = 50%**	$n_A = n_{IS} \times r_{A/IS}$ n_{IS} =0.02735*mmol* $r_{A/IS}$ = (0.65/1) / (1/3) = 1.95 n_A = 1.95 X 0.02735 = 0.0533*mmol* 0.222*mmol* in 0.9mL of DMSO **NMR Yield = 24%**

To conclude, we observed that the inclusion of electron-donating and electron-withdrawing groups on 3-hydroxyisoindolinones **112** do not influence the formation of either product, as seen in the cases of **161.1a** – **161.1c** & **161.2a** – **161.2c.** However, if an electron rich diene is used we see the preferential formation of the Diels-Alder product over the indene by-product and this effect is also observed with electron withdrawing

dienes but to a less extent. To minimise the formation of the side-product, electron-rich dienes should be chosen.

3.3.3. Unsymmetrical dienes

Finally, we then wanted to explore the reactivity of unsymmetrical dienes when exposed to our reaction conditions. We prepared unsymmetrical dienes following a known procedure from the literature. [38] Dienes **138** were synthesised using the Kumada cross coupling of an enol phosphate **163** and vinyl Grignard reagent *(Scheme 36)*.

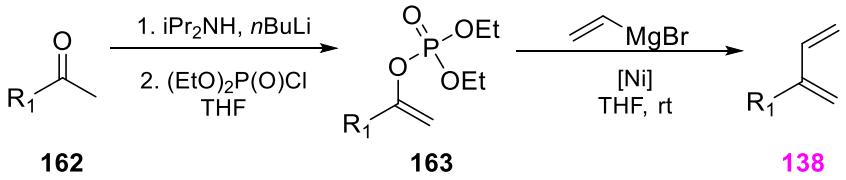

162 **163** **138**

Scheme 36. Preparation of unsymmetrical 1,3-dienes.

The Kumada coupling catalytic cycle is initiated by the oxidative addition of Ni*(0)* into the enol phosphate **163** which generates Ni*(II)* species **164.** The addition of the vinyl Grignard reagent to the reaction begins the transmetalation of magnesium and nickel to liberate magnesium-phosphate salt **138** and Ni*(II)* species **165.** Finally, this Ni*(II)* species undergoes *trans-cis* isomerisation which another Ni*(II)* species **166**, this species then undergoes reductive elimination to liberate the unsymmetrical diene **138** and reform the Ni*(0) (Scheme 37)*.

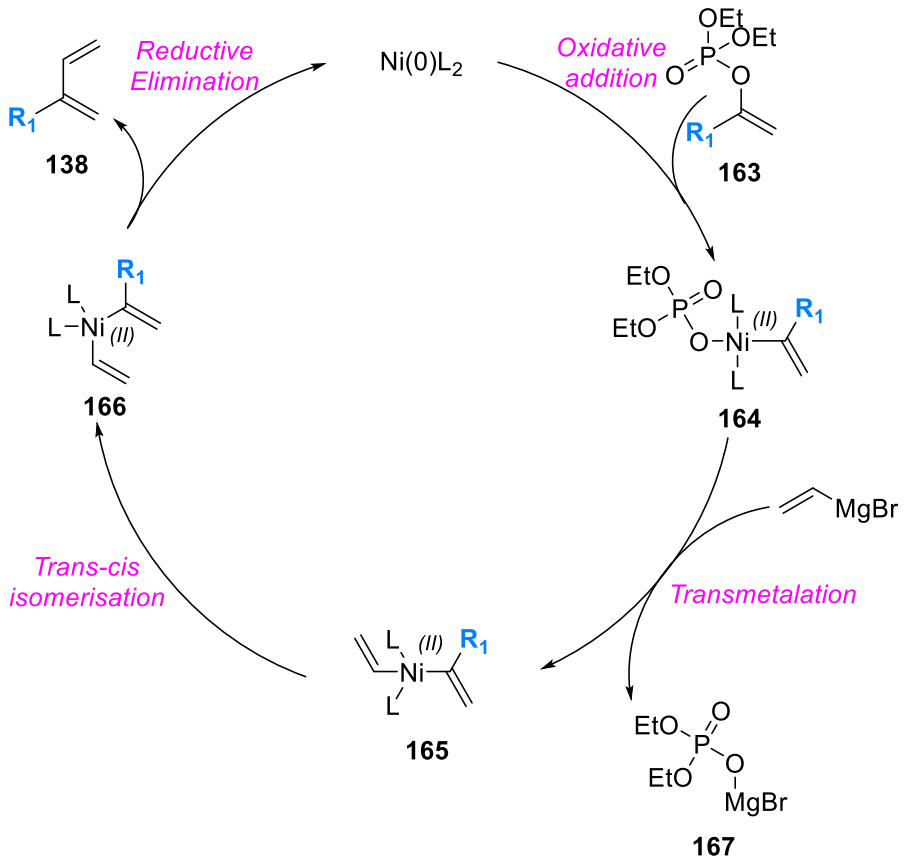

Scheme 37. Kumada cross coupling catalytic cycle.

Unsymmetrical dienes **138a** was synthesised in moderate yield, whereas unsymmetrical dienes **138b & 138c** were not synthesised. A Kumada cross coupling of vinyl Grignard reagent and enol phosphate **163** *(Table 15)*. Aromatic substrate **138a** was synthesised in moderate yield. Cyclic alkyl diene **138b** synthesis was unsuccessful as its enol phosphate precursor wasn't synthesised. Heterocyclic diene **138c** synthesis was also unsuccessful, as the Kumada coupling led to a complex inseparable mixture.

Table 15. Substrate scope of unsymmetrical 1,3-diene.

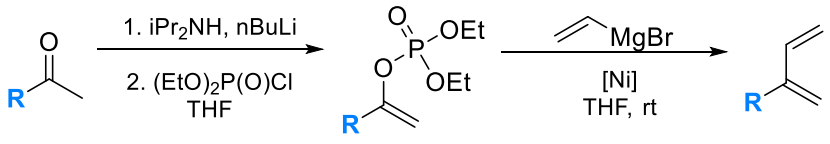

162 **163** **138**

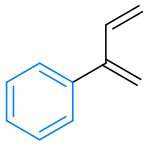	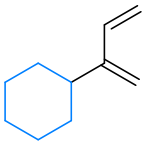	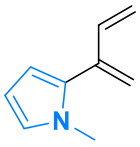
138a, 58%	**138b,** 0%	**138c,** 0%

The substrate scope of the formal [4+2] cycloaddition was probed over 7 substrates *(Table 16)*. Electron donating group **169b** worked well whereas electron withdrawing group **169c** saw a large decrease in yield. Para-halo substrate **169d** was also well tolerated. Meta substitution **169e** worked well. Heterocycles with Lewis basic atoms including nitrogen **169g**-**169h**, oxygen **169f** and sulfur **169f** were also tolerated in low to good yield. Substrate **169j** was synthesised in trace yield but then decomposition was observed.

Table 16. Diels-Alder reactions of 3-hydroxyisoindolinones and unsymmetrical dienes.

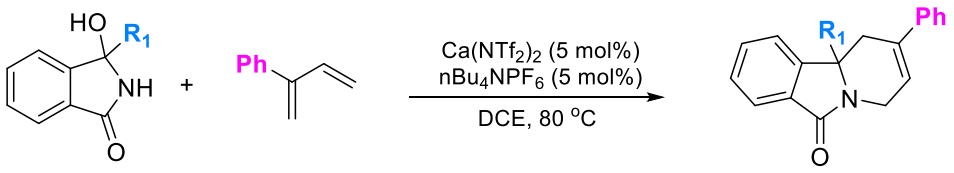

112 **168** **169**

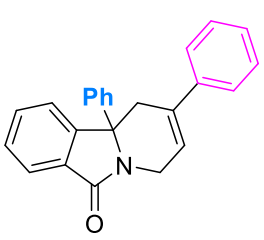

169a, 97%

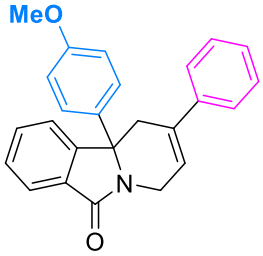

169b, 87%

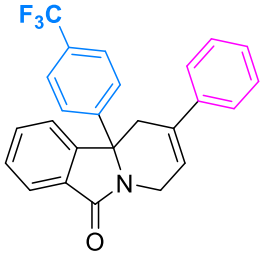

169c, 35%

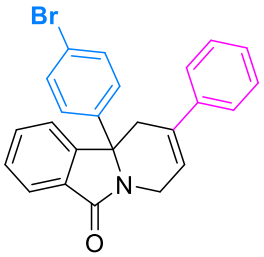

169d, 72%

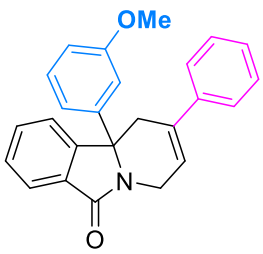

169e, 69%

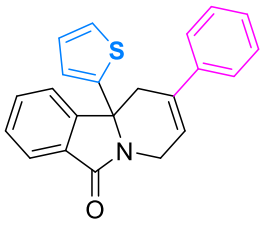

169f, 45%

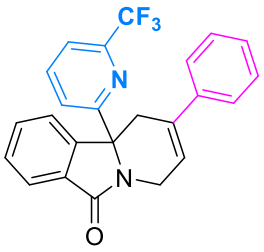

169g, 89%

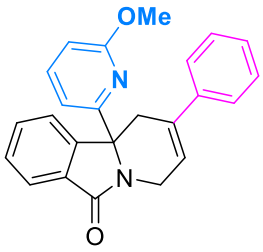

169h, 23%

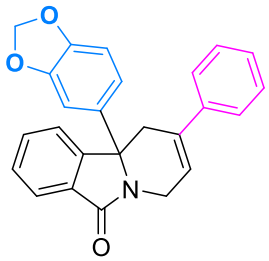

169i, 69%

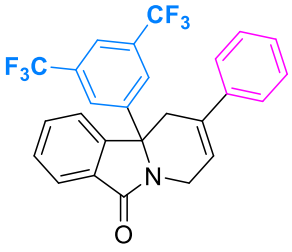

169j, 0%

Ongoing work in the McLaughlin group resulted in the production of diene **170**, which was subjected to the Aza-Diels-Alder reaction under the optimised conditions *(Scheme 38)*. When 3-hydroxyisoindolinone **126** and unsymmetrical diene **170** were subjected to the reaction conditions a complex inseparable mixture was observed.

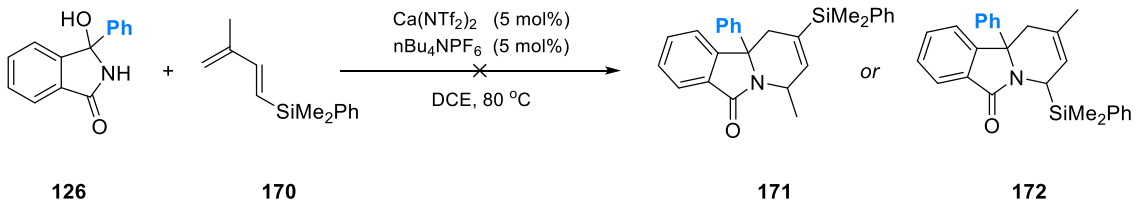

126 **170** **171** **172**

Scheme 38. Reaction of 3-hydroxyisoindolinone and silane diene.

3.4. Applications of 10bH-pyrido[2,1-a]isoindol-6-ones

After the successful synthesis of a range of 10bH-pyrido[2,1-a] isoindol-6-ones **173** we wanted to apply the novel structure to further well-known transformations to demonstrate the versatility of the products we synthesised. Illustrated in Figure 24 are some of the applications which can performed on the products of the Aza-Diels-Alder reaction and will be discussed individually.

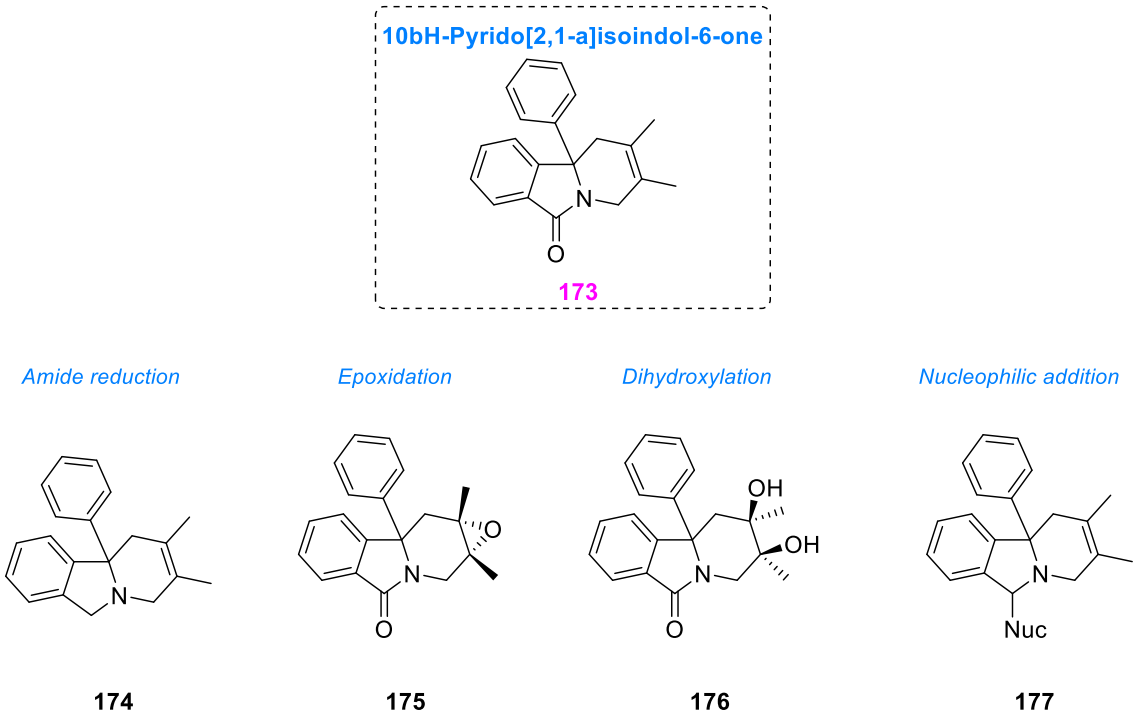

174 **175** **176** **177**

Figure 24. Possible applications of 10bH-pyrido[2,1-a]isoindol-6-ones.

3.4.1. Lactam reduction

The reduction of a lactam to a tertiary amine was carried out following a known procedure *(Scheme 39)*.[46]

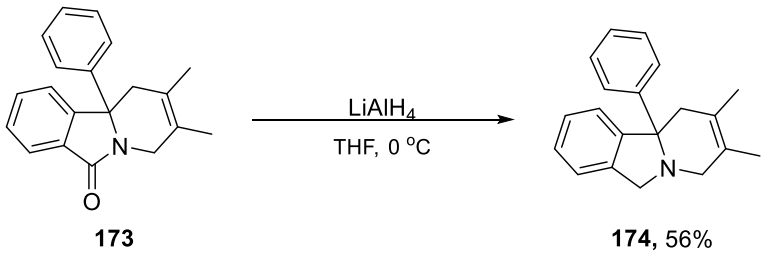

Scheme 39. Lactam reduction with $LiAlH_4$.

Reduction of the amide component of the 10bH-pyrido[2,1-a] isoindol-6-ones **173** was successful using lithium aluminium hydride, and yielded 56% of tertiary amine **174.**

The mechanism of the reduction is shown in Scheme 40. Lactam **173** and an excess of $LiAlH_4$ are reacted, a hydride attacks the electrophilic carbon of the carbonyl bond forming alkoxy **179**. This alkoxy then attacks the reducing agent to form leaving group shown on intermediate **180**, which then forms iminium ion **181** and Li_2AlH_3O. Iminium ion is then further reduced by another equivalent of hydride to give tertiary amide **174**.

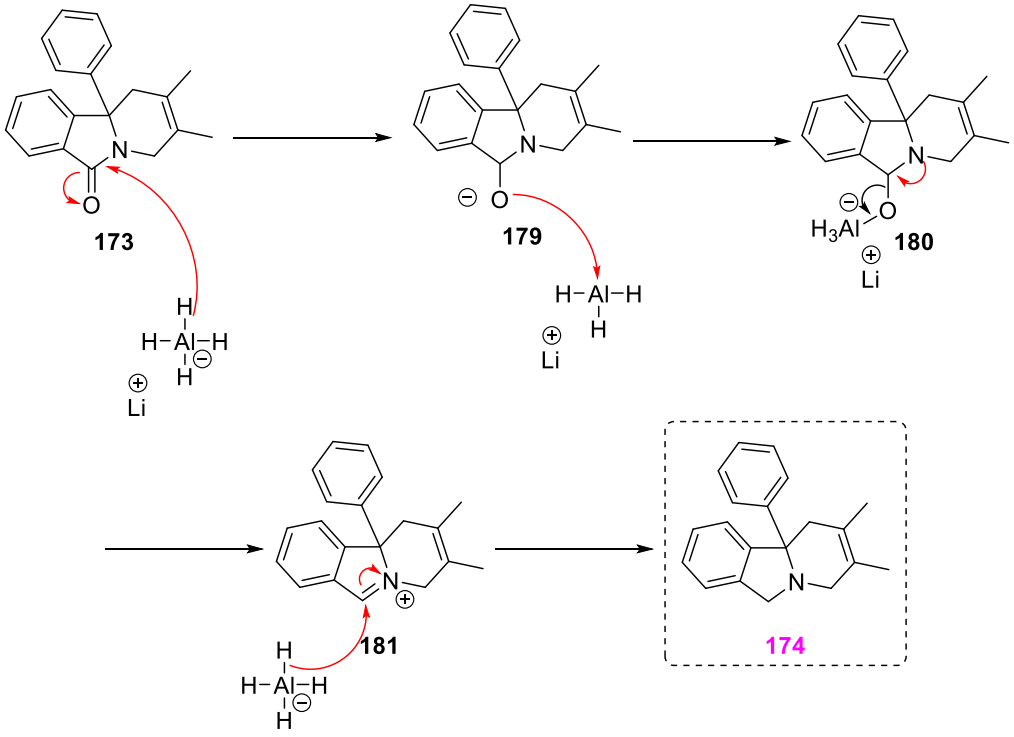

Scheme 40. Mechanism of lactam reduction.

3.4.2. Epoxidation of an olefin.

The epoxidation of the olefin bond in **173** was carried out following a known procedure *(Scheme 41)*.[47]

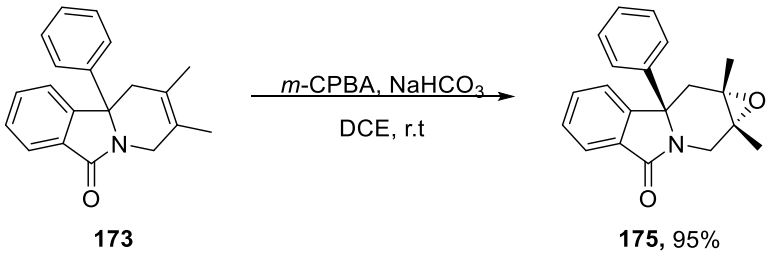

Scheme 41. Epoxidation with *m*-CPBA.

The epoxidation of olefin **173** saw full consumption of starting materials when left to stir at room temperature for 12 hours isolating the epoxide **175** in excellent yield. When *m*-CPBA is reacted with a base it's deprotonated to give anion species **182**, this species is then able to epoxidise an olefin to liberate an epoxide **175** and *m*-CBA **184** as a by-product.

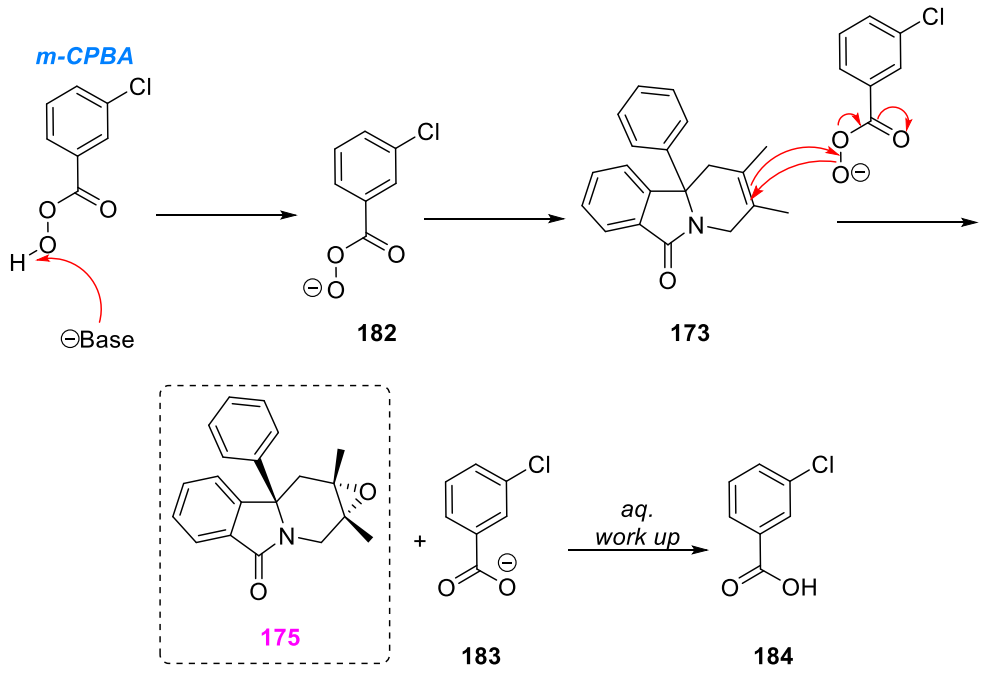

Scheme 42. Plausible mechanism for an *m*-CPBA epoxidation.

The introduction of the epoxide functional group to the products, introduces the ability to ring open and further functionalise.

Epoxides **185** can be used as starting materials for multiple transformations, a few of which are illustrated in Figure 25. The reduction of epoxides is well known and used to synthesis primary alcohols **186** employing $LiAlH_4$ or AlH_3 as a reducing agent. [48] The introduction of sulfur to the compounds is possible when epoxides are treated with thiourea, this produces a thiirane **187**. [49] The hydrolysis of an epoxide results in a *trans* diol product, **188.**

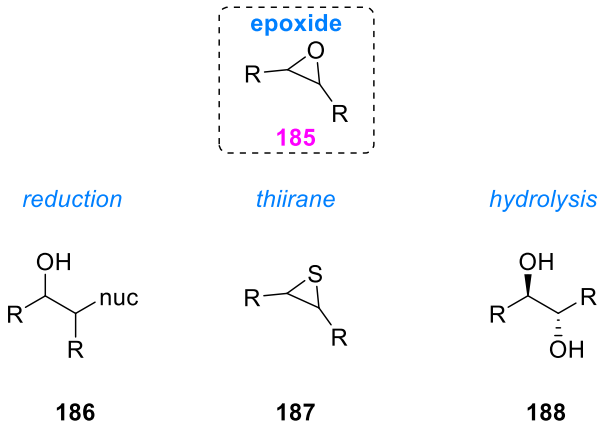

Figure 25 . Transformations with epoxides.

3.4.3. Upjohn Dihydroxylation

The Upjohn dihydroxylation of olefin bond in **173** was carried out following a known procedure *(Scheme 43)*.[50]

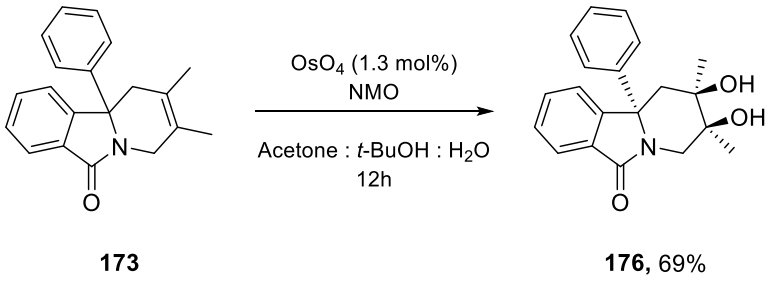

Scheme 43. Upjohn dihydroxylation.

The Upjohn dihydroxylation yielded 69% of diol **176**, when left to stir overnight at room temperature.

Olefin **189** enters the catalytic cycle and undergoes a cycloaddition with the osmium tetroxide to form osmium*(VI)* intermediate. Water then hydrolyses the osmium species to liberate diol **190** and osmium*(VI)*. The addition of NMO then oxidises osmium*(VI)* back

to osmium*(VIII)* and then catalytic cycle can continue with the sequential addition of an olefin. *(Scheme 44).*

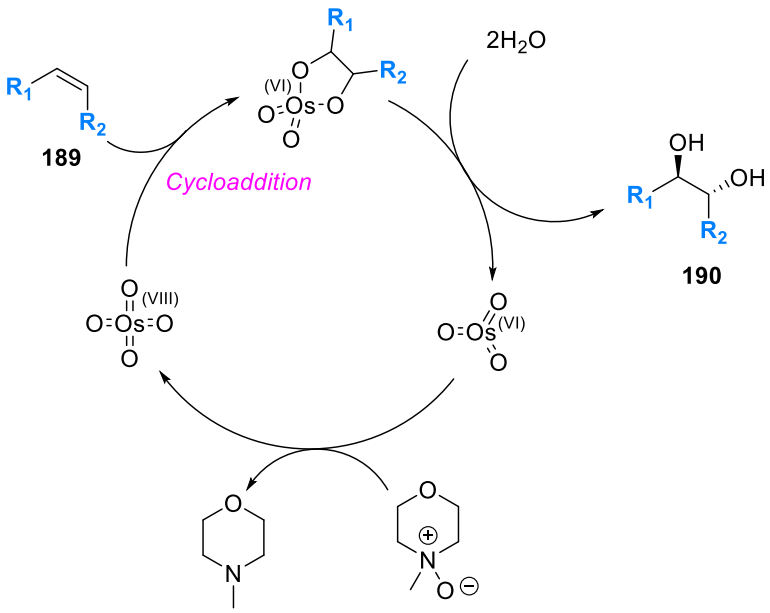

Scheme 44. Mechanism of Upjohn dihydroxylation.

3.4.4. Nucleophilic addition

The nucleophilic addition of nitrile functional group into compound **173** was carried out following known a procedure from the literature *(Scheme 45)*.[51]

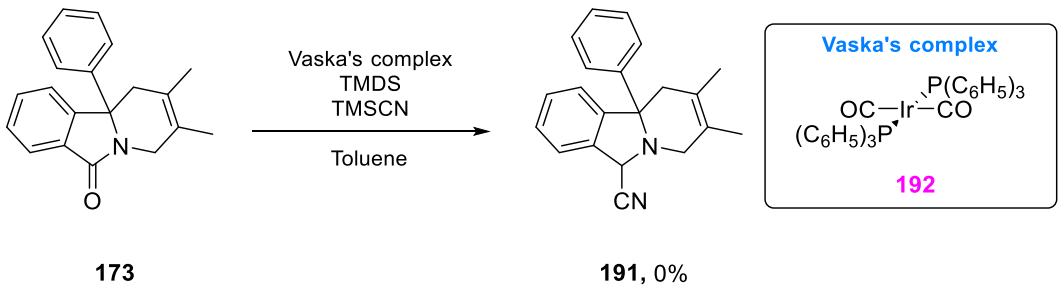

173 **191,** 0%

Scheme 45. Iridium-catalysed reductive Strecker reaction.

Reaction of 10bH-pyrido[2,1-a] isoindol-6-one **173** and TMSCN catalysed using Vaska's complex was unsuccessful. The reaction was left for 24 hours and no consumption of the starting material was observed.

3.5. N,O-Acetals

After the success of the cyclic N-acyliminium ions as dienophiles in the Diels-Alder we wanted to explore a different N-acyliminium ion precursor. Literature reports showed that N,O-acetals are precursors of N-acyliminium ions *(Scheme 46)*.[13]

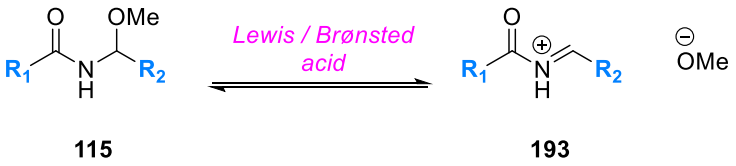

Scheme 46. N-acyliminium ion from N,O-acetal precursor.

Prior work done by the McLaughlin group found that when N,O-acetals **115** are reacted with calcium triflimidate and tetrabutylammonium hexafluorophosphate they liberate a methoxy anion to generate N-acyliminium ions **193**. [13] We predicted the reactivity of N-acyliminium ions **193** would be similar to isoindolinone N-acyliminium ions. Scheme 47 shows a plausible mechanism for the reactivity of N,O-acetals **115** with dimethyl butadiene **129**. Catalytic dehydration of N,O-acetal **115** will furnish N-acyliminium ion **193**, which can then undergo a formal Diels-Alder to form a new 6-membered ring intermediate **194**. Then, we postulate that the liberated methoxy anion would depronate the nitrogen, to liberate a methanol by-product and form product **195**.

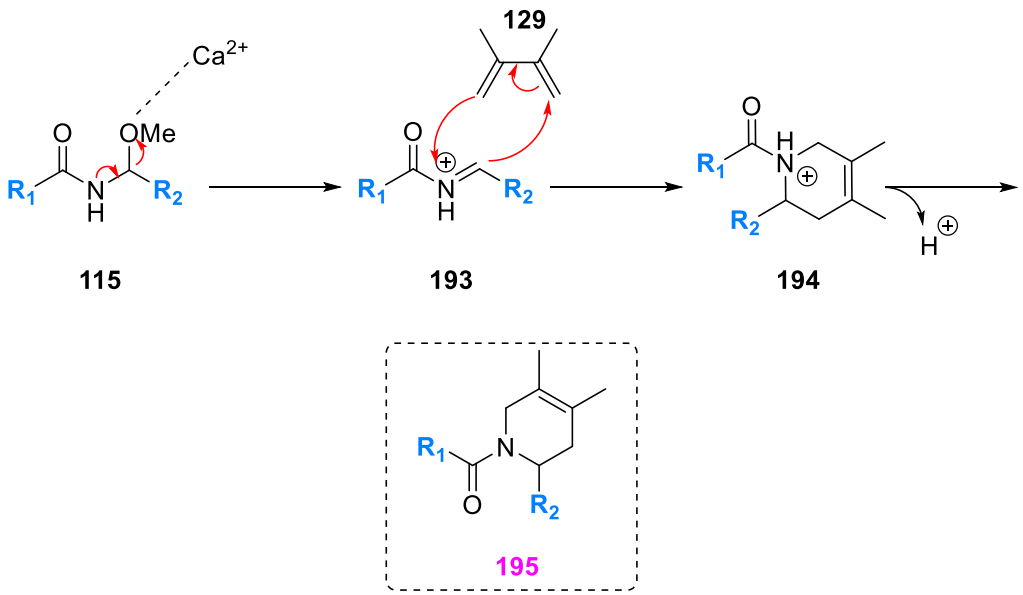

Scheme 47. Proposed mechanism of Diels-Alder of N,O-acetals.

3.5.1. Optimisation of reaction conditions

We predicted that our previously optimised reactions conditions would be a suitable starting point for the reaction of N-(methoxy(phenyl)methyl) benzamide **121** and dimethyl butadiene **129** *(Scheme 48)*.

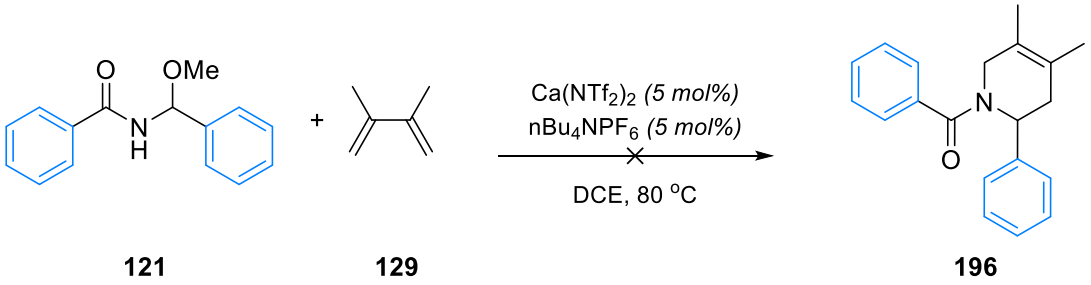

Scheme 48. Diels-Alder of N,O-acetal using optimised conditions.

After 30 minutes of stirring the reaction, analysis by TLC indicated a complex mixture. ^{1}H NMR of the crude product was taken to see if any peaks could be observed for the sp^{3} protons which correspond to the formation of the 6 membered ring *(Figure 26)*. However, these peaks were not observed.

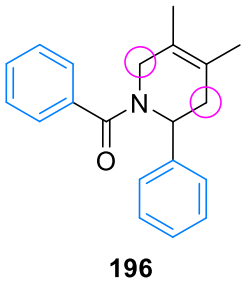

Figure 26. sp^{3} protons.

Re-optimisation of the reaction conditions was carried out to attempt to furnish the desired product **196** *(Table 17)*.

Results from the optimisation study proved the Diels-Alder of N,O-acetal **121** and dimethyl diene **129** was unsuccessful in furnishing desired product **198.** All cases led to no formation of **196**. After the initial reaction at 80 °C we decided to first lower the temperature to see if this was the cause of the complex mixture which was being observed. 3 reactions were set up *(entries 1-3)* at 40-50°C in DCM and EtOAc. The reactions were left stirring for up to 3 hours and TLC analysis indicated no consumption of starting material **121**. The reaction was also run in HFIP, which was left running

overnight, when analysed the following day we observed degradation of the starting material **121** which NMR analysis of the crude product confirmed *(entry 4)*. We concluded this finding was a result of HFIP being slightly acidic. Stochiometric amounts of catalyst also didn't furnish any product **196** *(entry 5)*. An increase to temperatures over 80 °C resulted in complex mixtures by TLC analysis *(entries 6-10)*.

Table 17. Optimisation study 3.

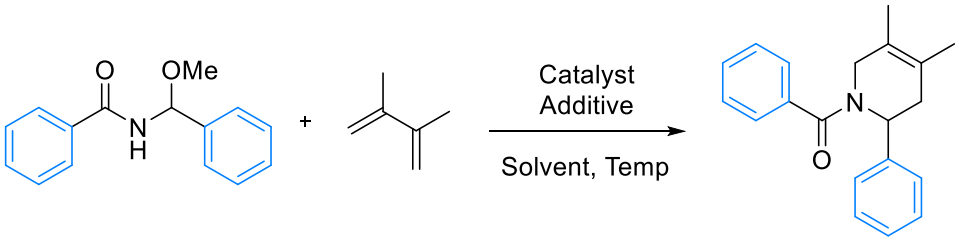

121 **129** **196**

Entry	Catalyst	Additive	Loading	Temp	Solvent	Time	Yield
1	$Ca(NTf_2)_2$	nBu_4NPF_6	10 mol%	40 °C	EtOAc	3h	n.r
2	$Ca(NTf_2)_2$	nBu_4NPF_6	10 mol%	50 °C	EtOAc	1h	n.r
3	$Ca(NTf_2)_2$	nBu_4NPF_6	10 mol%	40 °C	DCM	2h	n.r
4	$Ca(NTf_2)_2$	nBu_4NPF_6	10 mol%	40 °C	HFIP	12h	decomp of **121**
5	$Ca(NTf_2)_2$	nBu_4NPF_6	100 mol%	50 °C	DCM	1h	n.r
6	$Ca(NTf_2)_2$	nBu_4NPF_6	10 mol%	100 °C	DCE	12h	inseparable mix
7	$Ca(NTf_2)_2$	nBu_4NPF_6	10 mol%	100 °C	EtOAc	12h	inseparable mix
8	$Ca(NTf_2)_2$	nBu_4NPF_6	5 mol%	100 °C	DCE	3h	inseparable mix
9	$Ca(NTf_2)_2$	nBu_4NPF_6	10 mol%	100 °C	DCE	3h	inseparable mix
10	$Ca(NTf_2)_2$	nBu_4NPF_6	20 mol%	80 °C	Toluene	6h	inseparable mix

We postulated a reason for poor reactivity of N,O-acetals in the Diels-Alder reaction was the ability of the N,O-acetal **121** to react as a diene itself due to the positioning of the adjacent carbonyl bond *(Figure 27)*.

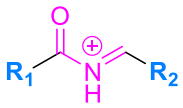

193

Figure 27. Diene reactivity of N-acyliminium ion.

After looking through the literature we found reports on the use of these structures as dienes in Diels-Alder reactions. [34]

3.5.2. Formation of bis-amide

After failing to optimise the transformation we decided that a simple control experiment would help to determine the cause of the degradation of starting material **121.** Upon

carrying out control experiments we observed an insoluble white solid, which we were able to isolate characterise and identify as bis-amide **197** *(Scheme 49)*.

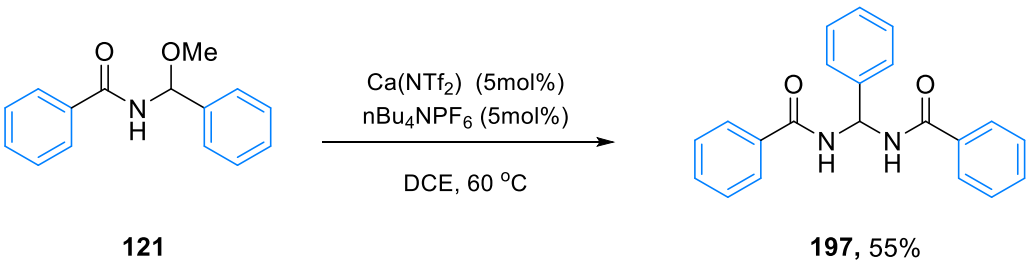

Scheme 49. Formation of bis-amide.

We postulated the formation of bis-amide **197** occurs when 2 reactions occur simultaneously. *A)* the formation of the N-acyliminium ion and *B)* the degradation of starting material which isn't undergoing catalytic dehydration.

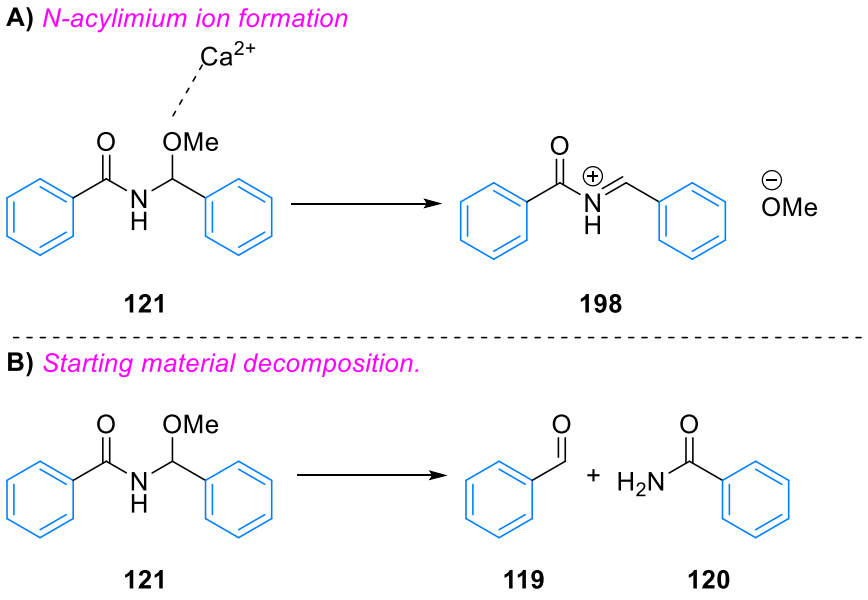

Scheme 50. Simultaneous reactions of N,O-acetal with calcium triflimidate.

If the reactions illustrated in Scheme 50 both occur at the same time we could see the nucleophilic addition of the amide **120** into the electrophilic N-acyliminium ion **198**.

Scheme 51 demonstrates a plausible mechanism for the formation of bis-amide **197** based on assumptions detailed in Scheme 50. It is possible that amide **120** will undergo an nucleophilic addition into the electrophilic N-acyliminium bond quenching the positive nitrogen charge and resulting in intermediate **199**. Intermediate **199** will then be susceptible to deprotonation which the previously liberated methoxy anion will come

back in and liberate methanol and bis-amide **197**. The yield of this reaction will be capped as both pathway A and B rely on each other for product formation, so complete turnover of either pathway will hinder the formation of bis-amide product.

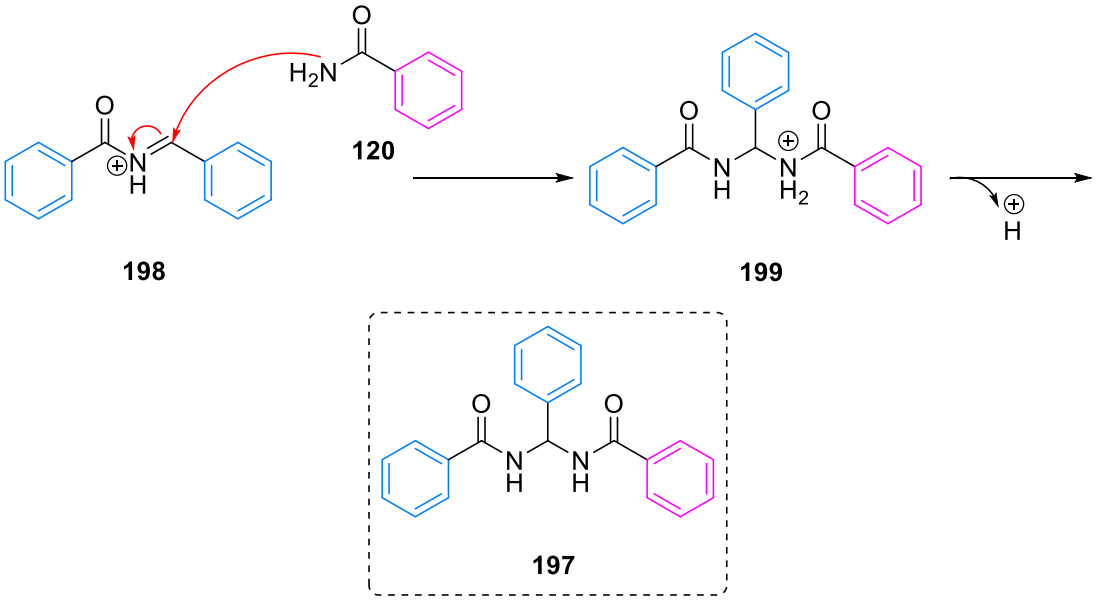

Scheme 51. Plausible mechanism for the formation of bis-amide.

3.6. Inverse electron demand Diels-Alder

We then turned our attention back to isoindolinones as N-acyliminium precursors as we knew their reactivity was reliable. This time we wanted to explore their reactivity as dienes in the inverse electron demand Diels-Alder.

They are many reports on N-acyliminium ions reactivity in the literature; most examples employ stoichiometric quantities of Lewis acid, which often comes with drawbacks. We aim to use our catalyst system to afford a more functional group tolerant reaction *(Scheme 52)*.

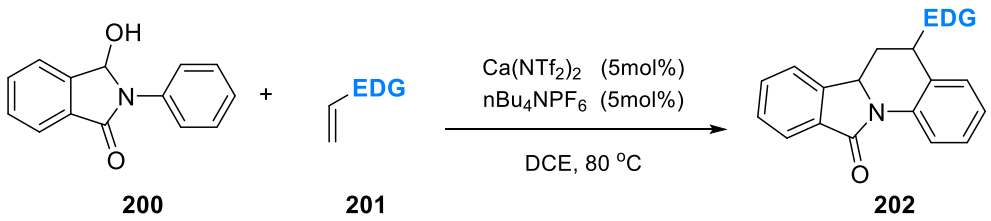

Scheme 52. Inverse electron demand Diels-Alder.

We proposed to take 3-hydroxyisoindolinone **200** and an electron rich dienophile **201** to synthesise a range of novel 6,5,6,6 cyclic systems **202**, using optimised reactions conditions.

We then identified a range of dienophiles we wanted to explore, we selected vinyl lactam **203** as it has been a previously noted as successful *(Figure 28)*. [31] We then wanted to investigate a range of enamines **204** – **206** to test dienophile reactivity coupled with the ease of synthesis making them a desirable scaffold to access.

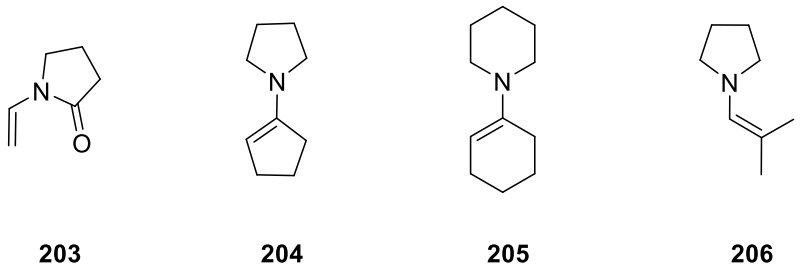

203 **204** **205** **206**

Figure 28. Proposed range of enamine dienophiles.

For N-acyliminium ions to react as dienes they must have an sp^2 substituent on the nitrogen. This sp^2 substituent will mean the N-acyliminium bond has an adjacent olefin bond which sets up diene functionality *(Figure 29)*.

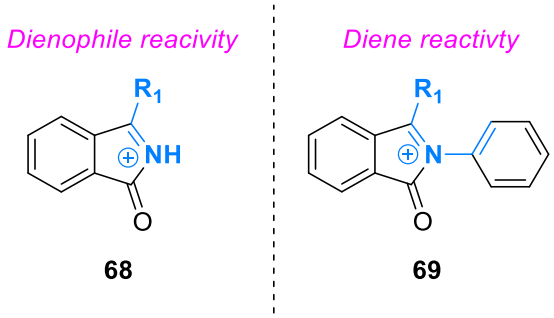

68 **69**

Figure 29. Reactivity of N-acyliminium ions.

Once we knew the dienophiles, we wanted employ we focussed on synthesising starting materials *(Scheme 53)*. We wanted to vary the sterics and electronics of the N-tethered phenyl **207** as well as the 3-position **210**.

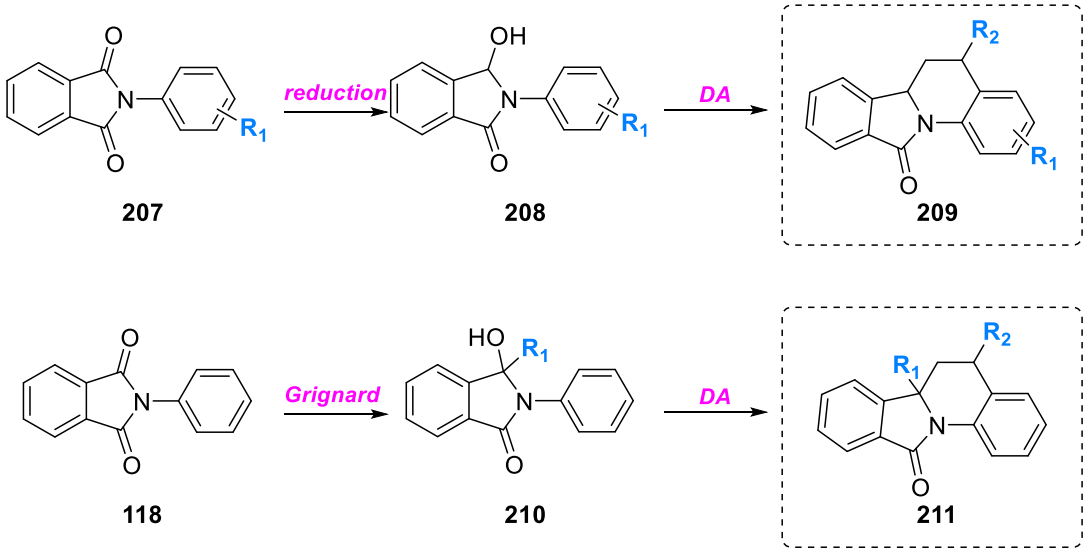

Scheme 53. Starting material substitution patterns.

3.6.1. Preparation of *N*-acyliminium precursors for diene reactivity

We had synthesised a batch of N-phenyl phthalimide **118** so that we could reduce it to the 3-hydroxy N-phenylpthalimide **212** which will then act as the N-acyliminium ion diene precursor.

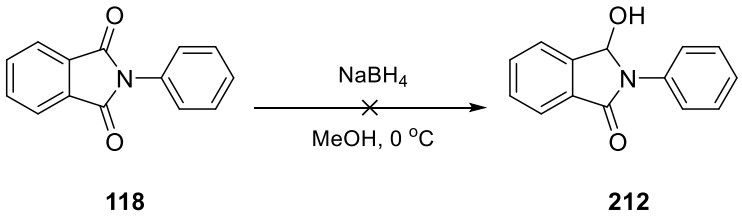

Scheme 54. Reduction with $NaBH_4$.

Scheme 54 shows the expected outcome of the reduction of N-phenylpthalimide **118** with sodium borohydride, using conditions from a known procedure, which reported high yields in excess of 80%. [31] However, when we repeated the procedure form the literature, we didn't see the formation of 3-hydroxy N-phenyl phthalimide **212**, but instead we saw for the formation of a different product, which we identified as benzamide, 2-(hydroxymethyl)-N-phenyl **213** *(Figure 30).*

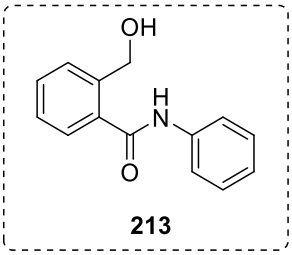

Figure 30. Structure of benzamide, 2-(hydroxymethyl)-N-phenyl

We postulated a potential mechanism for the formation of **213** shown in Scheme 55. Hydride attacks the electrophilic carbonyl in N-phenyl phthalimide **118** to generate an alkoxy intermediate **214**. This alkoxy then ring opens to generate species **215**, which was then further reduced to result in benzamide, 2-(hydroxymethyl)-N-phenyl **213**.

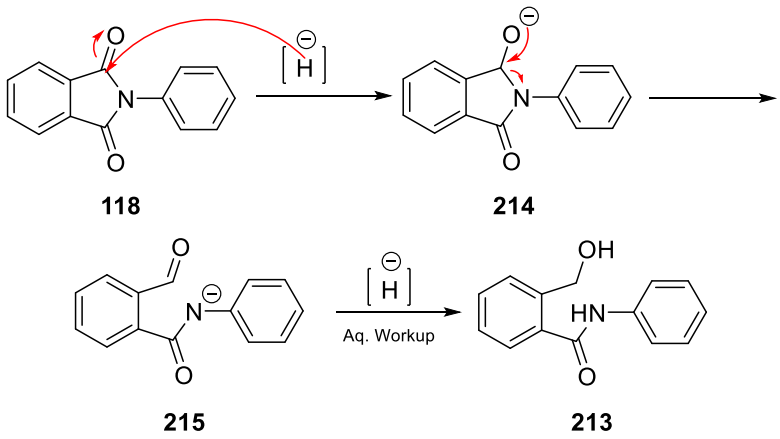

Scheme 55. Ring opening on N-phenyl phthalimide.

After this development, we consulted the literature and found reports that observed the same reactivity and formation of ring opening product **213**. [52] We then gathered procedures throughout the literature on different modes of reduction of N-phenyl phthalimides **118**, to see if any yielded the product we desired. After finding some procedures for the reduction of N-phenyl phthalimide. We attempted and adapted the procedures according to our findings; results can be seen in Table 18. We initially tried the reduction using $NaBH_4$ at 1.0 equivalent *(entry 1)* this was unsuccessful. Increasing the equivalents of reducing agent had no effect on the reaction outcome *(entries 2-3)*.[31] Another procedure In the literature used THF as solvent, however we again saw no impact on reactivity with both 1.00 and 5.00 equivalents.[53] We made the assumption that the collapse of alkoxy **214** which was causing the ring opening was happening at a greater rate than the reduction. We tried to counteract this by lowering the temperature *(entry*

6&7) and quenching at low temperature, however this was unsuccessful at preventing the formation of **213**. We then tried other reducing agents such as sodium triacetoxyborohydride and sodium cyanoborohydride at 1.00 and 5.00 equivalents, however analysis after 3 hours showed no consumption of the starting material **118** in either of the cases *(Table 18)*.

Table 18. Reduction conditions.

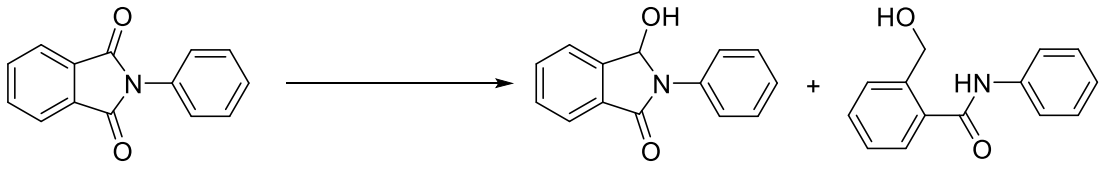

118 **212** **213**

Entry	Reducing agent	Equiv of RA	Solvent	Temp	aq. workup	Extract	Product
1	$NaBH_4$	1.00	MeOH	0 ºC to rt	HCl	EtOAc	**213**
2	$NaBH_4$	5.00	MeOH	0 °C to rt	HCl	EtOAc	**213**
3	$NaBH_4$	10.0	MeOH	0 °C to rt	HCl	EtOAc	**213**
4	$NaBH_4$	1.00	MeOH/THF	0 °C to rt	HCl	EtOAc	**213**
5	$NaBH_4$	5.00	MeOH/THF	0 °C to rt	HCl	EtOAc	**213**
6	$NaBH_4$	1.00	MeOH	-78 °C	HCl	EtOAc	**213**
7	$NaBH_4$	1.00	MeOH	0 ºC	HCl	EtOAc	**213**
8	$Na(CH_3COO)_3BH$	1.00	MeOH	0 ºC	-	-	n.r
9	$Na(CH_3COO)_3BH$	5.00	MeOH	0 ºC	-	-	n.r
10	$NaBH_3CN$	1.00	MeOH	0 ºC	-	-	n.r
11	$NaBH_3CN$	5.00	MeOH	0 ºC	-	-	n.r

After no success in reducing N-phenyl phthalimide **118** we focused on the grignard addition into N-phenyl phthalimide **118** as this is an alternate route to accessing the N-acyliminium precursor **216**.

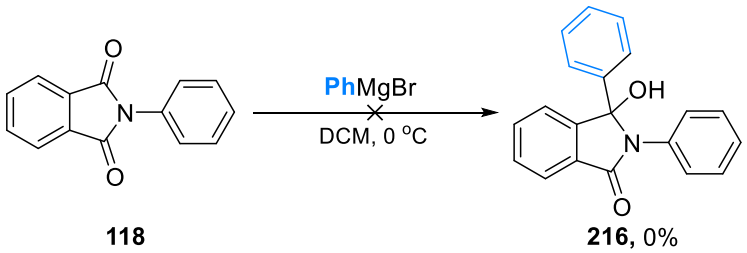

118 **216,** 0%

Scheme 56. Grignard addition into N-phenyl phthalimide.

We used a known procedure form the literature to carry out this grignard addition.[41] The reaction was unsuccessful and it resulted in a complex inseparable mixture.

4. Conclusions

In summary, we have developed the first Aza-Diels-Alder reaction which employs catalytically generated N-acyliminium ions for their use as electron deficient dienophiles. The optimised conditions were found to be 5 mol% calcium bistriflimide, 5 mol% tetrabutylammonium hexafluorophosphate and 1.5 equivalents of diene in DCE at 80 °C and allows access to 6,5,6 fused cyclic isoindolinone scaffolds.

The reaction was well tolerated by both dimethyl and diphenyl butadiene. Altering the electronics and sterics of the 3-hydroxyisoindolinone precursors was also well tolerated along with incorporating traditionally more difficult heterocyclic motifs. We were also able to carry out some well known transformations on the products synthesised, which allows scope for further functionalisation **215** – **217**.

However, the reaction was not tolerated by linear dienes indicating the importance of the positioning of the olefin bonds and more complex dienes such as Danishefsky's diene also were not tolerated. Switching the N-acyliminium ion precursors to N,O-acetals saw no formation of the desired products even when re-optimisation was attempted *(Scheme 57)*.

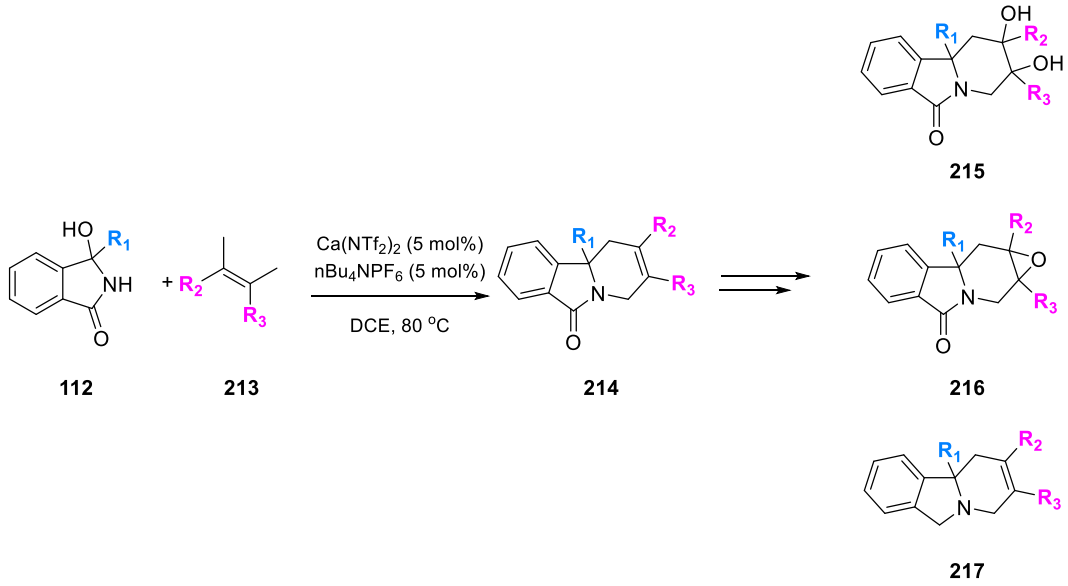

Scheme 57. Conclusion, first Aza-Diels-Alder employing catalytically generated N-acyliminium ions.

5. Future work

5.1. Diene component

We carried out an in-depth study into the reactivity of different dienes, which all had varying structural features, however we didn't explore the use of cyclic dienes and how their reactivity would differ and impact reaction outcome. Exploration of cyclic dienes **37** would be beneficial to build up a bigger picture of N-acyliminium ions and their reactivity as dienophiles *(Scheme 58)*.

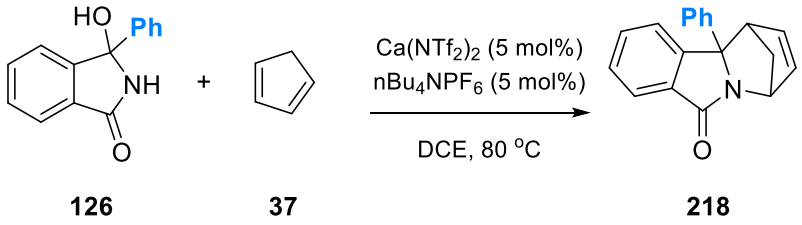

Scheme 58. Spirocycle synthesis employing Aza-Diels-Alder reactions.

5.2. Isoindolinones

We heavily explored the use of aromatic substitution at the 3 position of the 3-hydroxyisoinodline **126**. If we synthesised a range of 3-hydroisoindolinones with aliphatic substitution at the 3-position **222**, it may be possible to synthesis a range of spirocycles, using the same chemistry we have explored throughout this research.

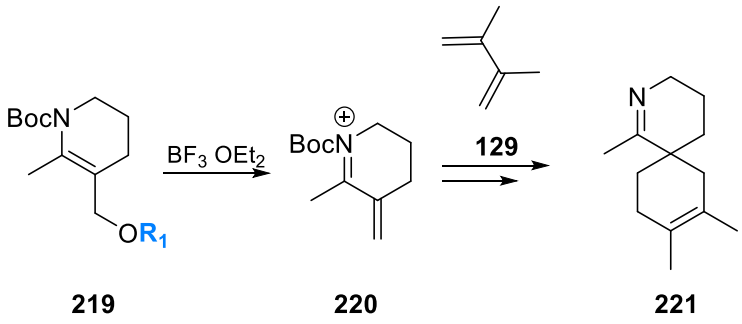

Scheme 59. Brimble's spirocycle synthesis from iminium ions.

Scheme 59 illustrates the synthesis of spirocycle **221**. Alpha-beta unsaturated iminium ion **220** and dimethyl diene **129** undergo a Diels-Alder reaction to produce spirocycle **221** beta to the nitrogen. [54] We would hope to observe complementary reactivity to install a

spirocycle onto the isoindolinone core alpha to the nitrogen, using an N-acyliminium as the intermediate the generate the dienophile *(Scheme 60)*.

When 3-hydroxyisoindolinones **222** are stirred with calcium triflimide, it generates N-acyliminium ion **224** is generated, with aliphatic substitution at the 3 position, we observe quenching on the N-acyliminium ion through elimination, as this is a facile process, this generates intermediate **225.** This intermediate then goes on to act as the dienophile in the Diels-Alder reaction to form spirocycle **223**.

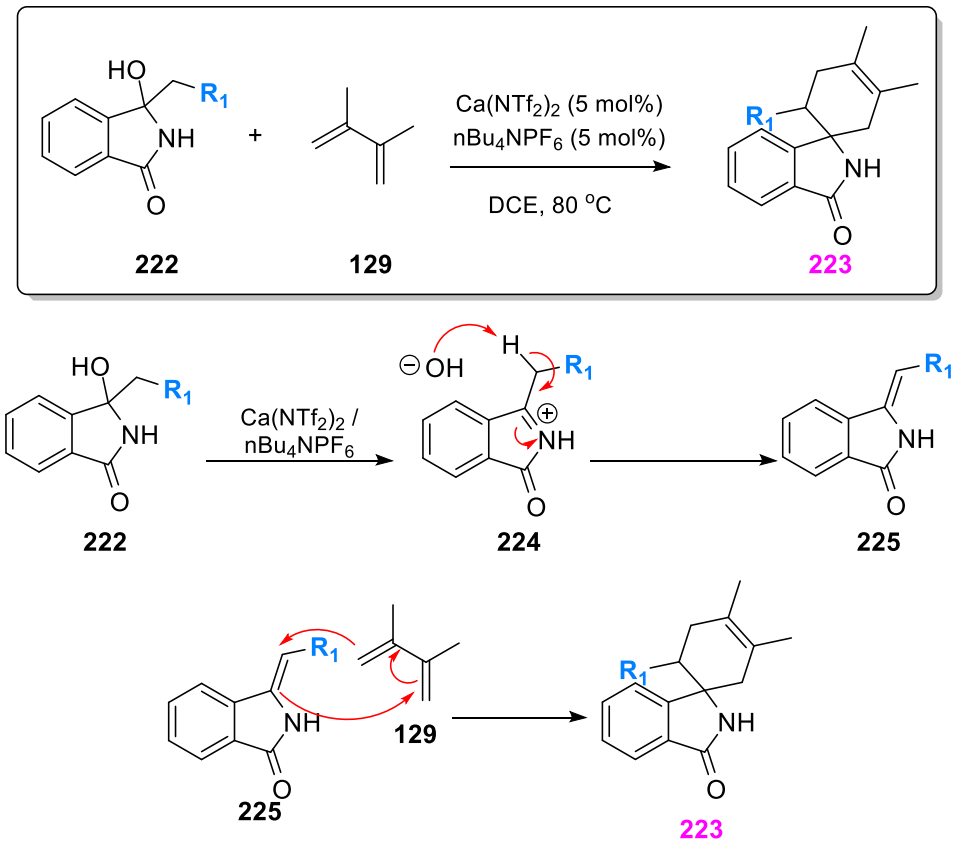

Scheme 60. Diels-Alder reaction to form spirocycle.

5.3. N,O-Acetals

After trying to use N,O-acetals **115** as dienophiles and having no success, we could explore their use as dienes, to synthesise a library of 1,3 oxazines **231**.

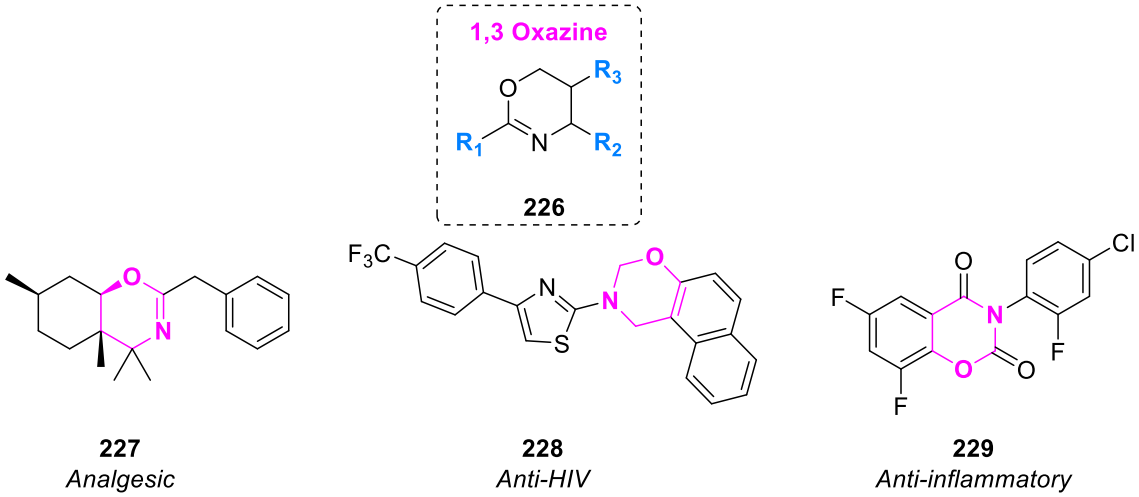

Figure 31. Biologically active oxazine containing compounds.

Oxazines are known to display a range of biologically activity, analgesic properties **227**, anti-HIV **228** and anti-inflammatory properties **229** *(Figure 31)*. [55-57]

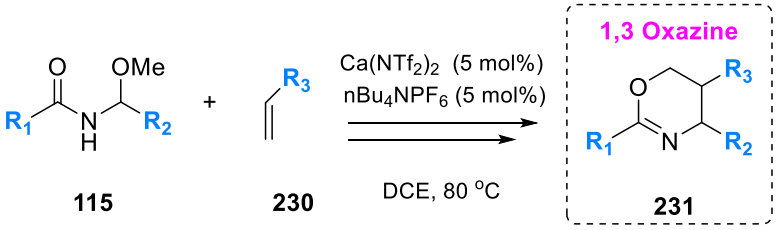

Scheme 61. 1,3 Oxazine synthesis.

The synthesis of oxazines using N-acyliminium ions and Diels-Alder reactions has been explored in the 1970's and again more recently in 2015 *(Scheme 15)*. [33, 34] Both studies presented drawbacks; first, the use of stoichiometric $BF_3{\cdot}Et_2O$ means reaction conditions are harsh and so functional group tolerance will be low and secondly there are minimal points of substitution. Using the catalytic system developed by the McLaughlin group we could further develop this methodology using mild conditions with increased points of substitution to create a range of novel scaffolds with an oxazine core **231** *(Scheme 61)*.

6. References

1. R. G. Pearson, J. Am. Chem. Soc. 1963, 85, 3533-3539.
2. A. Kate, L. K. Sahu, J. Pandey, M. Mishra and P. K. Sharma, Curr. Opin. Green Sustain. Chem. 2022, 5, 100248.
3. R. P. Allen J. Bard, Joseph Jordan, *Standard Potentials in Aqueous Solution*

1985.

4. A. D. Frankland, P. B. Hitchcock, M. F. Lappert and G. A. Lawless, *J. Chem. Soc, Chem. Commun*, 1994,
5. M. G. Hill, W. M. Lamanna and K. R. Mann, *Inorg Chem*, 1991, **30**, 4687-4690.
6. H. Ohtaki and T. Radnai, *Chem. Rev.* 1993, **93**, 1157-1204.
7. D. M. Gelman, C. M. Forsyth and P. Perlmutter, *Org. Lett.*, 2009, **11**, 4958-4960.
8. S. Haubenreisser and M. Niggemann, *Adv. Synth. Catal,* 2011, **353**, 469-474.
9. M. Niggemann and M. J. Meel, *Angew. Chem. Int. Ed.* 2010, **49**, 3684-3687.
10. D. Lebœuf, E. Schulz and V. Gandon, *Org. Lett.*, 2014, **16**, 6464-6467.
11. A. J. Basson and M. G. McLaughlin, *ChemComm*, 2019, **55**, 8317-8320.
12. A. J. Basson and M. G. McLaughlin, J. Org. Chem. 2020, **85**, 5615-5628.
13. A. J. Basson and M. G. McLaughlin, *ChemSusChem*, 2021, **14**, 1696-1699.
14. R. H. Wiley, *Chem. Rev.* 1945, **37**, 401-442.
15. S. Saito, T. Tsubogo and S. Kobayashi, J. Am. Chem. Soc. 2007, **129**, 5364-5365.
16. T. Tsubogo, Y. Yamashita and S. Kobayashi, *Angew. Chem. Int. Ed.* 2009, **48**, 9117-9120.
17. P. Vermeeren, T. A. Hamlin, I. Fernández and F. M. Bickelhaupt, *Angew. Chem., Int. Ed. Engl.*, 2020, **59**, 6201-6206.
18. T. A. Hamlin, F. M. Bickelhaupt and I. Fernández, *Acc Chem Res*, 2021, **54**, 1972-1981.
19. H. Kobayashi, J. Nie and T. Sonoda, *Chem. Lett.* 1995, **24**, 307-308.
20. M. Shi, L.-X. Shao and B. Xu, *Org. Lett.*, 2003, **5**, 579-582.
21. J. Wang, Z. Liu, J. Li, Z. Song, C. Hu and Z. Su, J. Org. Chem. 2019, **84**, 3940-3952.
22. C. Mannich and W. Krösche, *Arch Pharm*, 1912, **250**, 647-667.
23. A. Pictet and T. Spengler, *Berichte der deutschen chemischen Gesellschaft*, 1911, **44**, 2030-2036.
24. M. Hatano, T. Horibe and K. Ishihara, *Org. Lett.*, 2010, **12**, 3502-3505.
25. S.-i. Nakatsuka, H. Miyazaki and T. Goto, *Chem. Lett.* 1981, **10**, 407-410.
26. M. Petrini, *Chem. Rev.* 2005, **105**, 3949-3977.
27. T. Shono, Y. Matsumura and K. Tsubata, J. Am. Chem. Soc. 1981, **103**, 1172-1176.
28. S. M. Weinreb and P. M. Scola, *Chem. Rev.* 1989, **89**, 1525-1534.
29. M. G. Memeo and P. Quadrelli, *Eur. J. Chem.*, 2012, **18**, 12554-12582.
30. R. R. Schmidt, *Angew. Chem., Int. Ed. Engl.* 1973, **12**, 212-224.
31. A. Jha, T.-Y. Chou, Z. Aljaroudi, B. D. Ellis and T. S. Cameron, *Beilstein J. Org. Chem.* 2014, **10**, 848-857.
32. S. Suga, Y. Tsutsui, A. Nagaki and J.-i. Yoshida, *Bull Chem Soc Jpn*, 2005, **78**, 1206-1217.
33. J. Altman, R. Moshberg and D. Ben-Ishai, *Tetrahedron Lett.,* 1975, **16**, 3737-3740.
34. I. Colomer, O. Adeniji, G. M. Burslem, P. Craven, M. O. Rasmussen, A. Willaume, T. Kalliokoski, R. Foster, S. P. Marsden and A. Nelson, *Bioorg. Med. Chem,* 2015, **23**, 2736-2740.
35. Y. Ueda and S. C. Maynard, *Tetrahedron Lett.,* 1985, **26**, 6309-6312.
36. K. Speck and T. Magauer, *Beilstein J. Org. Chem.* 2013, **9**, 2048-2078.
37. R. Ben Othman, R. Affani, M.-J. Tranchant, S. Antoniotti, V. Dalla and E. Duñach, *Angew. Chem. Int. Ed.* 2010, **49**, 776-780.
38. C. Zhang, Y. Ding, Y. Gao, S. Li and G. Li, *Organic Letters*, 2018, **20**, 2595-2598.
39. A. J. Basson, N. R. Halcovitch and M. G. McLaughlin, *Eur. J. Chem.*, 2022, **n/a**, e202201107.
40. C. V. Gärtner and C. Schneider, *Org. Lett.*, 2022, **24**, 3560-3564.

41. J. Sućˊ, I. Dokli and M. Grediˇcak, *ChemComm*, 2016, **52**, 2071-2074.
42. J. Halli, K. Hofman, T. Beisel and G. Manolikakes, *Eur J Org Chem*, 2015, **2015**, 4624-4627.
43. Y.-C. Yuan, C. Bruneau, T. Roisnel and R. Gramage-Doria, J. Org. Chem. 2019, **84**, 12893-12903.
44. S. Danishefsky, *OrgSyn*, 1983, **61**, 147.
45. I. L. Alberts and H. F. Schaeffer, *Chem. Phys. Lett.,* 1989, **161**, 375-382.
46. N. Assimomytis, Y. Sariyannis, G. Stavropoulos, P. G. Tsoungas, G. Varvounis and P. Cordopatis, *Synlett*, 2009, **2009**, 2777-2782.
47. W. Liu, T. Leischner, W. Li, K. Junge and M. Beller, *Angew. Chem. Int. Ed.* 2020, **59**, 11321-11324.
48. B. Rickborn and W. E. Lamke, J. Org. Chem. 1967, **32**, 537-539.
49. F. G. Bordwell and H. M. Andersen, J. Am. Chem. Soc. 1953, **75**, 4959-4962.
50. G. A. Molander and R. Figueroa, *Org. Lett.*, 2006, **8**, 75-78.
51. Á. L. Fuentes de Arriba, E. Lenci, M. Sonawane, O. Formery and D. J. Dixon, *Angew. Chem. Int. Ed.* 2017, **56**, 3655-3659.
52. Z.-I. Horii, C. Iwata and Y. Tamura, J. Org. Chem. 1961, **26**, 2273-2276.
53. Z. Al-Jaroudi, P. P. Mohapatra and A. Jha, *Tetrahedron Lett.,* 2016, **57**, 772-777.
54. Z. Wang, N. Krogsgaard-Larsen, B. Daniels, D. P. Furkert and M. A. Brimble, J. Org. Chem. 2016, **81**, 10366-10375.
55. N. S. Li-Zhulanov, A. V. Pavlova, D. V. Korchagina, Y. V. Gatilov, K. P. Volcho, T. G. Tolstikova and N. F. Salakhutdinov, *Chem. heterocycl.* 2020, **56**, 936-941.
56. C.-L. Chen, C.-C. Lee, F.-L. Liu, T.-C. Chen, A. A. Ahmed Ali, D.-M. Chang and H.-S. Huang, *Eur. J. Med. Chem.*, 2016, **117**, 70-84.
57. R. Gawali, J. Trivedi, S. Bhansali, R. Bhosale, D. Sarkar and D. Mitra, *Eur. J. Med. Chem.,* 2018, **157**, 310-319.
58. A. Di Mola, A. Macchia, C. Tedesco, G. Pierri, L. Palombi, R. Filosa and A. Massa, *ChemistrySelect*, 2019, **4**, 4820-4826.
59. C. Ge, R.-X. Liang, R.-R. Liu, B. Xiang and Y.-X. Jia, *Tetrahedron Lett.,* 2017, **58**, 142-144.
60. J.-Q. Zhou, W.-J. Sheng, J.-H. Jia, Q. Ye, J.-R. Gao and Y.-X. Jia, *Tetrahedron Lett.,* 2013, **54**, 3082-3084.
61. A. V. Iosub and S. S. Stahl, J. Am. Chem. Soc., 2015, **137**, 3454-3457.
62. N. Yasukawa, H. Yokoyama, M. Masuda, Y. Monguchi, H. Sajiki and Y. Sawama, *Green Chemistry*, 2018, **20**, 1213-1217.
63. D. Fiorito, S. Folliet, Y. Liu and C. Mazet, *ACS Catalysis*, 2018, **8**, 1392-1398.
64. W. Wang, S. He, Y. Zhong, J. Chen, C. Cai, Y. Luo and Y. Xia, J. Org. Chem. 2022, **87**, 4712-4723.
65. R. J. Maza, E. Davenport, N. Miralles, J. J. Carbó and E. Fernández, *Org. Lett.*, 2019, **21**, 2251-2255.
66. M. Ohashi, I. Takeda, M. Ikawa and S. Ogoshi, J. Am. Chem. Soc. 2011, **133**, 18018-18021.
67. M. Shimizu, T. Kurahashi, K. Shimono, K. Tanaka, I. Nagao, S.-i. Kiyomoto and T. Hiyama, *Chem. Asian J.,* 2007, **2**, 1400-1408.
68. H. Jiang, L. He, X. Li, H. Chen, W. Wu and W. Fu, *ChemComm*, 2013, **49**, 9218-9220.
69. Z. Pei, X. Li, T. W. von Geldern, D. J. Madar, K. Longenecker, H. Yong, T. H. Lubben, K. D. Stewart, B. A. Zinker, B. J. Backes, A. S. Judd, M. Mulhern, S. J. Ballaron, M. A. Stashko, A. K. Mika, D. W. A. Beno, G. A. Reinhart, R. M. Fryer, L. C. Preusser, A. J. Kempf-Grote, H. L. Sham and J. M. Trevillyan, *J. Med. Chem.,* 2006, **49**, 6439-6442.
70. R. Nandi, P. K. Mandal, A. Kayet, T. Bhattachariya, S. Ghosh and D. K. Maiti, *Org. Lett.*, 2020, **22**, 3474-3478.

7. Experimental

General Information

Solvents & reagents

Reagents were purchased in the highest purity available from Acros Organics, Alfa Aesar, Fluorochem, TCI, Fisher Scientific or Sigma Aldrich. All solvents were purchased from commercial sources and used without purification (reagent grade). Metal salts and ligands were stored in a desiccator when not in use. Anhydrous solvent was prepared by storing solvent over activated 4Å MS for 72 hours. Standard vacuum line techniques were used and glassware was oven dried prior to use. Organic solvents were dried during workup using anhydrous Na_2SO_4. All reactions were performed using DrySyn heating mantles and pressure regulated vials or round bottom flasks.

Purification and chromatography.

Thin Layer Chromatography (TLC) was carried out using aluminium plates coated with 60 F254 silica gel. Plates were visualised using UV light (254 or 365 nm) and developed with iodine and basic permanganate solution. Flash chromatography was performed on VWR silica gel 60, 40–63 microns RE as the stationary phase and the solvents employed were of reagent grade.

Characterisation.

^{1}H NMR spectroscopic data were obtained at 400 MHz (Bruker Ultrashield 400 Plus) and ^{13}C data were obtained at 100 MHz (Bruker Ultrashield 400 Plus) at 298 K. The chemical shifts are reported in parts per million (δ) relative to residual $CHCl_3$ (δ_H = 7.26 ppm) and $CDCl_3$ (δ_C = 77.16 ppm, central line.) The assignment of the signals in the ^{1}H and ^{13}C NMR spectra was achieved through 2D-NMR techniques: COSY, HSQC and HMBC. Coupling constants (*J*) are quoted in Hertz. Infrared spectra were recorded on an Agilent Technologies Cary 630 FTIR spectrometer. High resolution mass spectrometry data were recorded using electron spray ionization (ESI) or atmospheric pressure chemical ionization (ESI) on a Shimadzu LCMS-IT-TOF mass spectrometer.

Synthesis of starting materials

General Procedure A – Grignard addition into phthalimides. [41]

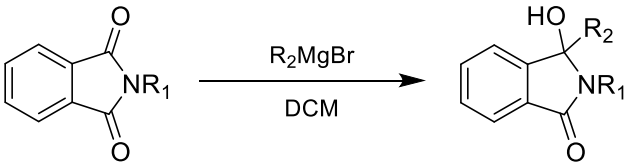

To an oven dried round bottom flask purged with nitrogen was added phthalimide (1.0 equiv) dissolved in DCM (0.25 M) and the flask cooled to 0°C. The Grignard reagent (3.0 equiv) was added dropwise and the reaction was warmed to room temperature and stirred until TLC analysis indicated full conversion. The reaction was then quenched with sat.aq. NH_4Cl and extracted with DCM (3 x 50 mL). The organic layers were dried over Na_2SO_4 filtered and concentrated *in vacuo*. The crude sample was purified using flash column chromatography, to result in the pure product.

General Procedure B – Synthesis of Grignards for addition into phthalimides. [41]

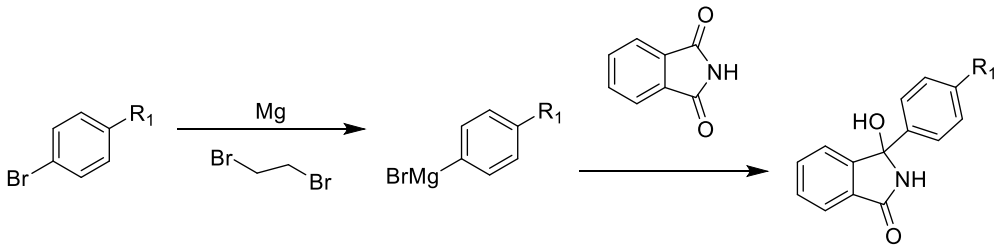

To an oven-dried round bottom flask purged with nitrogen was added magnesium turnings (3.1 equiv) and suspended in THF (1.0 M). Dibromoethane (0.1 equiv) was added followed by the corresponding aryl halide (3.0 equiv) dropwise (initiation occurred following the first few drops) and the resulting mixture was stirred for approximately 60 mins.

In a separate oven-dried round bottom flask purged with nitrogen was added phthalimide (1.0 equiv) dissolved in THF (0.25 M) and cooled to 0°C. The above Grignard reagent was then added dropwise and allowed to warm to room temperature, stirring until TLC analysis indicated completion. The mixture was quenched with 50.0 mL sat.aq. NH_4Cl and extracted with DCM (3 x 50 mL). The organic layer was dried over Na_2SO_4 filtered and

concentrated *in vacuo*. The crude sample was purified using flash column chromatography to afford the pure product.

General Procedure C – Halide lithium exchange for addition into phthalimides. [41]

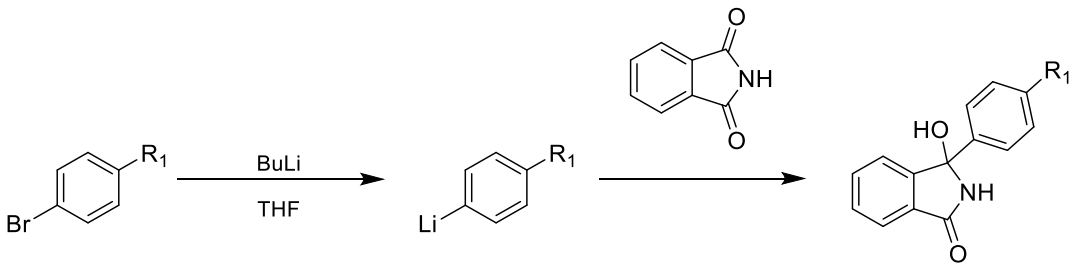

In an oven dried round bottom flask purged with nitrogen was added the required aryl halide (4.0 equiv) and dissolved in anhydrous THF (0.5 M) The flask was cooled to -78°C and nBuLi (2.5 M) (3.5 equiv) was added dropwise and stirred for 60 minutes. Phthalimide (1.0 equiv) dissolved in THF (0.5 M) was added to the reaction in a single portion. The reaction was then warmed to room temperature until TLC analysis indicated completion. The mixture was quenched with sat.aq. NH_4Cl and extracted with ethyl acetate (3X50 mL). The organic layer was dried over Na_2SO_4, filtered and concentrated in vacuo. The crude sample was purified using flash column chromatography to afford the pure product.

General procedure D – Synthesis of N,O-acetal. [42]

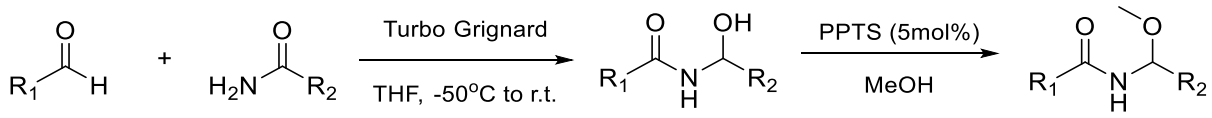

To a flame-dried round bottom flask purged with argon was added amide (1.0 equiv.) and dry THF (2mmol/amide). The resulting solution was cooled to -50°C and iPrMgCl.LiCl (1.05 equiv.) was added dropwise. The resulting solution was then warmed to room temperature and stirred for 30 min. The mixture was then cooled to 0 °C and the corresponding aldehyde (1.1 equiv.) was added as a single portion. The reaction mixture was warmed to room temperature and stirred until TLC analysis indicated full consumption of amide. The mixture was quenched with sat. aq. $NaHCO_3$, the organic layer separated, and the aqueous layer extracted three times with DCM. The combined organic layers were dried with Na_2SO_4, filtered and concentrated to afford the crude hemiaminal.

Pure hemiaminals were obtained by crystallisation from DCM:Hexane (9:1) The crude hemiaminal was then dissolved in methanol (3mL/mmol) and PPTS (5 mol%) was added. The reaction mixture was stirred at room temperature until complete consumption of the hemiaminal was observed via TLC. The mixture was quenched using sat. aq. $NaHCO_3$. The organic layer was separated, and the aqueous layer was extracted three times with

DCM. The combined organic layers were dried with Na_2SO_4, filtered, concentrated and purified by flash column chromatography (EtOAc:Hex, 1% NEt_3) to afford the pure product.

General Procedure E – Synthesis of 3-hydroxy N—phenyl phthalimides. [43]

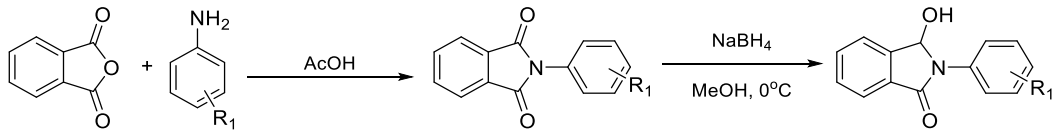

Phthalic anhydride (1.0 equiv) was dissolved in AcOH (0.2 M) and aniline derivative (1.2 equiv) was added. Reaction was stirred at r.t. until TLC analysis indicated completion. The reaction was then quenched with ice, and filtered to afford crude N-phenylpthalimide.

N-phenylpthalimide was dissolved in methanol (0.25 M) and cooled to 0°C, then reduced using $NaBH_4$ (2.0equiv) and stirred until TLC analysis indicated completion. The mixture was quenched with sat.aq. $NaHCO_3$. The organic layer was separated, and the aqueous layer was extracted three times with DCM (3 x 50mL), organic layer was dried over Na_2SO_4 filtered and concentrated to obtain the crude 3-hydroxy N—phenyl phthalimide. Pure product was obtained using flash chromatography.

3-Hydroxy-3-phenyl-isoindolin-1-one, 112o

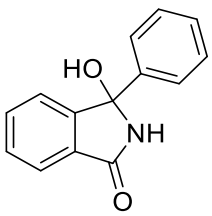

112o was prepared according to general procedure A from phthalimide (500 mg, 3.40 mmol, in 0.25 M DCM) and phenylmagnesium bromide (3.40 mL, 10.2 mmol) resulting in

the desired crude product. Purification by column chromatography (1:1 EtOAc:Hex) resulted in obtaining the pure product as a white solid (395 mg, 51%).

R_F (1:1 EtOAc:Hex) = 0.29

^{1}H NMR (400 MHz, DMSO-D_6)δ 9.23 (s, 1H), 7.64 (d, *J* = 7.2 Hz, 1H), 7.56 – 7.42 (m, 4H), 7.37 – 7.27 (m, 4H), 6.89 (s, 1H).

^{13}C NMR (101 MHz, DMSO-D_6) δ 168.3, 150.9, 142.1, 132.4, 130.6, 128.9, 128.2, 127.8, 125.5, 122.8, 122.6, 87.3.

Data in accordance with literature. [58]

3-Hydroxy-3-(4-methyloxyphenyl) isoindolin-1one, 112p

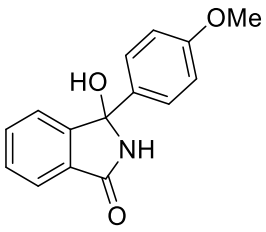

112p was prepared according to general procedure B from phthalimide (500 mg, 3.40 mmol, in 0.25 M THF), magnesium turnings (252 mg, 10.5 mmol in 1.0M THF), dibromoethane (0.063 mL, 0.34 mmol) and 4-bromoanisole (1.28 mL, 10.2 mmol) resulting in the desired crude product. Purification by column chromatography (1:1 EtOAc:Hex) resulted in the pure product as a white solid (144 mg, 17%).

R_F (1:1 EtOAc:Hex) = 0.17

^{1}H NMR (400 MHz, DMSO-D_6) δ 9.17 (s, 1H), 7.62 (d, *J* = 6.9 Hz, 1H), 7.52 (td, *J* = 7.4, 1.3 Hz, 1H), 7.45 (td, *J* = 7.4, 1.1 Hz, 1H), 7.38 (d, *J* = 9.0 Hz, 2H), 7.29 (d, *J* = 7.4 Hz, 1H), 6.89 (d, *J* = 9.0 Hz, 2H), 6.80 (s, 1H), 3.72 (s, 3H).

^{13}C NMR (101 MHz, DMSO-D_6) δ 168.1, 158.6, 150.9, 133.7, 132.1, 130.3, 128.6, 126.5, 122.5, 122.3, 113.3, 86.9, 54.9.

Data in accordance with literature. [59]

3-Hydroxy-3-[4-trifluoromethyl)phenyl]isoindolin-1one, 112a

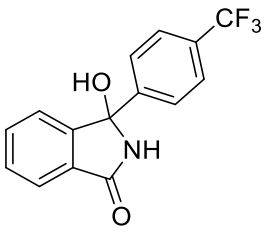

112a was prepared according to general procedure C from phthalimide (200 mg, 1.36 mmol, in 0.5 M THF), 4-bromobenzyltrifluoride (0.76 mL, 5.44 mmol in 0.5 M THF) and butyllithium (2.0 mL, 4.76 mmol) resulting in the desired crude product. Purification by column chromatography (3:1 EtOAc:Hex) resulted in obtaining the pure product as a white solid (194 mg, 49%).

R_F (1:1 EtOAc:Hex) = 0.29

^{1}H NMR (400 MHz, DMSO-D_6) δ 9.36 (s, 1H), 7.75 – 7.66 (m, 5H), 7.56 (td, *J* = 7.4, 1.4 Hz, 1H), 7.51 (td, *J* = 7.4, 1.2 Hz, 1H), 7.32 (d, *J* = 7.0 Hz, 1H), 7.15 (s, 1H).

^{13}C NMR (101 MHz, D_6-DMSO) δ 168.8, 150.6, 147.2, 133.1, 131.0, 129.7, 128.8 (q, *J* = 31.8 Hz), 126.9, 125.7 (q, *J* = 3.6 Hz), 123.2, 123.2, 87.4.

Not all *J* values were obtained due to lack of materiel.

^{19}F NMR (376 MHz, DMSO-D_6): -60.9

Data in accordance with literature.[59]

3-(1,3-Benzodioxol-5-yl)-3hydroxy-indan-1one, 112e

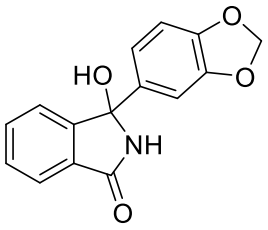

112e was prepared according to general procedure C from phthalimide (200 mg, 1.36 mmol, in 0.5 M THF), 5-bromo-1,3-benzodioxle (0.60 mL, 5.44 mmol in 0.5 M THF) and butyllithium (1.90 mL, 4.76 mmol), resulting in the desired crude product. Purification by column chromatography (3:1 EtOAc:Hex) resulted in obtaining the pure product as a white solid (165 mg, 45%).

R_F (1:1 EtOAc:Hex) = 0.15

^{1}H NMR (400 MHz, DMSO-D_6) δ 9.17 (s, 1H), 7.61 (d, *J* = 7.0 Hz, 1H), 7.53 (td, *J* = 7.4, 1.3 Hz, 1H), 7.46 (td, *J* = 7.4, 1.1 Hz, 1H), 7.32 (d, *J* = 7.4 Hz, 1H), 6.98 (d, *J* = 1.6 Hz, 1H), 6.92 (d, *J* = 1.8 Hz, 1H), 6.90 (d, *J* = 1.8 Hz, 1H), 6.85 (s, 1H), 5.99 (dd, *J* = 4.3, 0.9 Hz, 2H)

^{13}C NMR (101 MHz, DMSO-D_6) δ 168.3, 150.8, 147.2, 146.8, 136.1, 132.4, 130.5, 128.9, 122.7, 122.5, 118.8, 107.8, 106.2, 101.1, 87.2.

Data in accordance with literature. [11]

3-(2,4 Dimethoxyphenyl)-3-hydroxy-indan-1one, 112c

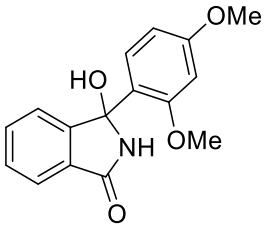

112c was prepared according to general procedure C from phthalimide (200 mg, 1.36 mmol, in 0.5 M THF), 1-bromo-2,4-dimethoxybenzene (0.70 mL, 5.44 mmol in 0.5 M THF) and butyllithium (1.90 mL, 4.76 mmol) resulting in the desired crude product. Purification by column chromatography (3:1 EtOAc:Hex) resulted in obtaining the pure product as a white solid (86 mg, 22%).

R_F (1:1 EtOAc:Hex) = 0.14

IR vmax (cm-1): 3278, 2939, 1682, 1621.

HRMS (APCI) m/z: $[M + H]^+$ Calcd for $C_{16}H_{16}NO_4$ 286.1074; Found 286.1071

^{1}H NMR (400 MHz, DMSO-D_6) δ 8.70 (s, 1H), 7.75 (d, *J* = 8.6 Hz, 1H), 7.59 (d, *J* = 5.2 Hz, 1H), 7.47 – 7.39 (m, 2H), 7.14 (d, *J* = 7.7 Hz, 1H), 6.55 (d, *J* = 6.6 Hz, 2H), 6.42 (d, *J* = 2.4 Hz, 1H), 3.74 (s, 3H), 3.30 (s, 3H).

^{13}C NMR (101 MHz, DMSO-D_6) δ 168.8, 160.6, 157.5, 131.6, 128.4, 128.2, 121.8, 121.8, 121.5, 104.2, 99.5, 85.2, 55.5, 55.2.

3-[3,5-Bis(trifluoromethyl)phenyl]-3-hydroxy-indan-1one, 104d

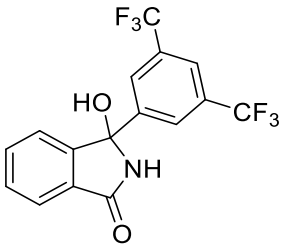

112d was prepared according to general procedure C from phthalimide (400 mg, 1.36 mmol, in 0.5 M THF), 1,3-bis(trifluoromethyl)-5-bromobenzene (1.95 mL, 5.44 mmol in 0.5 M THF) and butyllithium (4.00 mL, 4.76 mmol) resulting in the desired crude product. Purification by column chromatography (1:1 EtOAc:Hex) resulted in obtaining the pure product as a white solid (504 mg, 51%).

R_F (1:1 EtOAc:Hex) = 0.58

^{1}H NMR (400 MHz, DMSO-D_6) δ 9.45 (s, 1H), 8.14 (s, 1H), 8.04 (s, 2H), 7.75 – 7.67 (m, 1H), 7.63 – 7.52 (m, 2H), 7.48 (s, 1H), 7.44 – 7.38 (m, 1H).

^{13}C NMR (101 MHz, DMSO-D_6) δ 168.8, 149.4, 146.0, 133.1, 130.9 (q, J=32.9Hz), 130.7, 129.9, 127.4, 123.6 (q, J=272.9Hz), 123.1, 122.3, 86.7.

^{19}F NMR (376 MHz, DMSO-D_6): -61.3

Data in accordance with literature. [58]

3-Hydroxy-3-(3-methoxyphenyl)indan-1one, 112b

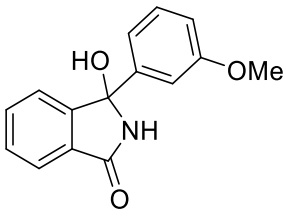

112b was prepared according to general procedure C from phthalimide (200 mg, 1.36 mmol, in 0.5 M THF), 3-bromoanisole (0.70 mL, 5.44 mmol in 0.5 M THF) and butyllithium (1.90 mL, 4.76 mmol) resulting in the desired crude product. Purification by column chromatography (3:1 EtOAc:Hex) resulted in obtaining the pure product as a white solid (271 mg, 79%).

R_F (1:1 EtOAc:Hex) = 0.19

^{1}H NMR (400 MHz, DMSO) δ 9.23 (s, 1H), 7.67 – 7.61 (m, 1H), 7.54 (td, *J* = 7.4, 1.3 Hz, 1H), 7.48 (td, *J* = 7.4, 1.1 Hz, 1H), 7.37 – 7.31 (m, 1H), 7.25 (t, *J* = 8.0 Hz, 1H), 7.09 (dd, *J* = 2.4, 1.7 Hz, 1H), 6.98 – 6.94 (m, 1H), 6.91 (s, 1H), 6.87 (ddd, *J* = 8.2, 2.6, 0.9 Hz, 1H).

^{13}C NMR (101 MHz, DMSO-D_6) δ 168.8, 159.6, 151.1, 144.3, 132.8, 130.9, 129.8, 129.3, 123.2, 122.9, 118.1, 113.4, 111.8, 87.6, 55.5.

Data in accordance with literature. [60]

3-Hydroxy-3-(6-methoxy-2-pyridyl)indan-1one, 112g

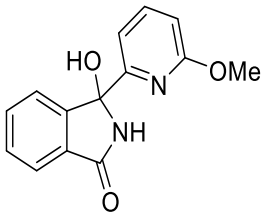

112g was prepared according to general procedure C from phthalimide (200 mg, 1.36 mmol, in 0.5 M THF), 6-bromo 2-methoxypyridine (0.70 mL, 5.44 mmol in 0.5 M THF) and butyllithium (1.90 mL, 4.76 mmol) resulting in the desired crude product. Purification by column chromatography (3:1 EtOAc:Hex) resulted in obtaining the pure product as a white solid (207 mg, 59%).

R_F (1:1 EtOAc:Hex) = 0.22

IR νmax (cm^{-1}): 3259, 3055, 1703, 1284.

HRMS (APCI) m/z: $[M + H]^+$ Calcd for $C_{14}H_{13}N_2O_3$ 257.0921; Found 257.0929

^{1}H NMR (400 MHz, DMSO-D_6) δ 9.13 (s, 1H), 7.79 – 7.71 (m, 1H), 7.62 (d, *J* = 7.4 Hz, 1H), 7.52 (dd, *J* = 7.4, 1.3 Hz, 1H), 7.49 – 7.39 (m, 3H), 6.94 (s, 1H), 6.71 (dd, *J* = 8.2, 0.7 Hz, 1H), 3.64 (s, 3H).

^{13}C NMR (101 MHz, DMSO-D_6) δ 168.8, 162.7, 157.9, 149.8, 139.8, 132.0, 131.5, 128.9, 123.0, 122.3, 113.0, 109.6, 87.6, 52.7.

3-Hydroxy-3-[6-(trifluoromethyl)-2-pyridyl]isoindolin-1one, 112h

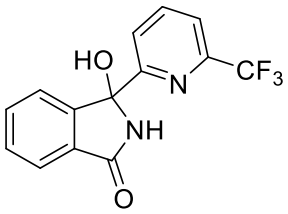

112h was prepared according to general procedure C from phthalimide (150 mg, 1.02 mmol, in 0.5 M THF), 2-bromo-6-(trifluoromethyl)pyridine (900 mg, 4.06 mmol in 0.5 M THF) and butyllithium (1.40 mL, 3.57 mmol) resulting in the desired crude product. Purification by column chromatography (3:1 EtOAc:Hex) resulted in obtaining the pure product as a white solid (204 mg, 68%).

R_F (1:1 EtOAc:Hex) = 0.21

IR νmax (cm^{-1}): 3309, 1697, 1340, 1123.

HRMS (APCI) m/z: $[M + H]^+$ Calcd for $C_{14}H_{10}F_3N_2O_2$ 295.0689; Found 295.0682

^{1}H NMR (400 MHz, DMSO-D_6) δ 8.46 (s, 1H), 7.41 – 7.30 (m, 2H), 7.00 (dd, *J* = 7.3, 1.4 Hz, 1H), 6.82 (ddd, *J* = 7.1, 1.3, 0.8 Hz, 1H), 6.74 – 6.62 (m, 2H), 6.60 – 6.51 (m, 1H), 6.43 (s, 1H).

^{13}C NMR (101 MHz, DMSO-D_6) δ 169.1, 161.6, 149.7, 149.1(q, *J*=34.0Hz), 140.0, 132.7, 131.8, 129.7, 124.7, 123.4, 123.0, 121.8 (q, *J*=274.7), 120.5, 88.0.

^{19}F NMR (376 MHz DMSO-D_6): -66.4

N-[Methoxy(phenyl)methyl]benzamide, 121

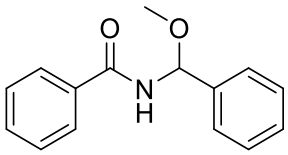

121 was prepared according to general procedure D from benzamide (1.00 g, 8.25 mmol) *i*PrMgCl.LiCl (6.7 mL, 8.67 mmol, 1.3M in THF) and benzaldehyde (0.93 mL, 9.10 mmol) in THF (20 mL) to afford the hemiaminal. Transacetalisation in MeOH (20 mL) and PPTS (88 mg, 0.35 mmol). Purification by column chromatography (1:3 EtOAc:Hex 1% NEt_3) resulted in obtaining the pure product as a white solid (1.58 g, 79%).

R_F (1:3 EtOAc:Hex) = 0.33

^{1}H NMR (400 MHz, DMSO-D_6) δ 9.20 (d, *J* = 9.0 Hz, 1H), 7.96 (dd, *J* = 5.3, 3.4 Hz, 2H), 7.62 – 7.52 (m, 1H), 7.52 – 7.43 (m, 4H), 7.42 – 7.37 (m, 2H), 7.35 – 7.30 (m, 1H), 6.28 (d, *J* = 9.0 Hz, 1H), 3.40 (s, 3H).

^{13}C NMR (101 MHz, DMSO-D_6) δ 166.9, 139.8, 133.8, 131.7, 128.3, 128.2, 128.0, 127.7, 126.4, 81.8, 55.3.

Data in accordance with literature. [13]

N-Phenyl phthalimide, 118

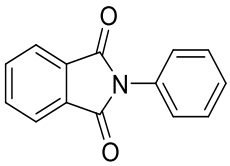

118 was prepared according to general procedure E from phthalic anhydride (10.0 g, 67.5 mmol) and aniline (7.40 mL, 81.0 mmol) dissolved in acetic acid (2.5 M) to produce a white solid of N-phenyl phthalimide (14.8 g, 98%).

R_F (1:1 EtOAc:Hex) = 0.63

^{1}H NMR (400 MHz, DMSO-D_6) δ 8.15 – 7.79 (m, 4H), 7.72 – 7.34 (m, 5H).

^{13}C NMR (101 MHz, DMSO-D_6) δ 167.2, 134.9, 132.1, 131.7, 129.0, 128.2, 127.6, 123.6.

Data in accordance with literature. [61]

Synthesis of dienes

General Procedure F – Wittig on B-unsaturated aldehydes. [62]

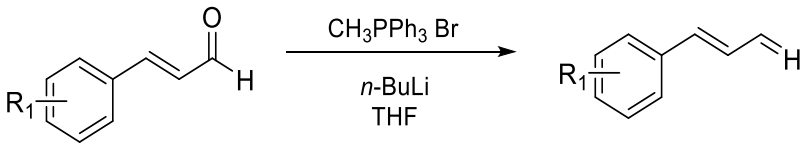

Methyltriphenylphosphonium bromide (0.6 equiv) was dissolved in THF (0.2 M) and stirred at -78°C under an inert atmosphere and N-BuLi (1.0 equiv) was added. After 15 mins a cinnamaldehyde derivative (1.0 equiv) was added. The reaction was warmed to room temperature. Once TLC analysis indicated completion, the reaction mixture was quenched with sat. NH4Cl aq. and extracted with EtOAc. The organic layer as dried over $MgSO_4$ filtered then concentrated in vacuo. The crude sample was purified using flash column chromatography to afford the pure product.

General Procedure G – Double Wittig on Benzils. [62]

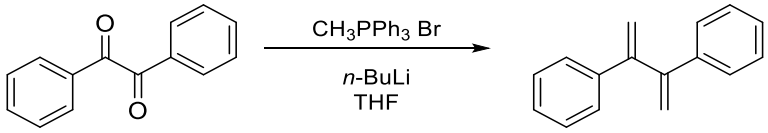

Methyltriphenylphosphonium bromide (2.4 equiv) was dissolved in THF (0.2 M) and stirred at -78°C under an inert atmosphere and nBuLi (2.4 equiv) was added. After 15 mins Benzil (1.0 equiv) was added. The reaction was warmed to room temperature. Once TLC analysis indicated completion, the reaction mixture was quenched with sat. NH4Cl aq. and extracted with EtOAc. The organic layer as dried over $MgSO_4$ filtered then concentrated in vacuo. The crude sample was purified using flash column chromatography, to afford the pure product.

General Procedure H – Synthesis of asymmetric dienes. [63]

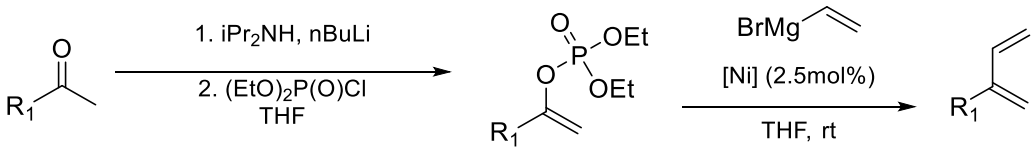

iPr_2NH (1.1 equiv) was stirred at -78°C under an inert atmosphere and n-BuLi (1.1 equiv) was added dropwise. After 15min, ketone was added (1.0 equiv) dropwise. A further

30mins later was added diethyl chlorophosphite (1.5 equiv) dropwise and stirred at -78°C until TLC analysis indicated completion. The resulting mixture was quenched with ethanol at -78°C, then sat. NH4Cl aq. was added at 0°C. The solution was extracted into diethyl ether (3X50 mL). The organic layer was dried over Na_2SO_4 filtered and concentrated in vacuo. The crude sample was purified using flash chromatography to afford the pure product.

[(dppe)$NiCl_2$] (2.5 mol%) was dissolved in anhydrous THF (0.25 M) in a Schlenk and cooled to 0 °C and enol phosphate was added (1.0 equiv) to the solution. Vinyl grignard (1.05 equiv) was added dropwise. The reaction was warmed up to room temperature and stirred for 1h. The reaction was then quenched with sat. NH_4Cl aq. at 0 °C and extracted with diethyl ether. The organic layer was dried over Na_2SO_4 filtered and concentrated in vacuo. The crude sample was purified using flash chromatography.

1 -(1,3-Butadien-1-yl)-2-methoxybenzene, 136b

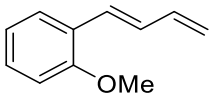

136b was prepared fowling general procedure F from Methyltriphenylphosphonium bromide (493 mg, 3.0 mmol), *n*BuLi (0.74 mL, 1.85 mmol), 2-methoxycinnmaldehyde (500 mg, 3.08 mmol) and THF (15.0 mL, 0.2 M). Purification by column chromatography (Hex) resulted in obtaining the pure product as a yellow oil (178 mg, 36%).

R_F (1:1 EtOAc:Hex) = 0.82

^{1}H NMR (400 MHz, $CDCl_3$) δ 7.48 (dd, *J* = 7.7, 1.7 Hz, 1H), 7.22 (ddd, *J* = 8.3, 7.4, 1.7 Hz, 1H), 7.02 – 6.74 (m, 1H), 6.54 (dt, *J* = 16.9, 10.1 Hz, 1H), 5.41 – 5.25 (m, 1H), 5.22.

^{13}C NMR (101 MHz, $CDCl_3$) δ 157.3, 138.4, 130.7, 129.1, 128.1, 126.9, 126.6, 121.1, 117.4, 111.4, 55.9.

Data in accordance with literature. [64]

(2-Methyl-1,3-butadien-1-yl) benzene, 136a

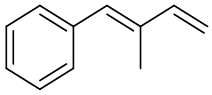

136a was prepared fowling general procedure F from Methyltriphenylphosphonium bromide (575 mg, 3.42 mmol), *n*BuLi (0.82 mL, 2.05 mmol), alpha-methyl-trans-cinnamaldehyde (500 mg, 3.42 mmol) and THF (17.0 mL, 0.2 M). Purification by column chromatography (Hex) resulted in obtaining the pure product as a clear oil (99 mg, 20%).

R_F (1:1 EtOAc:Hex) = 0.95

^{1}H NMR (400 MHz, $CDCl_3$) δ 7.36 (d, *J* = 7.7 Hz, 1H), 7.34 – 7.29 (m, 1H), 7.26 – 7.21 (m, 1H), 6.65 – 6.51 (m, 1H), 5.31 (d, *J* = 17.5 Hz, 1H), 5.14 (d, *J* = 10.7 Hz, 1H), 2.01 (d, *J* = 1.3 Hz, 1H).

^{13}C NMR (101 MHz, $CDCl_3$) δ 142.0, 137.9, 136.1, 131.8, 129.4, 129.3, 128.3, 128.2, 126.8, 113.1, 13.3.

Data in accordance with literature. [65]

1,4-Diphenyl-1,3-butadiene, 137a

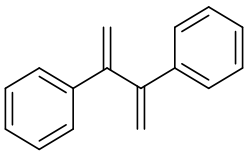

137a was prepared according to general procedure G from Benzil (2.50 g, 11.9 mmol), Methyltriphenylphosphonium bromide (10.2 g, 28.5 mmol) and *n*BuLi (11.4mL, 28.5 mmol) and THF (0.5 M). Purification by column chromatography (Hex) resulted in obtaining the pure product as a white solid (756 mg, 31%).

R_F (1:1 EtOAc:Hex) = 0.96

^{1}H NMR (400 MHz, $CDCl_3$) δ 7.42 – 7.35 (m, 4H), 7.28 (t, *J* = 1.8 Hz, 1H), 7.25 (dd, *J* = 3.6, 2.2 Hz, 3H), 7.20 (dt, *J* = 2.8, 2.0 Hz, 1H), 5.54 (d, *J* = 1.7 Hz, 2H), 5.31 (d, *J* = 1.7 Hz, 2H).

^{13}C NMR (101 MHz, $CDCl_3$) δ 149.9, 140.3, 128.3, 127.6, 116.5. *(1 Aromatic hidden)*

Data in accordance with literature. [66]

(4,4-Dimethoxydiphenyl)buta-1,3-diene, 137b

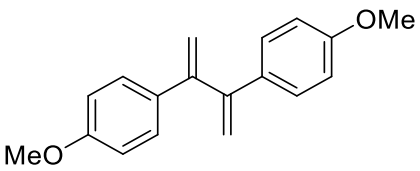

137b was prepared according to general procedure G from (3.00 g, 11.1 mmol), Methyltriphenylphosphonium bromide (9.52 g, 26.6 mmol) and *n*BuLi (10.7 mL, 26.6 mmol) and THF (0.5 M). Purification by column chromatography (Hex) resulted in obtaining the pure product as a white solid (700 mg, 24%).

R_F (1:1 EtOAc:Hex) = 0.71

^{1}H NMR (400 MHz, $CDCl_3$) δ 7.54 – 7.28 (m, 4H), 6.89 – 6.66 (m, 4H), 5.47 (d, *J* = 1.8 Hz, 2H), 5.24 (d, *J* = 1.8 Hz, 2H), 3.77 (s, 6H).

^{13}C NMR (101 MHz, $CDCl_3$) δ 159.2, 149.5, 132.8, 128.6, 114.5, 113.7, 55.4.

Data in accordance with literature.[67]

(4,4-Fluorodiphenyl)buta-1,3-diene, 137c

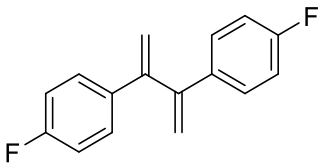

137c was prepared according to general procedure G from 4,4'-difluorobenzil (2.50 g, 10.2 mmol), Methyltriphenylphosphonium bromide (8.71 g, 24.4 mmol) and *n*BuLi (9.75 mL, 24.4 mmol) and THF (0.5 M). Purification by column chromatography (Hex) resulted in obtaining the pure product as a white solid (700 mg, 28%).

R_F (1:1 EtOAc:Hex) = 0.96

1H NMR (400 MHz, CDCl3) δ 7.67 – 7.61 (m, 4H), 7.26 (dd, *J* = 9.7, 7.8 Hz, 4H), 5.80 (d, *J* = 1.4 Hz, 2H), 5.61 (d, *J* = 1.3 Hz, 2H).

^{13}C NMR (101 MHz, $CDCl_3$) δ 162.5(d, *J* = 246.8Hz), 148.87, 136.1(d, *J* = 3.3Hz), 129.2(d, *J* = 8.1Hz), 116.4, 115.3(d, *J* = 21.4Hz)

^{19}F NMR (376 MHz, $CDCl_3$): -114.73

Data in accordance with literature.[68]

Diethyl 1-phenylvinyl phosphate, 163a

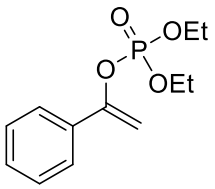

163aa was prepared following general procedure H from Acetophenone (971 µL, 8.32 mmol), diisoproylamine (1.28 mL, 9.16 mmol), *n*BuLi (3.66 mL, 9.16 mmol) and diethyl chlorophosphite (1.80 mL, 12.5 mmol) in a solution of THF (0.3 M). Purification by column chromatography (1:1 EtOAc:Hex) resulted in obtaining the pure product as a white solid (739 mg, 35%).

R_F (1:1 Hex:EtOAc) = 0.17

^{1}H NMR (400 MHz, $CDCl_3$) δ 7.59 (dd, *J* = 7.7, 2.1 Hz, 2H), 7.39 – 7.31 (m, 3H), 5.30 – 5.27 (m, 1H), 5.23 (dd, *J* = 2.8, 2.1 Hz, 1H), 4.20 (tdd, *J* = 7.0, 4.6, 3.5 Hz, 4H), 1.34 (td, *J* = 7.1, 1.1 Hz, 6H).

^{13}C NMR (101 MHz, $CDCl_3$) δ 152.4, 134.4 129.21, 128.51, 125.35, 97.4 64.7, 16.2

Data in accordance with literature.[63]

2-Phenyl-1,3-butadiene, 138a

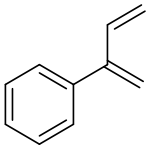

138a was prepared following general procedure H from XX (650 mg, 2.54 mmol) vinyl grignard (2.66 mL, 2.66 mmol), [Ni(dppe)Cl_2] (33 mg, 63.4 µmol) dissolved in THF (0.25 M) Purification by column chromatography (Pent, 1% NEt_3) resulted in obtaining the pure product as a white solid (192 mg, 58%).

R_F (1 pentane) = 0.77

^{1}H NMR (400 MHz, $CDCl_3$) δ 7.40 – 7.29 (m, 5H), 6.63 (dd, *J* = 17.3, 11.1 Hz, 1H), 5.35 – 5.27 (m, 1H), 5.26 – 5.13 (m, 3H).

^{13}C NMR (101 MHz, $CDCl_3$) δ 148.4, 139.9, 138.3, 128.4, 128.3, 127.6, 117.3, 117.0.

Data in accordance with literature.[69]

Synthesis of Diels-Alder products and their synthetic applications

General Procedure I – Diels alder of functionalised Isoindolinones.

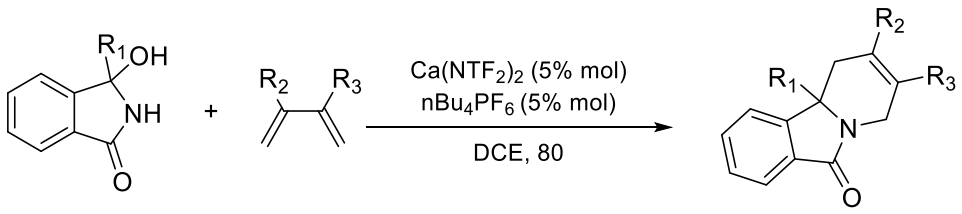

3-hydroxy Isoindolinone (1.0 equiv) was added to a pressure regulated vial with Calcium(ii) bis(trifluoromethanesulfonimide) (5 mol%) and tetrabutylammonium hexafluorophosphate (5 mol%) and dissolved in DCE (0.2 M). 2,3-Dimethyl-1,3-butadiene (1.50 equiv) was added to the solution, the reaction was stirred at 80°C until TLC analysis indicated completion. The pure product was obtained using flash chromatography.

General Procedure J – synthesis of bis-amide.

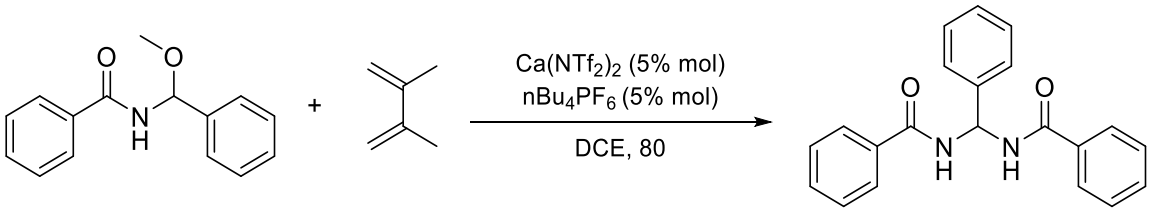

N,O-Acetal (1.0 equiv) was added to a pressure regulated vial with Calcium(ii) bis(trifluoromethanesulfonimide) (5 mol%) and tetrabutylammonium hexafluorophosphate (5 mol%) and dissolved in DCE (0.2 M). 2,3-Dimethyl-1,3-butadiene (1.50 equiv) was added to the solution, the reaction was stirred at 80°C until TLC analysis indicated completion. The pure product precipitated out of reaction and was filtered off.

General Procedure K – Amide reduction.[46]

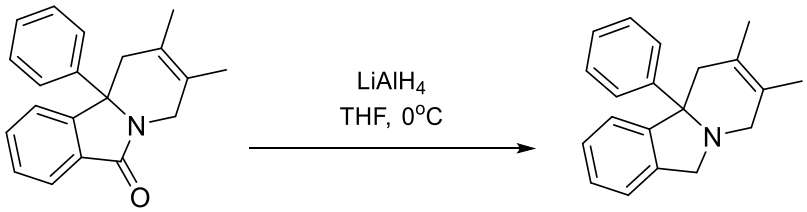

To an oven dried round bottom glass was added amide (1.0 equiv) dissolved in THF (0.025 M) and $LiAlH_4$ (10.0 equiv) was added dropwise at 0°C. The solution was then warmed to

r.t. and stirred until TLC analysis indicated completion. The reaction mixture was quenched at 0°C with H_2O and NaOH (1.0 M) and extracted with Et_2O. The organic layers were dried over Na_2SO_4 and concentrated in vacuo. The amine was isolated using flash chromatography to afford the pure product.

General Procedure L – m-CPBA epoxidation.[47]

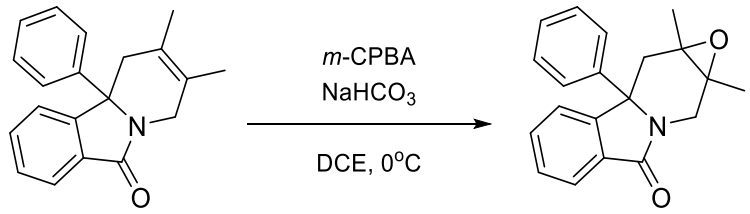

To an oven dried Schlenk flask under an inert atmosphere was added alkene (1.0 equiv), sodium hydrogen carbonate (1.3 equiv) dissolved in DCM. The reaction was then cooled to 0°C and *m*-CPBA (70 %, 1.2 equiv) was dissolved in DCM and added dropwise to the reaction over 20minuets. The reaction was stirred at 0°C for 1hour, then warmed to room temperature. Once TLC analysis indicate completion the reaction was quenched with $Na_2S_2O_4$ and extracted with DCM and washed with $NaHCO_3$ and brine. The organic layers were dried over Na_2SO_4 and concentrated in vacuo. The epoxide was isolated using flash chromatography.

General Procedure M – Upjohn dihydroxylation.[50]

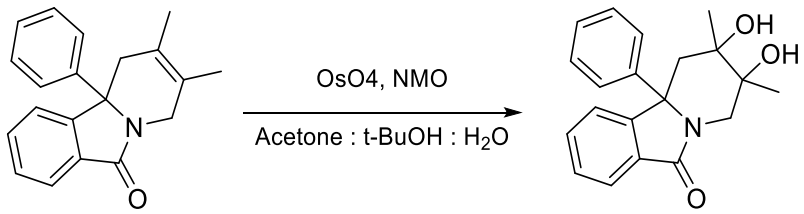

The olefin (1.0 equiv) was dissolved in a mixture of acetone, t-BuOH and water (18:1:1). To the solution was added a solution of 4% wt of OsO4 in H_2O followed by the addition of N-methyl morpholine N-oxide at rt. Reactions were monitored as possible by ^{1}H-NMR of aliquots. Upon completion, the reaction was quenched and extracted with Et_2O and washed with brine. The organic layers were dried over Na_2SO_4 and concentrated in vacuo. The diol was isolated using flash chromatography.

2,3-Dimethyl-10b-phenyl-1,4-dihydropyrido[2,1-a]isoindol-6-one, 132a

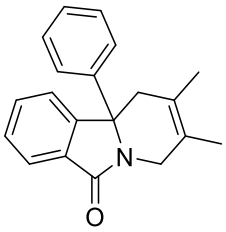

132a was prepared according to general procedure I from 3-hydroxy-3-phenyl-isoindolin-1-one (40.0 mg, 178 µmol), calcium(ii) bis(trifluoromethanesulfonimide) (5.0 mg, 8.88 µmol), tetrabutylammonium hexafluorophosphate (4.0 mg, 8.88 µmol) and 2,3-Dimethyl-1,3-butadiene (30.0 µL, 266 µmol) in DCE (0.2 M). Purification by column chromatography (1:1 EtOAc:Hex) resulted in obtaining the pure product as a white solid (35 mg, 88%).

R_F (1:1 EtOAc:Hex) = 0.66

IR νmax (cm^{-1}): 2920, 2829, 1690, 1671, 1397, 1099

HRMS (APCI) m/z: $[M + H]^+$ Calcd for $C_{20}H_{20}NO$ 290.1545; Found 290.1527

^1H NMR (400 MHz, $CDCl_3$) δ 7.90 (ddd, *J* = 7.6, 3.7, 2.9 Hz, 1H), 7.48 – 7.39 (m, 2H), 7.32 – 7.27 (m, 2H), 7.23 (dt, *J* = 2.8, 1.9 Hz, 1H), 7.20 – 7.14 (m, 3H), 4.53 (d, *J* = 18.6 Hz, 1H), 3.29 (d, *J* = 17.5 Hz, 1H), 3.18 (d, *J* = 16.6 Hz, 1H), 2.32 (d, *J* = 16.2 Hz, 1H), 1.77 (s, 3H), 1.63 – 1.56 (m, 3H).

^{13}C NMR (101 MHz, $CDCl_3$) δ 166.9, 152.1, 139.1, 131.9, 130.9, 128.9, 128.1, 127.8, 125.9, 124.1, 123.1, 122.1, 121.8, 65.1, 42.2, 39.1, 19.2, 16.0.

10b-(4-Methoxyphenyl)-2,3-dimethyl-1,4-dihydropyrido[2,1-a]isoindol-6-one, 132b

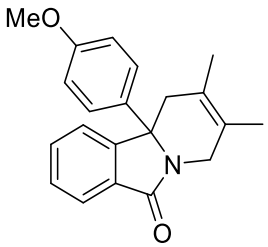

132b was prepared according to general procedure I from 3-hydroxy-3-(4-methyloxyohenyl)isoindolin-1one (30.0 mg, 118 µmol), calcium(ii) bis(trifluoromethanesulfonimide) (4.0 mg, 5.88 µmol), tetrabutylammonium

hexafluorophosphate (3.0 mg, 5.88 µmol) and 2,3-Dimethyl-1,3-butadiene (20.0 µL, 176 µmol) in DCE (0.2 M). Purification by column chromatography (1:1 EtOAc:Hex) resulted in obtaining the pure product as a white solid (30 mg, 79%).

R_F (1:1 EtOAc:Hex) = 0.58

IR νmax (cm^{-1}): 2922, 2836, 1690, 1246, 1028.

HRMS (APCI) m/z: $[M + H]^+$ Calcd for $C_{22}H_{22}NO_2$ 320.1635; Found 320.1635

^1H NMR (400 MHz, $CDCl_3$) δ 7.97 – 7.83 (m, 1H), 7.42 (pd, *J* = 7.4, 1.4 Hz, 2H), 7.17 (dd, *J* = 6.2, 1.5 Hz, 1H), 7.06 (d, *J* = 8.9 Hz, 2H), 6.80 (d, *J* = 8.9 Hz, 2H), 4.51 (d, *J* = 18.0 Hz, 1H), 3.76 (s, 1H), 3.26 (d, *J* = 17.6 Hz, 1H), 3.12 (d, *J* = 16.7 Hz, 1H), 2.29 (d, *J* = 16.7 Hz, 1H), 1.76 (s, 3H), 1.59 (s, 3H).

^{13}C NMR (101 MHz, $CDCl_3$) δ 166.8, 159.2, 152.6, 131.9, 131.0, 130.9, 128.2, 127.4, 124.1, 123.3, 122.2, 121.9, 114.4, 64.9, 55.5, 42.2, 39.4,19.3, 16.2.

2,3-Dimethyl-10b-[4-(trifluoromethyl)phenyl]-1,4-dihydropyridol[2,1-a]indol-6-one, 132c

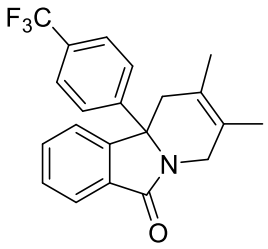

132c was prepared according to general procedure I from 3-hydroxy-3-[4-trifluoromethyl)phenyl]isoindolin-1one (50.0 mg, 171 µmol), calcium(ii) bis(trifluoromethanesulfonimide) (5.0 mg, 8.53 µmol), tetrabutylammonium hexafluorophosphate (3.0 mg, 8.53 µmol) and 2,3-Dimethyl-1,3-butadiene (30.0 µL, 256 µmol) in DCE (0.2 M). Purification by column chromatography (1:1 EtOAc:Hex) resulted in obtaining the pure product as a white solid (24 mg, 66%).

R_F (1:1 EtOAc:Hex) = 0.74

IR νmax (cm^{-1}): 2924, 2857, 1694, 1615, 1321, 717.

HRMS (APCI) m/z: $[M + H]^+$ Calcd for $C_{21}H_{19}F_3NO_2$ 358.1409; Found 358.1401

^{1}H NMR (400 MHz, $CDCl_3$) δ 7.92 (ddd, *J* = 3.4, 2.3, 0.7 Hz, 1H), 7.55 (d, *J* = 8.4 Hz, 2H), 7.50 – 7.42 (m, 2H), 7.29 (d, *J* = 8.2 Hz, 2H), 7.18 – 7.09 (m, 2H), 4.56 (d, *J* = 17.9 Hz, 1H), 3.27 (d, *J* = 17.9 Hz, 1H), 3.18 (d, *J* = 16.9 Hz, 1H), 2.37 (d, *J* = 16.9 Hz, 1H), 1.77 (s, 3H), 1.60 (s, 3H).

^{13}C NMR (101 MHz, $CDCl_3$) δ 166.9, 151.3, 143.5, 134.4, 132.1, 130.9, 130.14 (q, *J* = 32.6 Hz), 128.5, 126.4, 126.0 (d, *J* = 3.7 Hz), 124.3, 124.0 (q, *J* = 272.1 Hz), 123.4, 121.9, 121.8, 64.9, 42.2, 39.1, 19.2, 16.0.

^{19}F NMR (376 MHz, $CDCl_3$): -62.65

10b-(1,3-Benzodioxol-4-yl)-2,3-dimethyl-1,4-dihydropyrido[2,1-a]isoindol-6-one, 132f

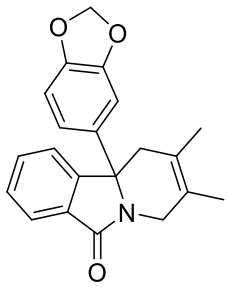

132f was prepared according to general procedure I from 3-(1,3-benzodioxol-5-yl)-3hydroxy-indan-1one (73.0 mg, 271 µmol), calcium(ii) bis(trifluoromethanesulfonimide) (8.0 mg, 13.6 µmol), tetrabutylammonium hexafluorophosphate (5.00 mg, 13.6 µmol) and 2,3-Dimethyl-1,3-butadiene (30.0 µL, 256 µmol) in DCE (0.2 M). Purification by column chromatography (1:1 EtOAc:Hex) resulted in obtaining the pure product as a white solid (60 mg, 67%).

R_F (1:1 EtOAc:Hex) = 0.42

IR νmax (cm^{-1}): 3047, 2853, 692, 1671, 1231, 1097.

HRMS (APCI) m/z: $[M + H]^+$ Calcd for $C_{21}H_{20}NO_3$ 334.1443; Found 334.1433

^{1}H NMR (400 MHz, $CDCl_3$) δ 7.98 – 7.83 (m, 1H), 7.44 (ddd, *J* = 7.8, 7.0, 1.3 Hz, 2H), 7.24 – 7.16 (m, 1H), 6.69 (dt, *J* = 8.2, 5.0 Hz, 2H), 6.57 (d, *J* = 1.7 Hz, 1H), 5.92 (dd, *J* = 7.6, 1.4 Hz, 2H), 4.51 (d, *J* = 17.8 Hz, 1H), 3.30 (d, *J* = 17.9 Hz, 1H), 3.07 (d, *J* = 16.8 Hz, 1H), 2.29 (d, *J* = 16.7 Hz, 1H), 1.75 (s, 3H), 1.61 (s, 3H).

^{13}C NMR (101 MHz, $CDCl_3$) δ 166.8, 152.2, 148.3, 147.2, 132.9, 131.9, 130.8, 128.2, 124.1, 123.1, 122.0, 121.7, 119.4, 108.5, 106.7, 101.4, 65.0, 42.1, 39.4, 19.2, 16.1.

10b-(2,4-Dimethoxyphenyl)-2,3-dimethyl-1,4-dihydropyrido[2,1-a]isoindol-6-one, 132e

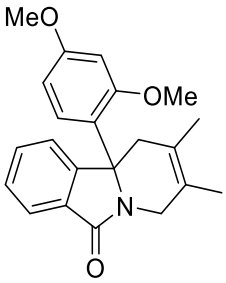

132e was prepared according to general procedure I from 3-(2,4dimethoxyphenyl)-3hydroxy-indan-1one (50 mg, 175 µmol), calcium(ii) bis(trifluoromethanesulfonimide) (5.00 mg, 8.76 µmol), tetrabutylammonium hexafluorophosphate (3.00 mg, 8.76 µmol) and 2,3-Dimethyl-1,3-butadiene (30.00 µL, 263 µmol) in DCE (0.2 M). Purification by column chromatography (1:1 EtOAc:Hex) resulted in obtaining the pure product as a white solid (22 mg, 60%).

R_F (1:1 EtOAc:Hex) = 0.42

IR νmax (cm^{-1}): 2920, 2851, 1690, 1669, 1466, 1028.

HRMS (APCI) m/z: $[M + H]^+$ Calcd for $C_{22}H_{24}NO_3$ 350.1756; Found 350.1734

^{1}H NMR (400 MHz, $CDCl_3$) δ 8.01 – 7.75 (m, 1H), 7.53 – 7.33 (m, 2H), 7.25 (s, 1H), 7.05 (t, *J* = 19.1 Hz, 1H), 6.52 – 6.27 (m, 2H), 4.49 (d, *J* = 17.6 Hz, 1H), 3.77 (s, 3H), 3.44 (s, 3H), 3.36 – 3.11 (m, 2H), 2.15 (d, *J* = 16.6 Hz, 1H), 1.76 (s, 3H), 1.59 (s, 3H).

^{13}C NMR (101 MHz, $CDCl_3$) δ 166.8, 160.8, 159.5, 152.5, 132.1, 131.2, 129.2, 127.5, 123.5, 122.8, 122.3, 120.9, 118.5, 104.1, 100.1, 64.2, 55.5, 55.3, 42.3, 40.4, 18.9, 15.9.

10b-(3-Methoxyphenyl)-2,3-dimethyl-1,4-dihydropyrido[2,1-a]isoindol-6-one, 132d

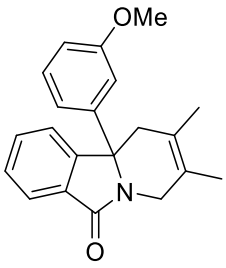

132d was prepared according to general procedure I from 3-hydroxy-3-(3-methoxyphenyl)indan-1one (50 mg, 196 µmol), calcium(ii) bis(trifluoromethanesulfonimide) (6.00 mg, 9.79 µmol), tetrabutylammonium hexafluorophosphate (4.00 mg, 9.79 µmol) and 2,3-Dimethyl-1,3-butadiene (30.00 µL, 294 µmol) in DCE (0.2 M). Purification by column chromatography (3:1 EtOAc:Hex) resulted in obtaining the pure product as a white solid (47 mg, 75%).

R_F (1:1 EtOAc:Hex) = 0.60

IR νmax (cm^{-1}): 2963,2853, 1686, 1669, 1399, 1034.

HRMS (APCI) m/z: $[M + H]^+$ Calcd for $C_{22}H_{21}NO_2$ 320.1651; Found 320.1648

^{1}H NMR (400 MHz, $CDCl_3$) δ 7.88 (dd, *J* = 8.0, 6.4 Hz, 1H), 7.43 (p, *J* = 7.2 Hz, 2H), 7.22 (dd, *J* = 9.2, 7.0 Hz, 2H), 6.85 – 6.63 (m, 3H), 4.54 (d, *J* = 17.8 Hz, 1H), 3.74 (s, 3H), 3.34 (d, *J* = 17.5 Hz, 1H), 3.14 (d, *J* = 16.7 Hz, 1H), 2.30 (d, *J* = 16.4 Hz, 1H), 1.75 (s, 3H), 1.58 (d, *J* = 9.7 Hz, 3H).

^{13}C NMR (101 MHz, $CDCl_3$) δ 167.3, 160.4, 152.3, 141.2, 132.2, 131.2, 130.3, 128.5, 124.4, 123.4, 122.4, 122.1, 118.5, 112.9, 112.6, 65.5, 55.7, 42.6, 39.6, 19.5, 16.4.

10b-(6-Methoxy-2-pyridyl)-2,3-dimethyl-1,4-dihydropyrido[2,1-a]isoindol-6-one, 132h

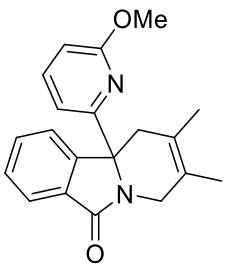

132h was prepared according to general procedure I from 3-hydroxy-3-(6-methoxy-2-pyridyl)indan-1one (50 mg,195 µmol), calcium(ii) bis(trifluoromethanesulfonimide) (6.00 mg, 9.76 µmol), tetrabutylammonium hexafluorophosphate (4.00 mg, 9.76 µmol) and 2,3-Dimethyl-1,3-butadiene (30 µL, 293 µmol) in DCE (0.2 M). Purification by column chromatography (1:1 EtOAc:Hex) resulted in obtaining the pure product as a white solid (22 mg, 37%).

R_F (1:1 EtOAc:Hex) = 0.72

IR νmax (cm^{-1}): 2976, 2853,1694, 1464, 1320, 1023.

HRMS (APCI) m/z: $[M + H]^+$ Calcd for $C_{20}H_{21}N_2O_2$ 321.1603; Found 321.1608

^1H NMR (400 MHz, $CDCl_3$) δ 7.97 – 7.82 (m, 1H), 7.58 – 7.36 (m, 4H), 6.65 (ddd, *J* = 14.3, 7.8, 0.6 Hz, 2H), 4.62 (d, *J* = 18.6 Hz, 1H), 4.05 (s, *J* = 19.2 Hz, 3H), 3.79 (dd, *J* = 20.1, 13.9 Hz, 1H), 3.59 (d, *J* = 17.9 Hz, 1H), 2.23 (d, *J* = 15.8 Hz, 1H), 1.71 (s, 3H), 1.62 (s, 3H).

^{13}C NMR (101 MHz, $CDCl_3$) δ 168.0, 164.3, 156.7,151.0, 139.9, 132.1, 130.9, 128.6, 124.3, 123.2, 122.3, 121.9, 112.2, 109.9, 67.2, 53.7, 43.1, 39.1, 19.6, 16.4.

2,3-Dimethyl-10b-[6-(trifluoromethyl)-2-pyridyl]-1,4-dihydropyrido[2,1-a]isoindol-6-one, 132g

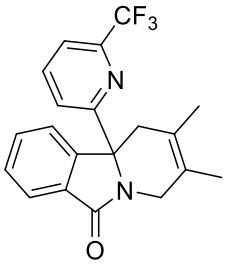

132g was prepared according to general procedure I from 3-hydroxy-3-[6-(trifluoromethyl)-2-pyridyl]isoindolin-1one (50 mg, 170 µmol), calcium(ii) bis(trifluoromethanesulfonimide) (5.00 mg,8.50 µmol), tetrabutylammonium hexafluorophosphate (3.00 mg, 8.50 µmol) and 2,3-Dimethyl-1,3-butadiene (30.00 µL, 255 µmol) in DCE (0.2 M). Purification by column chromatography (1:1 EtOAc:Hex) resulted in obtaining the pure product as a white solid (36 mg, 60%).

R_F (1:1 EtOAc:Hex) = 0.60

IR νmax (cm^{-1}): 2994, 2916, 1695, 1593, 1338, 1112, 993.

HRMS (APCI) m/z: $[M + H]^+$ Calcd for $C_{20}H_{18}F_3N_2O$ 359.1371; Found 359.1369

^1H NMR (400 MHz, $CDCl_3$) δ 7.99 – 7.81 (m, 1H), 7.73 (ddd, *J* = 7.8, 3.4, 1.7 Hz, 1H), 7.54 (dt, *J* = 9.2, 4.6 Hz, 1H), 7.51 – 7.36 (m, 3H), 7.22 (d, *J* = 8.0 Hz, 1H), 4.64 (d, *J* = 18.0 Hz, 1H), 3.91 (dd, *J* = 33.3, 16.0 Hz, 1H), 3.54 (t, *J* = 14.8 Hz, 1H), 2.40 – 2.19 (m, 1H), 1.67 (s, 3H), 1.58 (s, 3H).

^{13}C NMR (101 MHz, $CDCl_3$) δ 167.7, 159.8, 149.6, 148.0 (d, *J* = 35.4 Hz), 138.4, 132.0, 130.3, 128.4, 123.9, 123.5 (q, *J* = 274.1 Hz), (123.3, 122.2, 122.0, 121.0, 119.1 (q, *J* = 2.6 Hz), 66.9, 42.7, 38.5, 19.0, 15.9.

^{19}F NMR (376 MHz, $CDCl_3$): -68.24

2,3-Dimethyl-10b-(2-thienyl)-1,4-dihydropyridol[2,1-a]isoindol-6-one, 132i

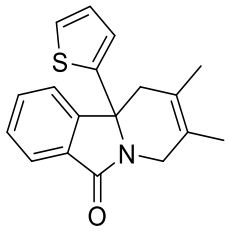

132i was prepared according to general procedure I from 3-hydroxy-3-(2-thienyl)isoindolin-1-one (25 mg, 108 µmol), calcium(ii) bis(trifluoromethanesulfonimide) (3.24 mg, 5.40 µmol), tetrabutylammonium hexafluorophosphate (2.09 mg, 5.40 µmol) and 2,3-Dimethyl-1,3-butadiene (18.0 µL, 162 µmol) in DCE (0.2 M). Purification by column chromatography (1:1 EtOAc:Hex) resulted in obtaining the pure product as a white solid (18 mg, 56%).

R_F (1:1 EtOAc:Hex) = 0.75

IR νmax (cm^{-1}): 2920, 2845, 1690, 1390.

HRMS (APCI) m/z: $[M + H]^+$ Calcd for $C_{18}H_{18}NOS$ 296.1109 ; Found 296.1098

^1H NMR (400 MHz, $CDCl_3$) δ 7.95 – 7.82 (m, 1H), 7.48 (dtd, *J* = 22.4, 7.4, 1.2 Hz, 2H), 7.39 – 7.34 (m, 1H), 7.17 (dd, *J* = 5.1, 1.2 Hz, 1H), 6.90 (dd, *J* = 5.1, 3.6 Hz, 1H), 6.84 (dd, *J* = 3.6, 1.2 Hz, 1H), 4.54 (d, *J* = 17.9 Hz, 1H), 3.50 (d, *J* = 17.9 Hz, 1H), 3.01 (d, *J* = 16.6 Hz, 1H), 2.40 (d, *J* = 17.1 Hz, 1H), 1.75 (s, 3H), 1.66 (s, 3H).

^{13}C NMR (101 MHz, $CDCl_3$) δ 166.3, 151.2, 144.5, 131.9, 130.5, 128.5, 127.2, 125.1, 124.6, 124.1, 123.1, 121.9, 121.9, 63.3, 42.3, 41.9, 19.2, 16.1

2,3, 10b-Triphenyl-1,4-dihydropyridol[2,1-a]isoindol-6-one, 161.1a

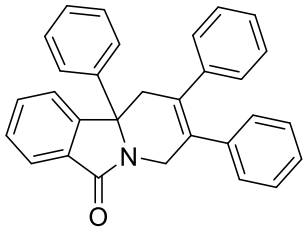

161.1a was prepared according to general procedure I from 3-hydroxy-3-phenyl-isoindolin-1-one (80.0 mg, 355 µmol), calcium(ii) bis(trifluoromethanesulfonimide) (10.7 mg, 17.8 µmol), tetrabutylammonium hexafluorophosphate (6.88 mg, 17.8 µmol) and 2,3-Diphenyl-1,3-butadiene (110 mg, 533 µmol) in DCE (0.2 M). Purification by column chromatography (1:3 EtOAc:Hex) resulted in obtaining the pure product as a white solid (47 mg, 32%).

R_F (1:1 EtOAc:Hex) = 0.74

IR νmax (cm^{-1}): 3022, 2839, 1684, 1392.

HRMS (APCI) m/z: $[M + H]^+$ Calcd for $C_{30}H_{24}NO$ 414.1858 ; Found 414.1851

^{1}H NMR (400 MHz, $CDCl_3$) δ 7.97 (dd, *J* = 6.5, 1.7 Hz, 1H), 7.55 – 7.43 (m, 2H), 7.43 – 7.30 (m, 5H), 7.17 (ddd, *J* = 18.6, 9.5, 3.0 Hz, 5H), 7.11 – 7.04 (m, 3H), 7.04 – 6.99 (m, 2H), 6.93 – 6.86 (m, 2H), 5.09 (dd, *J* = 18.6, 2.5 Hz, 1H), 3.85 – 3.68 (m, 2H), 2.82 (d, *J* = 17.0 Hz, 1H).

^{13}C NMR (101 MHz, $CDCl_3$) δ 167.1, 151.7, 141.7, 139.0, 138.7, 132.4, 132.2, 130.9, 130.9, 129.1, 129.1, 128.9, 128.4, 128.3, 128.1, 128.1, 127.1, 126.9, 126.1, 124.2, 121.9, 65.1, 42.4, 39.8.

3-Phenyl-3-[(2-phenyl-3H-inden-1-yl)methyl]isoindolin-1-one, 161.2a

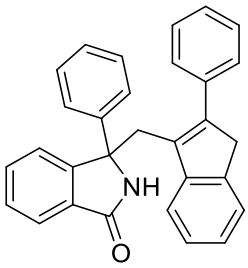

161.2a was prepared according to general procedure I from 3-hydroxy-3-phenyl-isoindolin-1-one (80.0 mg, 355 µmol), calcium(ii) bis(trifluoromethanesulfonimide) (10.7 mg, 17.8 µmol), tetrabutylammonium hexafluorophosphate (6.88 mg, 17.8 µmol) and 2,3-Diphenyl-1,3-butadiene (110 mg, 533 µmol) in DCE (0.2 M). Purification by column chromatography (1:3 EtOAc:Hex) resulted in obtaining the pure product as a yellow solid (84 mg, 57%).

R_F (1:1 EtOAc:Hex) = 0.59

IR νmax (cm^{-1}): 3165, 3056, 1694, 1466.

HRMS (APCI) m/z: $[M + H]^+$ Calcd for $C_{30}H_{24}NO$ 414.1852 ; Found 414.1846

^1H NMR (400 MHz, $CDCl_3$) δ 7.61 – 7.55 (m, 1H), 7.41 – 7.33 (m, 3H), 7.34 – 7.27 (m, 3H), 7.25 – 7.20 (m,52H), 7.20 – 7.14 (m, 4H), 7.10 (ddd, *J* = 9.5, 7.5, 1.5 Hz, 3H), 5.95 (s, 1H), 3.90 (s, 1H), 3.55 (q, *J* = 22.9 Hz, 2H).

^{13}C NMR (101 MHz, $CDCl_3$) δ 170.0, 150.7, 147.1, 146.7, 142.7, 142.4, 138.3, 132.9, 132.3, 130.5, 129.1, 129.1, 128.5, 128.4, 128.1, 127.5, 126.8, 125.7, 125.1, 123.9, 123.8, 123.2, 119.9, 67.8, 43.3, 34.7.

10b-(4-Methoxyphenyl)-2,3-diphenyl-1,4-dihydropyrido[2,1-a]isoindol-6-one, 161.1b

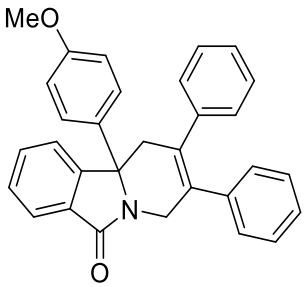

161.1b was prepared according to general procedure I from 3-hydroxy-3-(4-methyloxyohenyl)isoindolin-1one (50.0 mg, 196 µmol), calcium(ii) bis(trifluoromethanesulfonimide) (5.88 mg, 9.79 µmol), tetrabutylammonium hexafluorophosphate (3.79 mg, 9.79 µmol) and 2,3-Diphenyl-1,3-butadiene (60.6 mg, 294 µmol) in DCE (0.2 M). Purification by column chromatography (1:3 EtOAc:Hex) resulted in obtaining the pure product as a yellow solid (17 mg, 20%).

R_F (1:1 EtOAc:Hex) = 0.67

IR νmax (cm^{-1}): 2924, 2849, 1684, 1509 1246.

HRMS (APCI) m/z: $[M + H]^+$ Calcd for $C_{31}H_{26}NO_2$ 444.1964 ; Found 444.1940

^1H NMR (400 MHz, $CDCl_3$) δ 8.14 – 7.86 (m, 1H), 7.61 – 7.41 (m, 2H), 7.30 – 7.14 (m, 5H), 7.14 – 7.09 (m, 3H), 7.07 – 7.03 (m, 2H), 6.97 – 6.87 (m, 4H), 5.17 – 4.96 (m, 1H), 3.97 – 3.78 (s, 3H), 3.81 – 3.65 (m, 2H), 2.82 (dt, *J* = 17.1, 3.2 Hz, 1H).

^{13}C NMR (101 MHz, $CDCl_3$) δ 166.7, 159.0, 151.7, 141.4, 138.7, 132.1, 131.8, 130.7, 130.6, 130.1, 128.8, 128.6, 128.0, 127.9, 127.8, 127.2, 126.8, 126.6, 123.9, 121.6, 114.1, 64.4, 55.1, 41.9, 39.6.

3-(4-Methoxyphenyl)-3-[(2-phenyl-3H-inden-1-yl)methyl]isoindolin-1-one, 161.2b

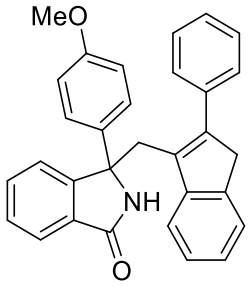

161.2b was prepared according to general procedure I from 3-hydroxy-3-(4-methyloxyohenyl)isoindolin-1one (50.0 mg, 196 µmol), calcium(ii) bis(trifluoromethanesulfonimide) (5.88 mg, 9.79 µmol), tetrabutylammonium hexafluorophosphate (3.79 mg, 9.79 µmol) and 2,3-Diphenyl-1,3-butadiene (60.6 mg, 294 µmol) in DCE (0.2 M). Purification by column chromatography (1:3 EtOAc:Hex) resulted in obtaining the pure product as a yellow solid (13 mg, 15%).

R_F (1:1 EtOAc:Hex) = 0.37

IR νmax (cm-1): 3132, 2853, 1695, 1507.

HRMS (APCI) m/z: $[M + H]^+$ Calcd for $C_{30}H_{26}NO_2$ 444.1958 ; Found 444.1944

^{1}H NMR (400 MHz, $CDCl_3$) δ 7.69 – 7.54 (m, 1H), 7.36 (d, *J* = 7.3 Hz, 1H), 7.29 (tt, *J* = 4.5, 4.0 Hz, 3H), 7.19 (dd, *J* = 3.5, 1.9 Hz, 5H), 7.17 – 7.07 (m, 5H), 6.72 (d, *J* = 8.9 Hz, 2H), 5.96 (s, 1H), 3.85 (dt, *J* = 19.9, 9.9 Hz, 2H), 3.76 (s, 3H), 3.55 (q, *J* = 22.9 Hz, 2H).

^{13}C NMR (101 MHz, $CDCl_3$) δ 169.9, 159.4, 151.1, 147.0, 146.8, 142.7, 138.3, 134.3, 132.9, 132.3, 130.3, 129.1, 128.5, 128.4, 127.5, 126.9, 126.8, 125.1, 124.0, 123.8, 123.1, 119.9, 114.4, 67.4, 55.7, 43.3, 34.9.

2,3-Diphenyl-10b-[4-(trifluoromethyl)phenyl]-1,4-dihydropyrido[2,1-a]isoinol-6-one, 161.1c

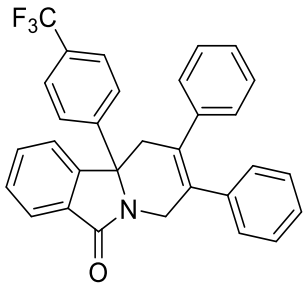

161.1c was prepared according to general procedure I from 3-hydroxy-3-[4-trifluoromethyl)phenyl]isoindolin-1one (31.0 mg, 105 µmol), calcium(ii) bis(trifluoromethanesulfonimide) (3.16 mg, 5.27 µmol), tetrabutylammonium hexafluorophosphate (2.04 mg, 5.27 µmol) and 2,3-Diphenyl-1,3-butadiene (32.6 mg, 158 µmol) in DCE (0.2 M). Purification by column chromatography (1:3 EtOAc:Hex) resulted in obtaining the pure product as a white solid (11 mg, 23%).

R_F (1:1 EtOAc:Hex) = 0.70

IR νmax (cm^{-1}): 3003, 2834, 1659, 1593.

HRMS (APCI) m/z: $[M + H]^+$ Calcd for $C_{31}H_{23}F_3NO$ 482.1732; Found 482.1729

^{1}H NMR (400 MHz, $CDCl_3$) δ 8.01 (dd, *J* = 5.7, 2.8 Hz, 1H), 7.84 (ddd, *J* = 45.0, 5.5, 3.1 Hz, 1H), 7.66 (d, *J* = 8.3 Hz, 2H), 7.57 – 7.49 (m, 4H), 7.24 – 7.10 (m, 6H), 7.07 – 6.89 (m, 4H), 5.13 (dd, *J* = 18.7, 2.5 Hz, 1H), 3.87 – 3.62 (m, 2H), 2.90 (d, *J* = 17.1 Hz, 1H).

^{13}C NMR (101 MHz, $CDCl_3$) δ 167.2, 150.9, 143.1, 141.4, 138.7, 134.5, 132.6, 132.5, 130.8, 130.6, 129.0, 128.9, 128.8, 128.4, 128.2, 127.3, 127.1, 126.6, 126.3(q, J=3.7Hz), 124.5, 123.8, 121.9, 64.9, 42.4, 39.6.

^{19}F NMR (376 MHz, $CDCl_3$): -62.62

3-[(2-Phenyl-3H-inden-1-yl)methyl]-3-[4-(trifluoromethyl)phenyl]isoindolin-1-one, 161.2c

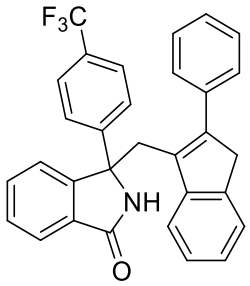

161.2c was prepared according to general procedure I from 3-hydroxy-3-[4-trifluoromethyl)phenyl]isoindolin-1one (31.0 mg, 105 µmol), calcium(ii) bis(trifluoromethanesulfonimide) (3.16 mg, 5.27 µmol), tetrabutylammonium hexafluorophosphate (2.04 mg, 5.27 µmol) and 2,3-Diphenyl-1,3-butadiene (32.6 mg, 158 µmol) in DCE (0.2 M). Purification by column chromatography (1:3 EtOAc:Hex) resulted in obtaining the pure product as a white solid (19 mg, 38%).

R_F (1:1 EtOAc:Hex) = 0.53

IR νmax (cm^{-1}): 3100, 2953, 1686, 1587.

HRMS (APCI) m/z: $[M + H]^+$ Calcd for $C_{31}H_{23}F_3NO$ 482.1726; Found 482.1731

^{1}H NMR (400 MHz, $CDCl_3$) δ 7.67 (ddd, *J* = 4.2, 2.2, 0.6 Hz, 1H), 7.39 (q, *J* = 8.5 Hz, 5H), 7.31 (ddd, *J* = 7.0, 5.9, 3.8 Hz, 7H), 7.26 – 7.20 (m, 2H), 7.19 – 7.07 (m, 1H), 7.06 – 6.99 (m, 2H), 6.43 (s, 1H), 3.87 (dd, *J* = 108.1, 13.9 Hz, 2H), 3.55 (dd, *J* = 54.3, 22.9 Hz, 2H)

^{13}C NMR (101 MHz, $CDCl_3$) δ 149.9, 146.9, 146.2, 145.7, 142.4, 137.8, 132.3, 132.2, 128.9, 128.6, 128.1, 127.3, 126.7, 125.8, 125.5 (q, J=3.7Hz), 125.1, 123.9, 123.8, 122.6, 119.7, 67.4, 43.0, 34.8.

^{19}F NMR (376 MHz, $CDCl_3$): -62.71

2,3-Bis(4-methoxyphenyl)-10b-phenyl-1,4-dihydropyrido[2,1-a]isoindol-6-one, 161.1d

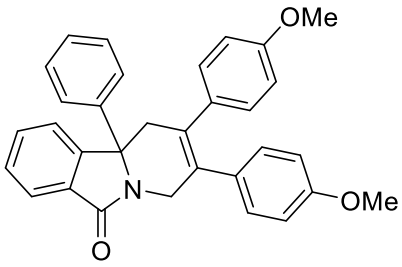

161.1d was prepared according to general procedure I from 3-hydroxy-3-phenyl-isoindolin-1-one (80.0 mg, 355 µmol), calcium(ii) bis(trifluoromethanesulfonimide) (10.7 mg, 17.8 µmol), tetrabutylammonium hexafluorophosphate (6.88 mg, 17.8 µmol) and 4,4-dimethoxydiphenyl)buta-1,3-diene (142 mg, 533 µmol) in DCE (0.2 M). Purification by column chromatography (1:1 EtOAc:Hex) resulted in obtaining the pure product as a white solid (148 mg, 88%).

R_F (3:1 EtOAc:Hex) = 0.63

IR νmax (cm^{-1}): 2984, 2930, 1684, 1507, 1241.

HRMS (APCI) m/z: $[M + H]^+$ Calcd for $C_{32}H_{28}NO_3$ 474.2069 ; Found 474.2052

^1H NMR (400 MHz, $CDCl_3$) δ 8.08 – 7.82 (m, 1H), 7.50 – 7.43 (m, 2H), 7.38 – 7.29 (m, 5H), 7.24 (d, *J* = 3.3 Hz, 1H), 6.96 (d, *J* = 8.7 Hz, 2H), 6.83 (d, *J* = 8.8 Hz, 2H), 6.72 (d, *J* = 8.8 Hz, 2H), 6.64 (d, *J* = 8.8 Hz, 2H), 5.06 (d, *J* = 18.2 Hz, 1H), 3.79 – 3.56 (m, 8H), 2.86 – 2.66 (m, 1H).

^{13}C NMR (101 MHz, $CDCl_3$) δ 167.2, 158.3, 151.8, 138.7, 134.2, 132.1, 131.5, 131.1, 130.9, 130.2, 130.0, 129.7, 129.1, 128.4, 128.1, 126.1, 124.2, 121.9, 113.7, 113.6, 65.2, 55.3, 42.4, 39.9.

3-[[5-Methoxy-2-(4-methoxyphenyl)-3H-inden-1-yl]methyl]-3-phenyl-isoindolin-1-one, 161.2d

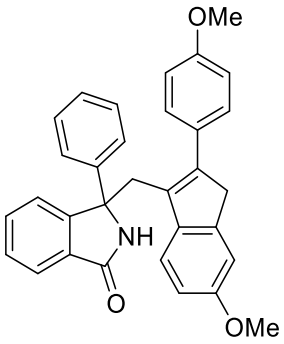

161.2d was prepared according to general procedure I from 3-hydroxy-3-phenyl-isoindolin-1-one (80.0 mg, 355 µmol), calcium(ii) bis(trifluoromethanesulfonimide) (10.7 mg, 17.8 µmol), tetrabutylammonium hexafluorophosphate (6.88 mg, 17.8 µmol) and 4,4-dimethoxydiphenyl)buta-1,3-diene (142 mg, 533 µmol) in DCE (0.2 M). Purification by column chromatography (3:1 EtOAc:Hex) resulted in obtaining the pure product as a yellow solid (14 mg, 8.7%).

R_F (3:1 EtOAc:Hex) = 0.87

IR νmax (cm^{-1}): 3058, 2877, 1602, 1577.

HRMS (APCI) m/z: $[M + H]^+$ Calcd for $C_{32}H_{28}NO_3$ 474.2069 ; Found 474.2043

^{1}H NMR (400 MHz, $CDCl_3$) δ 7.70 – 7.55 (m, 1H), 7.38 (dd, *J* = 4.8, 3.1 Hz, 2H), 7.28 – 7.16 (m, 7H), 7.05 – 6.96 (m, 3H), 6.93 (d, *J* = 2.2 Hz, 1H), 6.87 – 6.81 (m, 2H), 6.71 (dd, *J* = 8.4, 2.4 Hz, 1H), 6.10 (s, 1H), 4.06 – 3.68 (m, 8H), 3.47 (q, *J* = 22.6 Hz, 2H).

^{13}C NMR (101 MHz, $CDCl_3$) δ 169.6, 158.6, 157.6, 150.5, 144.0, 143.9, 142.1, 139.5, 131.7, 131.3, 130.4, 130.1, 129.1, 128.6, 128.0, 127.7, 125.3, 123.4, 122.8, 119.7, 114.1, 111.8, 109.9, 67.4, 55.5, 42.7, 34.6.

2,3,10b-Tris(4-methoxyphenyl)-1,4-dihydropyrido[2,1-a]isoindol-6-one, 161.1e

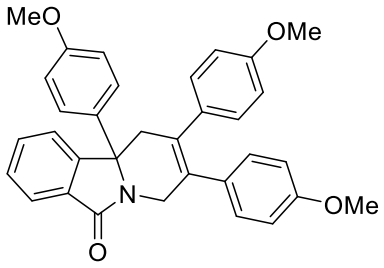

161.1e was prepared according to general procedure I from 3-hydroxy-3-(4-methyloxyohenyl)isoindolin-1one (80.0 mg, 313 µmol), calcium(ii) bis(trifluoromethanesulfonimide) (9.14 mg, 14.7 µmol), tetrabutylammonium hexafluorophosphate (6.07 mg, 15.7 µmol) and 4,4-dimethoxydiphenyl)buta-1,3-diene (125 mg, 470 µmol) in DCE (0.2 M). Purification by column chromatography (1:1 EtOAc:Hex) resulted in obtaining the pure product as a white solid (138 mg, 88%).

R_F (3:1 EtOAc:Hex) = 0.56

IR νmax (cm^{-1}): 2929, 2834, 1684, 1604, 1243.

HRMS (APCI) m/z: $[M + H]^+$ Calcd for $C_{33}H_{30}NO_4$ 504.2175 ; Found 504.2162

^{1}H NMR (400 MHz, $CDCl_3$) δ 8.06 – 7.87 (m, 1H), 7.53 – 7.41 (m, 2H), 7.25 – 7.20 (m, 3H), 6.99 – 6.94 (m, 2H), 6.90 – 6.81 (m, 4H), 6.76 – 6.70 (m, 2H), 6.68 – 6.61 (m, 2H), 5.02 (dd, *J* = 18.4, 2.4 Hz, 1H), 3.84 – 3.59 (m, 11H), 2.73 (d, *J* = 17.1 Hz, 1H).

^{13}C NMR (101 MHz, $CDCl_3$) δ 166.9, 159.3, 158.5, 158.3, 152.1, 134.2, 132.1, 131.6, 131.1, 130.9, 130.5, 130.2, 130.0, 129.7, 128.3, 127.5, 124.2, 121.9, 114.4, 113.7, 113.6, 64.7, 55.4, 55.3, 55.3, 42.2, 40.0.

2,3-Bis(4-methoxyphenyl)-10b-[4-(trifluoromethyl)phenyl]-1,4-dihydropyrido[2,1-a]isoindol-6-one, 161.1f

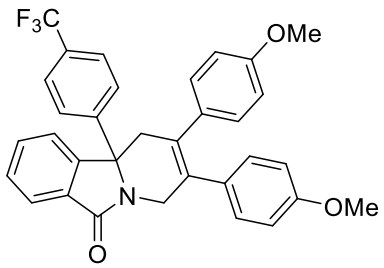

161.1f was prepared according to general procedure I from 3-hydroxy-3-[4-trifluoromethyl)phenyl]isoindolin-1one (80mg, 273µmol), calcium(ii) bis(trifluoromethanesulfonimide) (8.19mg, 13.6µmol), tetrabutylammonium hexafluorophosphate (5.28mg, 13.6µmol) and 4,4-dimethoxydiphenyl)buta-1,3-diene (109mg, 409µmol) in DCE (0.2M). Purification by column chromatography (1:3 EtOAc:Hex) resulted in obtaining the pure product as a pale red solid (32 mg, 22%).

R_F (3:1 EtOAc:Hex) = 0.59

IR νmax (cm^{-1}): 3003, 2834, 1659, 1593.

HRMS (APCI) m/z: $[M + H]^+$ Calcd for $C_{33}H_{27}F_3NO_3$ 542.1943 ; Found 542.1922

^1H NMR (400 MHz, $CDCl_3$) δ 8.02 – 7.97 (m, 1H), 7.64 (d, *J* = 8.3 Hz, 2H), 7.56 – 7.43 (m, 4H), 7.24 (d, *J* = 4.4 Hz, 1H), 7.01 – 6.94 (m, 2H), 6.89 – 6.82 (m, 2H), 6.78 – 6.71 (m, 2H), 6.70 – 6.63 (m, 2H), 5.09 (dd, *J* = 18.6, 2.5 Hz, 1H), 3.90 – 3.69 (m, 8H), 2.91 – 2.79 (m, 1H).

^{13}C NMR (101 MHz, $CDCl_3$) δ 167.2, 158.6, 158.5, 150.9, 143.2, 133.8, 132.4, 131.2, 131.2, 130.9, 130.1, 129.9, 129.3, 128.8, 126.6, 126.2(q, J=3.8Hz), 124.5, 121.9, 113.8, 113.6, 64.9, 55.3, 55.3, 42.4, 39.7.

^{19}F NMR (376 MHz, $CDCl_3$): -62.62

10b-(1,3-Benzodioxol-5-yl)-2,3-bis(4-methoxyphenyl)-1,4-dihydropyrido[2,1-a]isoindol-6-one, 161.1g

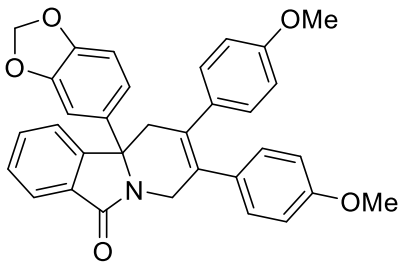

161.1g was prepared according to general procedure I from 3-(1,3-benzodioxol-5-yl)-3hydroxy-indan-1one (50 mg, 186 µmol), calcium(ii) bis(trifluoromethanesulfonimide) (5.57 mg, 9.28 µmol), tetrabutylammonium hexafluorophosphate (3.60 mg, 9.28 µmol) and 4,4-dimethoxydiphenyl)buta-1,3-diene (74.2 mg, 279 µmol) in DCE (0.2 M).

Purification by column chromatography (1:1 EtOAc:Hex) resulted in obtaining the pure product as a pale orange solid (71 mg, 74%).

R_F (1:1 EtOAc:Hex) = 0.60

IR νmax (cm^{-1}): 2959, 1690, 1570, 1120.

HRMS (APCI) m/z: $[M + H]^+$ Calcd for $C_{33}H_{28}NO_5$ 518.1967; Found 518.1937

^1H NMR (400 MHz, $CDCl_3$) δ 7.99 – 7.89 (m, 1H), 7.47 (td, *J* = 6.5, 1.4 Hz, 2H), 7.01 – 6.93 (m, 2H), 6.92 – 6.84 (m, 3H), 6.78 (d, *J* = 8.2 Hz, 1H), 6.74 – 6.69 (m, 3H), 6.68 – 6.63 (m, 2H), 5.94 (dd, *J* = 5.5, 1.4 Hz, 2H), 5.04 (dd, *J* = 18.4, 2.5 Hz, 1H), 3.86 – 3.53 (m, 8H), 2.72 (d, *J* = 17.1 Hz, 1H).

^{13}C NMR (101 MHz, $CDCl_3$) δ 166.9, 158.5, 158.3, 151.9, 148.5, 147.4, 134.0, 132.5, 132.1, 131.5, 130.9, 130.8, 130.2, 130.0, 129.6, 128.4, 124.2, 121.8, 119.5, 113.7, 113.5, 108.5, 106.7, 101.4, 64.9, 55.2, 55.2, 42.2, 40.1.

2,3-Bis(4-methoxyphenyl)-10b-[6-(trifluoromethyl)-2-pyridyl]-1,4-dihydropyrido[2,1-a]isoindol-6-one, 161.1h

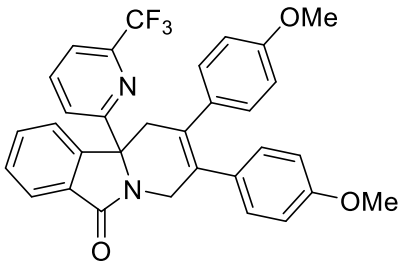

161.1h was prepared according to general procedure I from 3-hydroxy-3-[6-(trifluoromethyl)-2-pyridyl]isoindolin-1one (50 mg, 170 µmol), calcium(ii) bis(trifluoromethanesulfonimide) (5.10 mg, 8.50 µmol), tetrabutylammonium hexafluorophosphate (3.29 mg, 8.50 µmol) and 4,4-dimethoxydiphenyl)buta-1,3-diene (67.9 mg, 255 µmol) in DCE (0.2 M). Purification by column chromatography (1:1 EtOAc:Hex) resulted in obtaining the pure product as a pale orange solid (60 mg, 65%).

R_F (1:1 EtOAc:Hex) = 0.57

IR νmax (cm^{-1}): 2836, 1686, 1606, 1177.

HRMS (APCI) m/z: $[M + H]^+$ Calcd for $C_{32}H_{26}F_3N_2O_3$ 543.1896 ; Found 543.1982

^{1}H NMR (400 MHz, $CDCl_3$) δ 7.99 – 7.94 (m, 1H), 7.80 – 7.72 (m, 1H), 7.63 (dd, *J* = 7.7, 0.7 Hz, 1H), 7.54 – 7.44 (m, 3H), 7.28 (s, 1H), 7.08 (d, *J* = 8.8 Hz, 2H), 6.79 (d, *J* = 8.9 Hz, 2H), 6.70 (d, *J* = 8.8 Hz, 2H), 6.62 (d, *J* = 8.9 Hz, 2H), 5.31 (dd, *J* = 18.5, 2.6 Hz, 1H), 4.51 (d, *J* = 16.7 Hz, 1H), 3.73 (dd, *J* = 12.7, 8.6 Hz, 7H), 2.55 (d, *J* = 16.8 Hz, 1H).

^{13}C NMR (101 MHz, $CDCl_3$) δ 167.8, 159.6, 158.3, 158.3, 149.3, 148.1(q, J=34.8Hz), 138.7, 133.7, 132.3, 131.3, 131.2, 130.6, 130.4, 130.1, 129.0, 128.8, 124.1, 122.9, 122.3, 119.4(q, J=2.8Hz), 113.4, 66.8, 55.1, 55.1, 42.6, 39.6.

^{19}F NMR (376 MHz, $CDCl_3$): -68.24

2,10b-Diphenyl-1,4-dihydropyrido[2,1-a]isoindol-6-one, 169a

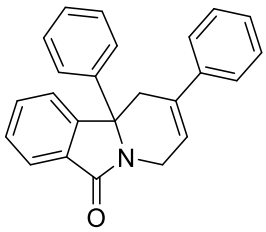

169a was prepared according to general procedure I from 3-hydroxy-3-phenyl-isoindolin-1-one (20.0 mg, 88.8 µmol), calcium(ii) bis(trifluoromethanesulfonimide) (2.60 mg, 4.44 µmol), tetrabutylammonium hexafluorophosphate (1.72 mg, 4.44 µmol) and 2-phenyl-1,3-butadiene (23.0 µL, 133 µmol) in DCE (0.2 M). Purification by column chromatography (1:1 EtOAc:Hex) resulted in obtaining the pure product as a white solid (29 mg, 97%).

R_F (1:1 EtOAc:Hex) = 0.69

IR νmax (cm^{-1}): 3052, 2838, 1686, 1388.

HRMS (APCI) m/z: $[M + H]^+$ Calcd for $C_{24}H_{20}NO$ 338.1545 ; Found 338.1541

^{1}H NMR (400 MHz, $CDCl_3$) δ 8.04 – 7.85 (m, 1H), 7.48 (ddd, *J* = 6.5, 4.6, 1.5 Hz, 2H), 7.43 – 7.34 (m, 4H), 7.34 – 7.27 (m, 4H), 7.21 (ddd, *J* = 10.7, 5.5, 2.8 Hz, 3H), 6.01 (dt, *J* = 3.6, 2.7 Hz, 1H), 4.92 (dt, *J* = 19.2, 3.3 Hz, 1H), 3.78 (dd, *J* = 16.6, 1.3 Hz, 1H), 3.69 – 3.56 (m, 1H), 2.73 (dd, *J* = 16.6, 3.5 Hz, 1H).

^{13}C NMR (101 MHz, $CDCl_3$) δ 167.2, 151.9, 140.7, 138.5, 133.6, 132.2, 130.9, 129.1, 128.8, 128.4, 128.0, 127.8, 126.1, 125.4, 124.2, 121.9, 120.9, 65.1, 38.5, 35.9.

10b-(4-Methoxyphenyl)-2-phenyl-1,4-dihydropyrido[2,1-a]isoindol-6-one, 169b

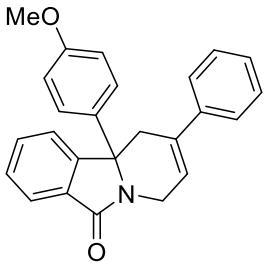

169b was prepared according to general procedure I from 3-hydroxy-3-(4-methyloxyohenyl)isoindolin-1one (25.0 mg, 97.9 µmol), calcium(ii) bis(trifluoromethanesulfonimide) (2.94 mg, 4.90 µmol), tetrabutylammonium hexafluorophosphate (1.90 mg, 4.90 µmol) and 2-phenyl-1,3-butadiene (26.0 µL, 147 µmol) in DCE (0.2 M). Purification by column chromatography (1:1 EtOAc:Hex) resulted in obtaining the pure product as a white solid (31 mg, 87%).

R_F (1:1 EtOAc:Hex) = 0.42

IR νmax (cm^{-1}): 3050, 2836, 1682, 1388.

HRMS (APCI) m/z: $[M + H]^+$ Calcd for $C_{25}H_{22}NO_2$ 368.1651 ; Found 368.1648

^1H NMR (400 MHz, $CDCl_3$) δ 8.01 – 7.89 (m, 1H), 7.52 – 7.43 (m, 2H), 7.39 (t, *J* = 4.4 Hz, 4H), 7.31 (ddd, *J* = 5.7, 4.4, 1.9 Hz, 1H), 7.26 – 7.22 (m, 1H), 7.09 (d, *J* = 8.9 Hz, 2H), 6.79 (d, *J* = 8.9 Hz, 2H), 6.01 (d, *J* = 3.7 Hz, 1H), 4.90 (dt, *J* = 19.2, 3.3 Hz, 1H), 3.81 – 3.67 (m, 4H), 3.65 – 3.49 (m, 1H), 2.70 (dd, *J* = 16.6, 3.4 Hz, 1H).

^{13}C NMR (101 MHz, $CDCl_3$) δ 167.0, 159.2, 152.2, 140.7, 133.6, 132.1, 130.9, 130.3, 128.8, 128.3, 127.8, 127.4, 125.4, 124.1, 121.9, 120.9, 114.3, 64.7, 55.3, 38.4, 36.0.

2-Phenyl-10b-[4-(trifluoromethyl)phenyl]-1,4-dihydropyrido[2,1-a]isoindol-6-one, 169c

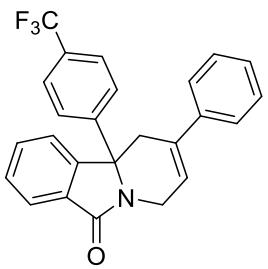

169c was prepared according to general procedure I from from 3-hydroxy-3-[4-trifluoromethyl)phenyl]isoindolin-1one (75.0 mg, 256 µmol), calcium(ii) bis(trifluoromethanesulfonimide) (7.68 mg, 12.8 µmol), tetrabutylammonium hexafluorophosphate (4.95 mg, 12.8 µmol) and 2-phenyl-1,3-butadiene (68.0 µL, 384 µmol) in DCE (0.2 M). Purification by column chromatography (1:3 EtOAc:Hex) resulted in obtaining the pure product as a white solid (36 mg, 35%).

R_F (1:1 EtOAc:Hex) = 0.76

IR νmax (cm^{-1}): 2955, 2881, 1601, 1358.

HRMS (APCI) m/z: $[M + H]^+$ Calcd for $C_{25}H_{19}F_3NO$ 406.1419 ; Found 406.1425

^1H NMR (400 MHz, $CDCl_3$) δ 8.02 – 7.88 (m, 1H), 7.59 – 7.44 (m, 4H), 7.39 (d, *J* = 4.4 Hz, 4H), 7.33 (dd, *J* = 7.1, 4.7 Hz, 3H), 7.25 – 7.22 (m, 1H), 6.03 (d, *J* = 3.6 Hz, 1H), 4.94 (dt, *J* = 19.3, 3.3 Hz, 1H), 3.78 (dd, *J* = 16.6, 1.1 Hz, 1H), 3.62 (d, *J* = 19.3 Hz, 1H), 2.78 (dd, *J* = 16.6, 3.3 Hz, 1H).

^{13}C NMR (101 MHz, $CDCl_3$) δ 151.0, 142.9, 140.3, 133.4, 132.4, 130.8, 130.3 (q, J= 32.6Hz), 128.9, 128.8, 128.0, 126.1 (q, J= 3.7Hz), 125.4, 124.4, 121.9, 121.0, 64.9, 38.6, 35.9.

^{19}F NMR (376 MHz, $CDCl_3$): -62.70

2-Phenyl-10b-[6-(trifluoromethyl)-2-pyridyl]-1,4-dihydropyrido[2,1-a]isoindol-6-one, 169g

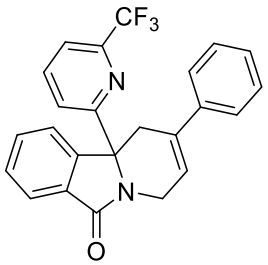

169g was prepared according to general procedure I from 3-hydroxy-3-[6-(trifluoromethyl)-2-pyridyl]isoindolin-1one (25.0 mg, 85.0 µmol), calcium(ii) bis(trifluoromethanesulfonimide) (2.55 mg, 4.25 µmol), tetrabutylammonium hexafluorophosphate (1.65 mg, 4.25 µmol) and 2-phenyl-1,3-butadiene (23.0 µL, 127 µmol) in DCE (0.2 M). Purification by column chromatography (3:1 EtOAc:Hex) resulted in obtaining the pure product as a white solid (31 mg, 89%).

R_F (3:1 EtOAc:Hex) = 0.48

IR νmax (cm^{-1}): 2924, 2851, 1694, 1340.

HRMS (APCI) m/z: $[M + H]^+$ Calcd for $C_{24}H_{18}F_3N_2O$ 407.1371; Found 407.1368

^1H NMR (400 MHz, $CDCl_3$) δ 7.97 – 7.84 (m, 1H), 7.80 – 7.71 (m, 1H), 7.57 (dd, *J* = 7.7, 0.7 Hz, 1H), 7.51 (ddd, *J* = 8.7, 5.3, 1.0 Hz, 2H), 7.51 – 7.42 (m, 3H), 7.40 – 7.29 (m, 4H), 5.82 (d, *J* = 3.0 Hz, 1H), 5.00 (dt, *J* = 19.3, 3.1 Hz, 1H), 4.59 (dd, *J* = 16.3, 0.9 Hz, 1H), 3.97 – 3.75 (m, 1H), 2.51 (dq, *J* = 16.2, 3.3 Hz, 1H).

^{13}C NMR (101 MHz, $CDCl_3$) δ 168.2, 159.6, 149.4, 148.3(q, J=34.9Hz), 140.9, 138.9, 135.5, 132.5, 130.4, 128.9, 128.6, 127.8, 126.2, 124.2, 122.9, 122.4, 122.40 120.2, 119.6, 119.5(q, J=2.7Hz), 67.2, 39.3, 36.2.

^{19}F NMR (376 MHz, $CDCl_3$): -68.05

10b-(6-Methoxy-2-pyridyl)-2-phenyl-1,4-dihydropyrido[2,1-a]isoindol-6-one, 169h

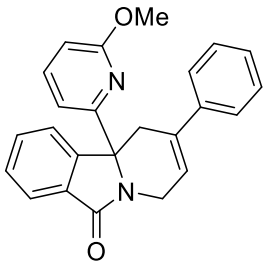

169h was prepared according to general procedure I from 3-hydroxy-3-(6-methoxy-2-pyridyl)indan-1one (25.0 mg, 97.6 µmol), calcium(ii) bis(trifluoromethanesulfonimide) (2.93 mg, 4.88 µmol), tetrabutylammonium hexafluorophosphate (1.89 mg, 4.88 µmol) and 2-phenyl-1,3-butadiene (26.0 µL, 146 µmol) in DCE (0.2 M). Purification by column chromatography (1:1 EtOAc:Hex) resulted in obtaining the pure product as a white solid (8.3 mg, 23%).

R_F (1:1 EtOAc:Hex) = 0.49

IR νmax (cm^{-1}): 2924, 2853, 1694, 1340.

HRMS (APCI) m/z: $[M + H]^+$ Calcd for $C_{24}H_{21}N_2O_2$ 369.1603 ; Found 369.1599

^{1}H NMR (400 MHz, $CDCl_3$) δ 8.14 – 8.05 (m, 1H), 7.95 (ddd, *J* = 9.8, 4.9, 4.3 Hz, 1H), 7.51 (pd, *J* = 7.4, 1.4 Hz, 2H), 7.44 – 7.34 (m, 4H), 7.34 – 7.26 (m, 2H), 7.25 – 7.23 (m, 1H), 7.19 (dd, *J* = 8.8, 2.7 Hz, 1H), 6.72 – 6.54 (m, 1H), 6.06 (tt, *J* = 21.0, 10.5 Hz, 1H), 4.91 (dt, *J* = 19.3, 3.3 Hz, 1H), 3.88 (s, 3H), 3.79 – 3.65 (m, 1H), 3.62 – 3.50 (m, 1H), 2.72 (ddd, *J* = 16.6, 6.6, 3.1 Hz, 1H).

^{13}C NMR (101 MHz, $CDCl_3$) δ 166.9, 163.9, 151.4, 144.9, 140.2, 137.3, 133.4, 132.4, 130.9, 128.8, 127.9, 126.9, 125.4, 124.3, 121.9, 120.9, 111.5, 63.3, 53.7, 38.4, 35.7.

10b-(1,3-Benzodioxol-5-yl)-2-phenyl-1,4-dihydropyrido[2,1-a]isoindol-6-one, 169i

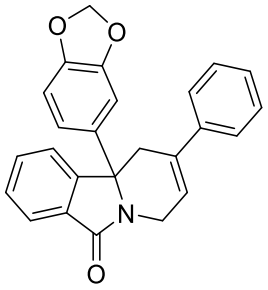

169i was prepared according to general procedure I from 3-(1,3-benzodioxol-5-yl)-3hydroxy-indan-1one (25.0 mg, 92.8 µmol), calcium(ii) bis(trifluoromethanesulfonimide) (2.79 mg, 4.64 µmol), tetrabutylammonium hexafluorophosphate (1.80 mg, 4.64 µmol) and 2-phenyl-1,3-butadiene (25.0 µL, 139 µmol) in DCE (0.2 M). Purification by column chromatography (1:1 EtOAc:Hex) resulted in obtaining the pure product as a white solid (25 mg, 69%).

R_F (1:1 EtOAc:Hex) = 0.64

IR νmax (cm^{-1}): 2920, 2853, 1682, 1610.

HRMS (APCI) m/z: $[M + H]^+$ Calcd for $C_{25}H_{20}NO_3$ 382.1443 ; Found 382.1447

^{1}H NMR (400 MHz, $CDCl_3$) δ 7.99 – 7.83 (m, 1H), 7.48 (ddd, *J* = 8.7, 7.1, 1.3 Hz, 2H), 7.42 – 7.29 (m, 6H), 6.77 – 6.65 (m, 2H), 6.59 (d, *J* = 1.5 Hz, 1H), 6.03 (d, *J* = 3.7 Hz, 1H), 5.90 (dd, *J* = 9.5, 1.4 Hz, 2H), 4.90 (dt, *J* = 19.1, 3.3 Hz, 1H), 3.72 – 3.59 (m, 2H), 2.78 – 2.62 (m, 1H).

^{13}C NMR (101 MHz, $CDCl_3$) δ 167.0, 151.9, 148.4, 147.4, 140.6, 133.6, 132.3, 132.2, 130.7, 128.8, 128.4, 127.8, 125.4, 124.2, 121.8, 120.9, 119.5, 108.5, 106.7, 101.4, 64.9, 38.5, 36.2.

10b-(3-Methoxyphenyl)-2-phenyl-1,4-dihydropyrido[2,1-a]isoindol-6-one, 169e

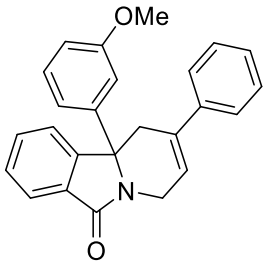

169e was prepared according to general procedure I from 3-hydroxy-3-(3-methoxyphenyl)indan-1one (25.0 mg, 97.9 µmol), calcium(ii) bis(trifluoromethanesulfonimide) (2.94 mg, 4.90 µmol), tetrabutylammonium hexafluorophosphate (1.90 mg, 4.90 µmol) and 2-phenyl-1,3-butadiene (26.0 µL, 147 µmol) in DCE (0.2 M). Purification by column chromatography (1:1 EtOAc:Hex) resulted in obtaining the pure product as a white solid (25 mg, 69%).

R_F (1:1 EtOAc:Hex) = 0.43

IR νmax (cm^{-1}): 2922, 2849, 1681, 1451.

HRMS (APCI) m/z: $[M + H]^+$ Calcd for $C_{25}H_{22}NO_2$ 368.1651 ; Found 368.1649

^{1}H NMR (400 MHz, $CDCl_3$) δ 8.07 – 7.80 (m, 1H), 7.47 (td, *J* = 6.6, 1.4 Hz, 2H), 7.42 – 7.34 (m, 4H), 7.33 – 7.26 (m, 2H), 7.20 (t, *J* = 8.0 Hz, 1H), 6.95 – 6.60 (m, 3H), 6.00 (d, *J* = 3.7 Hz, 1H), 4.92 (dt, *J* = 19.2, 3.3 Hz, 1H), 3.85 – 3.57 (m, 5H), 2.70 (dd, *J* = 16.5, 3.3 Hz, 1H).

^{13}C NMR (101 MHz, $CDCl_3$) δ 167.3, 160.2, 151.7, 140.7, 140.3, 133.7, 132.1, 130.8, 130.1, 128.7, 128.4, 127.8, 125.4, 124.2, 121.9, 120.9, 118.3, 112.9, 112.3, 65.1, 55.3, 38.6, 36.2.

10b-(4-Bromophenyl)-2-phenyl-1,4-dihydropyrido[2,1-a]isoindol-6-one, 169d

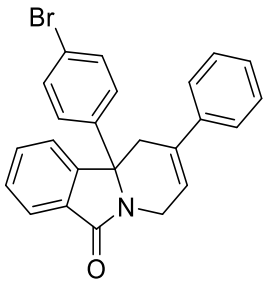

169d was prepared according to general procedure I from 3-hydroxy-3-(4-bromophenyl)-isoindolin-1-one (25.0 mg, 82.2 µmol), calcium(ii) bis(trifluoromethanesulfonimide) (2.47 mg, 4.11 µmol), tetrabutylammonium hexafluorophosphate (1.59 mg, 4.11 µmol) and 2-phenyl-1,3-butadiene (22.0 µL, 123 µmol) in DCE (0.2 M). Purification by column chromatography (1:1 EtOAc:Hex) resulted in obtaining the pure product as a white solid (25 mg, 72%).

R_F (1:1 EtOAc:Hex) = 0.68

IR νmax (cm^{-1}): 3022, 2924, 1682, 1388.

HRMS (APCI) m/z: $[M + H]^+$ Calcd for $C_{24}H_{19}BrNO$ 416.0650 ; Found 416.0648

^1H NMR (400 MHz, $CDCl_3$) δ 7.95 (dd, *J* = 6.9, 1.3 Hz, 1H), 7.57 – 7.46 (m, 2H), 7.39 (dd, *J* = 8.0, 5.9 Hz, 6H), 7.22 (ddd, *J* = 13.0, 5.2, 3.4 Hz, 2H), 7.05 (d, *J* = 8.7 Hz, 2H), 6.02 (d, *J* = 3.5 Hz, 1H), 4.91 (dt, *J* = 19.2, 3.3 Hz, 1H), 3.80 – 3.55 (m, 2H), 2.73 (dd, *J* = 16.6, 3.2 Hz, 1H).

^{13}C NMR (101 MHz, $CDCl_3$) δ 167.1, 151.3, 140.4, 137.8, 133.5, 132.3, 132.2, 128.8, 128.7, 127.9, 127.9, 125.4, 125.4, 124.3, 122.1, 121.8, 120.9, 64.7, 38.5, 35.9.

2-Phenyl-10b-(2-thienyl)-1,4-dihydropyrido[2,1-a]isoindol-6-one, 169f

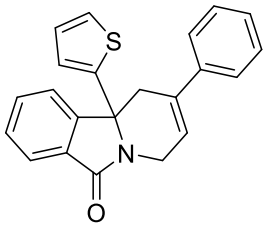

169f was prepared according to general procedure I from 3-hydroxy-3-(2-thienyl)isoindolin-1-one (25.0 mg, 108 µmol), calcium(ii)

bis(trifluoromethanesulfonimide) (3.24 mg, 5.40 µmol), tetrabutylammonium hexafluorophosphate (2.09 mg, 5.40 µmol) and 2-phenyl-1,3-butadiene (23.0 µL, 133 µmol) in DCE (0.2 M). Purification by column chromatography (1:1 EtOAc:Hex) resulted in obtaining the pure product as a brown solid (17 mg, 45%).

R_F (1:1 EtOAc:Hex) = 0.66

IR νmax (cm^{-1}): 2924, 2849, 1682, 1444, 1388.

HRMS (APCI) m/z: $[M + H]^+$ Calcd for $C_{22}H_{18}NOS$ 344.1109; Found 344.1111

^1H NMR (400 MHz, $CDCl_3$) δ 7.93 (d, *J* = 7.2 Hz, 1H), 7.58 – 7.46 (m, 2H), 7.40 (tt, *J* = 9.3, 4.7 Hz, 4H), 7.31 (d, *J* = 6.8 Hz, 1H), 7.18 (dd, *J* = 5.0, 1.3 Hz, 1H), 6.91 (ddd, *J* = 8.6, 4.3, 2.5 Hz, 2H), 6.06 (dd, *J* = 6.4, 2.8 Hz, 1H), 4.93 (dt, *J* = 19.2, 3.3 Hz, 1H), 3.97 – 3.78 (m, 1H), 3.64 (dd, *J* = 16.6, 1.3 Hz, 1H), 2.78 (dd, *J* = 16.6, 3.3 Hz, 1H).

^{13}C NMR (101 MHz, $CDCl_3$) δ 166.7, 151.1, 143.9, 140.6, 133.4, 132.2, 130.3, 128.8, 128.7, 127.9, 127.3, 125.6, 125.4, 124.8, 124.3, 121.9, 120.9, 63.2, 38.7, 38.6.

N,N'-(Phenylmethylene)bis[benzamide], 197

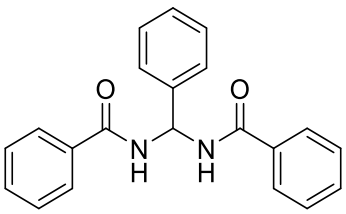

197 was prepared following procedure J from N-[methoxy(phenyl)methyl]benzamide (50 mg, 207 µmol), calcium(ii) bis(trifluoromethanesulfonimide) (12.4 mg, 20.7 µmol), tetrabutylammonium hexafluorophosphate (8.04 mg, 20.7 µmol) and 2,3-Dimethyl-1,3-butadiene (30.0 µL, 259 µmol) in DCE (0.2 M). Followed by filtration of the pure product to result in a white solid (33 mg, 55%).

^1H NMR (400 MHz, DMSO-D_6) δ 9.00 (d, *J* = 7.8 Hz, 2H), 7.94 – 7.85 (m, 4H), 7.60 – 7.51 (m, 2H), 7.51 – 7.44 (m, 6H), 7.41 – 7.27 (m, 3H), 7.03 (s, 1H).

^{13}C NMR (101 MHz, DMSO-D_6) δ 165.8, 140.5, 134.1, 131.8, 128.5, 128.5, 127.9, 127.7, 126.7, 58.9.

Data in accordance with literature [70]

11,13-Dimethyl-1-phenyl-12-oxa-9-azatetracyclotetradeca-2(7),3,5-trien-8-one, 175

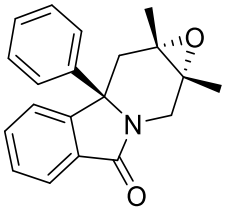

175 was prepared according to general procedure K from 2,3-dimethyl-10b-phenyl-1,4-dihydropyrido[2,1-a]isoindol-6-one (200 mg, 691 µmol), m-CPBA 70% (204 mg, 829 µmol) and sodium hydrogen carbonate (75.5 mg, 898 µmol) in DCM (70 mM). Purification by column chromatography (1:1 EtOAc:Hex) resulted in obtaining the pure product as a yellow solid (200 mg, 95%).

R_F (1:1 EtOAc:Hex) = 0.38

IR νmax (cm^{-1}): 2955, 2909, 1682, 1466, 1397.

HRMS (APCI) m/z: $[M + H]^+$ Calcd for $C_{20}H_{20}NO_2$ 306.1494; Found 306.1475

^1H NMR (400 MHz, $CDCl_3$) δ 7.92 – 7.81 (m, 1H), 7.49 – 7.37 (m, 2H), 7.39 – 7.28 (m, 3H), 7.19 – 7.05 (m, 3H), 4.50 (d, *J* = 14.8 Hz, 1H), 3.05 (d, *J* = 15.4 Hz, 1H), 2.86 (d, *J* = 14.8 Hz, 1H), 2.14 (d, *J* = 15.4 Hz, 1H), 1.53 (s, 3H), 1.25 (s, 3H).

^{13}C NMR (101 MHz, $CDCl_3$) δ 167.6, 152.0, 139.0, 132.5, 131.2, 129.6, 128.7, 128.6, 126.7, 124.5, 121.9, 64.4, 59.8, 59.7, 41.0, 39.1, 21.6, 17.1.

2,3-Dimethyl-10b-phenyl-4,6-dihydro-1H-pyrido[2,1-a]isoindole, 174

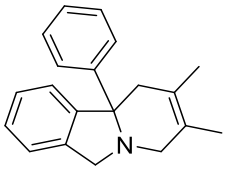

174 was prepared according to procedure L from 2,3-dimethyl-10b-phenyl-1,4-dihydropyrido[2,1-a]isoindol-6-one (100 mg, 346 µmol) and $LiAlH_4$ (1.40 mL, 3.46 mmol) in THF (0.025 M). Purification by column chromatography (1:3 EtOAc:Hex) resulted in obtaining the pure product as a yellow oil (52 mg, 54%).

R_F (1:1 EtOAc:Hex) = 0.91

IR νmax (cm^{-1}): 2888, 2829, 2758, 1444.

HRMS (APCI) m/z: $[M + H]^+$ Calcd for $C_{20}H_{22}N$ 276.1752; Found 276.1751

^1H NMR (400 MHz, $CDCl_3$) δ 7.36 – 7.31 (m, 2H), 7.29 – 7.23 (m, 3H), 7.22 – 7.12 (m, 2H), 7.10 (d, *J* = 7.3 Hz, 1H), 6.80 (d, *J* = 7.2 Hz, 1H), 4.26 (d, *J* = 12.3 Hz, 1H), 4.08 (d, *J* = 12.2 Hz, 1H), 3.22 – 3.01 (m, 2H), 2.56 (d, *J* = 17.3 Hz, 1H), 2.34 – 2.22 (m, 1H), 1.70 (s, 3H), 1.52 (s, 3H).

^{13}C NMR (101 MHz, $CDCl_3$) δ 151.24 143.7, 139.4, 128.1, 127.8, 126.8, 126.8, 126.5, 124.2, 124.1, 122.7, 121.9, 68.0, 56.5, 50.2, 35.4, 19.2, 16.2.

2-Hydroxy-2,3,3-trimethyl-10b-phenyl-1,4-dihydropyrido[2,1-a]isoindol-6-one;hydrate, 176

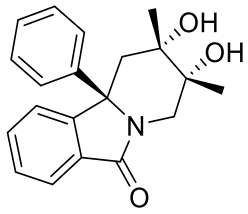

176 was prepared according to procedure M from 2,3-dimethyl-10b-phenyl-1,4-dihydropyrido[2,1-a]isoindol-6-one (100 mg, 346 µmol), OsO_4 (22 µL, 3.46 µmol) and NMO (93 µL, 449 µmol) dissolved in a mixture of acetone : *t*-BuOH : water (18:1:1). Purification by column chromatography (1:3 EtOAc:Hex) resulted in obtaining the pure product as a white solid (77 mg, 69%).

R_F (3:1 EtOAc:Hex) = 0.26

IR νmax (cm^{-1}): 3516, 3365, 2929, 1666, 1595.

HRMS (APCI) m/z: $[M + H]^+$ Calcd for $C_{20}H_{22}NO_3$ 324.1600 ; Found 324.1580

^1H NMR (400 MHz, $CDCl_3$) δ 7.72 (d, *J* = 7.1 Hz, 1H), 7.41 (dd, *J* = 6.9, 1.4 Hz, 3H), 7.34 (ddd, *J* = 13.5, 6.0, 0.9 Hz, 5H), 4.50 (d, *J* = 14.3 Hz, 1H), 3.91 (s, 1H), 3.11 – 3.01 (m, 2H), 2.87 (d, *J* = 13.5 Hz, 1H), 2.16 (d, *J* = 13.6 Hz, 1H), 1.27 (s, 3H), 0.83 (s, 3H).

^{13}C NMR (101 MHz, $CDCl_3$) δ 169.5, 152.0, 139.3, 132.3, 129.3, 128.9, 127.9, 127.8, 125.0, 124.3, 121.6, 72.9, 72.8, 68.2, 46.2, 44.3, 23.2, 20.3.